Corrosion of Thermal Sprayed Aluminium (TSA) in Marine Mud

Lars Krogstad Lien

MASTEROPPGAVE
Våren 2013
for
stud.techn. Lars Krogstad Lien

Korrosjon av termisk sprøytet aluminium i marin leire
(Corrosion of thermal sprayed aluminum in marine clay)

Bakgrunn:

I en rørledning skal fluidet kjøles ned den første kilometeren. Dette gjøres ved at røret ikke isoleres, men at man påfører et godt termisk ledende belegg i stedet, dvs termisk sprøytet aluminium (TSA). Røret skal ligge på havbunnen og man regner med at det etter hvert delvis vil dekkes av marin leire. Belegget er ikke fullstendig dekkende, så det er påkrevet med katodisk beskyttelse i tillegg. Aluminium offeranoder vil derfor monteres på røret.

Problem:

Når TSA polariseres av anodene vil det gå en svak katodisk strøm til røret, i størrelsesorden 10 mA/m². Katodereaksjonen er en blanding av hydrogenutvikling og oksygenreduksjon. Begge reaksjonene produserer hydroksid, hvilket kan føre til at pH stiger ved rørets overflate. Siden røret delvis er dekket av marin leire vil den dannede hydroksiden trolig vanskelig diffundere bort. Man kan derfor forestille seg at pH stiger ved overflata på TSA belegget. Aluminium er ikke immunt ved det potensialet som oppnås med aluminiumsanoder, men bare passivt. Hvis pH stiger over ca 9 vil aluminium ikke være passivt lenger, men starte å korrodere. Belegget vil da ikke få den levetiden som er ønsket. I tillegg vil den høye temperaturen gjøre at alle prosesser går raskere, hvilket kan redusere levetiden til belegget ytterligere.

Oppgaven:

1. Gjøre et litteratursøk på korrosjon av TSA og aluminium i sjøvann, med fokus på effekt av katodisk beskyttelse, høy temperatur og tildekning av marin leire.
2. Gjøre korrosjonsforsøk med TSA tildekket av marin leire for å måle korrosjonshastigheten under ulike betingelser.
3. Lage en enkel sensor for å måle pH på overflata av TSA under korrosjonsforsøkene.

Masteroppgave våren 2013 for stud.techn. Lars Krogstad Lien

Vår dato   Vår referanse
28.01.2013   KEDA

Oppgaveløsningen skal basere seg på eventuelle standarder og praktiske retningslinjer som foreligger og anbefales. Dette skal skje i nært samarbeid med veiledere og fagansvarlig. For øvrig skal det være et aktivt samspill med veiledere.

Innen tre uker etter at oppgaveteksten er utlevert, skal det leveres en forstudierapport som skal inneholde følgende:

- En analyse av oppgavens problemstillinger.

- En beskrivelse av de arbeidsoppgaver som skal gjennomføres for løsning av oppgaven. Denne beskrivelsen skal munne ut i en klar definisjon av arbeidsoppgavenes innhold og omfang.

- En tidsplan for fremdriften av prosjektet. Planen skal utformes som et Gantt-skjema med angivelse av de enkelte arbeidsoppgavenes terminer, samt med angivelse av milepæler i arbeidet.

Forstudierapporten er en del av oppgavebesvarelsen og skal innarbeides i denne. Det samme skal senere fremdrifts- og avviksrapporter. Ved bedømmelsen av arbeidet legges det vekt på at gjennomføringen er godt dokumentert.

Besvarelsen redigeres mest mulig som en forskningsrapport med et sammendrag både på norsk og engelsk, konklusjon, litteraturliste, innholdsfortegnelse etc. Ved utarbeidelsen av teksten skal kandidaten legge vekt på å gjøre teksten oversiktlig og velskrevet. Med henblikk på lesning av besvarelsen er det viktig at de nødvendige henvisninger for korresponderende steder i tekst, tabeller og figurer anføres på begge steder. Ved bedømmelsen legges det stor vekt på at resultatene er grundig bearbeidet, at de oppstilles tabellarisk og/eller grafisk på en oversiktlig måte og diskuteres utførlig.

Materiell som er utviklet i forbindelse med oppgaven, så som programvare eller fysisk utstyr er en del av besvarelsen. Dokumentasjon for korrekt bruk av dette skal så langt som mulig også vedlegges besvarelsen.

Eventuelle reiseutgifter, kopierings- og telefonutgifter må bære av studenten selv med mindre andre avtaler foreligger.

Hvis kandidaten under arbeidet med oppgaven støter på vanskeligheter, som ikke var forutsett ved oppgavens utforming og som eventuelt vil kunne kreve endringer i eller utelatelse av enkelte spørsmål fra oppgaven, skal dette straks tas opp med instituttet.

Oppgaveteksten skal vedlegges besvarelsen og plasseres umiddelbart etter tittelsiden.

Innleveringsfrist: 24. juni 2013.

Masteroppgave våren 2013 for stud.techn. Lars Krogstad Lien

Vår dato
28.01.2013

Vår referanse
KEDA

Besvarelsen skal innleveres i 1 elektronisk eksemplar (pdf-format) og 2 eksemplar (innbundet).

Ansvarlig faglærer:

Professor Olav Egeland
Institutt for produksjons- og kvalitetsteknikk
E-post: olav.egeland@ntnu.no
Telefon: 73 59 71 12

Veileder:

Professor II Ole Øystein Knutsen
Institutt for produktutvikling og materialer
E-post: Ole.O.Knudsen@sintef.no
Mobile Telephone: 982 30 420

**INSTITUTT FOR PRODUKSJONS-
OG KVALITETSTEKNIKK**

Per Schjølberg
førsteamanuensis/instituttleder

Olav Egeland
ansvarlig faglærer

PREFACE

This master thesis is submitted as the final work for the degree Master of Science in Subsea Technology, NTNU. The project was done for SINTEF Material and Chemistry, and was carried out the spring of 2013. The experimental work was performed at SINTEF Material and Chemistry's laboratory facility at Perleporten, NTNU.

I would like to thank my supervisor Ole Øystein Knudsen for help and guidance in this project and supplying information from his work for my use. Further on, I like to thank SINTEF Material and Chemistry for letting me work in their laboratory facility.

Lars Krogstad Lien

Trondheim, 09.06.13

ABSTRACT

A solution for cooling down reservoir fluid in an oil and gas pipeline has been suggested. By removal of the thermal isolation coating on the first kilometer of the pipeline and replacing it with thermal sprayed aluminum (TSA) will the increased thermal conductivity of the pipe speed up the cooling rate of the fluid.

A challenge with this solution is heating of TSA at the outside of the pipe. At higher temperatures is it expected an elevated corrosion rate of aluminum compered to normal service temperatures. In addition to the high temperature is there another concern. The pipe will be protected with sacrificial anodes to prevent rapid corrosion of the TSA. As a result of the cathodic protection will a cathodic reaction occur on the TSA surface, and hydroxide will be produced. What will happen when the pipe sinks into the sea bottom end gets covered by mud is unknown. A suggested theory is that the mud will hinder diffusion of the hydroxide produced from the cathodic reaction on the TSA surface. If so, will this lead to a pH increase near the TSA surface. In case of a the pH increase to about 9 the aluminum will change from being passive to active, this results in rapid corrosion of the TSA coating. The combination of the high temperature and the possible high pH can lead to a very short lifetime for the TSA coating, as the aluminum will corrode very rapidly.

To investigate the corrosion rate of TSA at the conditions mentioned over, has an experiments been conducted. Five samples TSA coated steel, coated in accordance with ISO 209 Grade 1100, with thickness of about 250µm were tested. A sealer was applied to all the samples. No coating failure was fabricated at any of the samples.

The test set up involved exposure at 95 °C, blanketing of the TSA with mud, and polarization to different potentials. The test duration was five weeks. During the test period hourly logging of current, potential, temperature and pH at the surface of the TSA were done by using KorrosjonsLogger©. For measuring the corrosion rate linear polarization resistance (LPR) measurements were conducted weekly. Together with Tafel curves recordings at test termination.

To measure the pH at the TSA surface was a sensor fabricated. A conventional glass electrode could not be used because of the harsh conditions. Trough a literature study was it decided to fabricate iridium oxide electrodes to use for the pH measurements. An iridium wire and lithium carbonate were obtained, and seven iridium oxide electrodes were made by the carbonate melt method. Prior to the utilization in the corrosion test was the stability and pH response of the iridium oxide electrodes measured.

After the test period did neither of the samples, which were cathodic polarized, show any visible degradation of the TSA coating. The sample that was anodic

polarized suffered from a leakage, because of corrosion of the TSA after 14 days, and was then removed from the experiment. For the samples that completed the test the cathodic current was between 23 mA/m^2 and 38 mA/m^2 and the corrosion rate between 10 μm/year and 15 μm/year after five weeks exposure.

SAMMENDRAG

En foreslått løsning for å kjøle ned reservoar væske i en undervanns olje og gas rørledning er forslått. Forslaget innebærer å fjerne det termisk isolerende belegget på den første kilometeren av rørledningen og erstatte det med termisk sprøytet aluminium (TSA). Dette vil føre til økt termiskkonduktivitet for rørledningen å føre til raskere nedkjøling av væsken inne i rørledningen.

En utfordring ved denne løsningen er at TSA belegget på utsiden av rørledningen vil bli varmet opp av den varme væsken inne i røret. Ved høye temperaturer er det forventet at aluminium vil korrodere hurtigere enn ved normale driftstemperaturer. I tillegg til den høye temperaturen er den en mulig at det vil oppstå enda en utfordring for TSA belegget. Rørledningen vil være beskyttet mot korrosjon av aluminiums offeranoder i tillegg til TSA belegget. Dette fører til polarisering av TSA belegget. Når TSA polariseres av anodene vil det gå en svak katodisk strøm til røret, i størrelsesorden 10 mA/m². Katodereaksjonen er en blanding av hydrogenutvikling og oksygenreduksjon. Begge reaksjonene produserer hydroksid, hvilket kan føre til at pH stiger på TSA overflaten. Rørledningen befinner seg på havets bunn og kommer til å delvis synke ned i sjøbunnen, og dermed bli dekket av marin leire. Dette vil trolig føre til at det blir vanskeligere for den produserte hydroksiden å diffundere bort fra overflaten til TSA belegget. I så fall vil dette føre til en høyere pH på overflaten av TSA belegget. Dette kan gi betydelige konsekvenser for TSA belegget. Aluminium er ikke immunt ved det potensialet som oppnås med aluminiums anoder, kun passivt. Hvis pH stiger til over ca. 9 vil aluminium ikke være passivt lenger, men starte å korrodere. Belegget vil da ikke oppnå den levetiden som er ønsket. I tillegg vil den høye temperaturen gjøre at alle prosesser og reaksjoner går raskere, hvilket kan redusere levetiden til belegget ytterligere.

For å kartlegge korrosjonshastigheten ved de nevnte forholdene over, ble det gjennomført et korrosjons forsøk. Fem prøveplater av stål belagt med TSA, etter ISO 209 Grade 1000, med tykkelse 250 μm ble testet. Det ble ikke påført skader i belegget.

I korrosjons forsøket ble prøveplatene eksponert ved 95°C, tildekket av marin leire og polarisert til forskjellig potensialer. Test perioden var fem uker. Under test perioden ble det gjennomført logging av: strøm, potensial, temperatur og pH på TSA overflaten hver time ved bruk av KorrosjonsLogger©. Korrosjonshastighets målinger ble gjennomført hver uke ved bruk av linear polarization resistance (LPR). I tillegg ble det tatt opp Tafel kurver ved test slutt.

For måling av pH ved TSA overflaten ble det fabrikkert pH sensorer, dette siden en vanlig glass elektrode ikke kan gjennomføre kontinuerlige målinger ved testens forhold. Gjennom litteratur søk ble det besluttet å produsere iridium oksid elektroder for å bruke til pH målingene. En iridium tråd og litiumkarbonat

ble kjøpt inn, og sju iridium oksid elektroder ble produsert ved bruk av karbonat smelte metoden. Før elektrodene ble brukt til pH målinger i korrosjons testen ble det gjennomført kartlegging av pH responsen og stabiliteten til elektrodene.

Ved test slutt viste ingen av prøvene, som var katodisk polarisert, nedbryting av TSA belegget. Den ene prøven som ble anodisk polarisert led av en lekkasje i en tetning som følge av korrosjon av TSA belegget etter 14 dager. Og dermed ble denne prøven fjernet fra testen etter 14 dager. For prøvene som gjennomførte testen var den katodiske strømmen mellom 23 mA/m^2 og 38 mA/m^2 ved test slutt, og korrosjonshastigheten mellom 10 μm/år og 15 μm/år ved test slutt.

Table of Contents

LIST OF FIGURES:

LIST OF TABLES:

1. INTRODUCTION

1.1. BACKGROUND

The high demand of oil and gas is pushing the industry to develop new techniques. The results are the arrival of new challenges and demands for the industry. An arising demand is cooling of the reservoir fluid within the pipeline that transports the fluid from the well. A proposed technique is involving use of the first kilometer of pipeline from the well to cool down the fluid inside. A normal subsea oil and gas pipeline that is located close to the well is normally isolated with a tick coating. In this situation is desirable to get the heat out of the fluid inside the pipe. To achieve this new solutions are required.

The proposed solution is to apply a coating that has good thermal conductivity and good corrosion protection qualities, therefore is thermal sprayed aluminum (TSA) chosen. The coating will serve as anodic corrosion protection for the steel pipe, and the nature of aluminum does that it will provide good thermal conductivity as well.

1.2. MOTIVATION

To aid the TSA with the corrosion protection are sacrificial anodes of aluminum installed on the pipeline. The anodes will polarize the TSA and a small cathodic current in the order of 10 mA/m^2 will run in the pipe. This results in a cathodic reaction that will produce hydroxide. The produced hydroxide will lead to an increased pH at the surface of the pipe. The pipe is located at the seabed, and it is expected that the pipe will sink into the seabed and be covered with seabed mud. This leads to a concern regarding the produced hydroxide. The mud can possible hinders the diffusion of the produced hydroxide. If so will an elevation of the pH occur at the TSA surface. Increased pH can lead to a big problem for the sustainability of TSA. At the potential that are introduced by the sacrificial anodes is aluminum passive, not immune. If the pH risers over ~9 will aluminum change from being passive ta active, in other words start to corrode heavily. This in combination with the high temperature will lead to a short lifetime for the TSA coating.

There is not a certainty that the hydroxide ions will be hindered to diffuse by the mud. The aim of this thesis is to investigate if the coverage of the TSA by mud will lead to rapid corrosion of the TSA coating. The three main tasks of this thesis are presented below:

- Conduct a literature study regarding corrosion of TSA and aluminum in seawater, with special focus on cathodic protection, high temperature and coverage by marine mud.
- Do a corrosion experiment with TSA covered by mud to measure the corrosion rate at 95°C and polarized to different potentials.
- Fabricate a sensor to measure the pH at the surface of the TSA while the corrosion experiments are running.

2. THEORY

2.1. CORROSION OF ALUMINIUM

Destruction or deterioration of a material by reaction with its environment is Mars G. Fontana definition of corrosion.[1] A more specific definition is material dissolution by a chemical reaction.

Aluminum is a very reactive material and should have bad qualities in terms of corrosion resistance. However aluminum is know as a corrosion resistant material because of it`s stable oxide, and is totally dependent on a good oxide layer to maintain the good corrosion resistance. The oxide layer forms very quickly, and a scratch in the oxide that reveals pure aluminum will be followed directly by re-oxidation of the surface. The oxide layer can be formed without dissolved oxygen in the solution, by splitting water molecules. [2]

2.1.1. INFLUENCE OF THE ENVIRONMENT

Aluminium is passive in an environment with near neutral pH and has good anti-corrosion qualities. Yet as the pH changes the stability of the oxide changes. The oxide is thermodynamically unstable both in acidic and alkaline environments for all potentials higher than -1.7 V vs. SHE according to the Pourbaix diagram in Figure 1. The diagram is presenting the equilibrium potential between the metal and its different oxidized species plotted as a function of pH. The Pourbaix diagram is constructed by utilising the Nernst equation (1) where T is the absolute temperature, R the universal gas constant, F the Faraday constant and z the number of electrons in the reaction. The concentration of the products of all the species that appears on the reduced and oxidized side is notated as [reduced] and [oxidized] respectively.

$$E_e = E° - \frac{RT}{zF} \ln \frac{[reduced]}{[oxidised]} \tag{1}$$

One of the most vital factors for corrosion of aluminium regarding the environment the aluminium is the pH. As the environment gets acidic or alkaline will the corrosion rate of aluminium increase, see Figure 2.
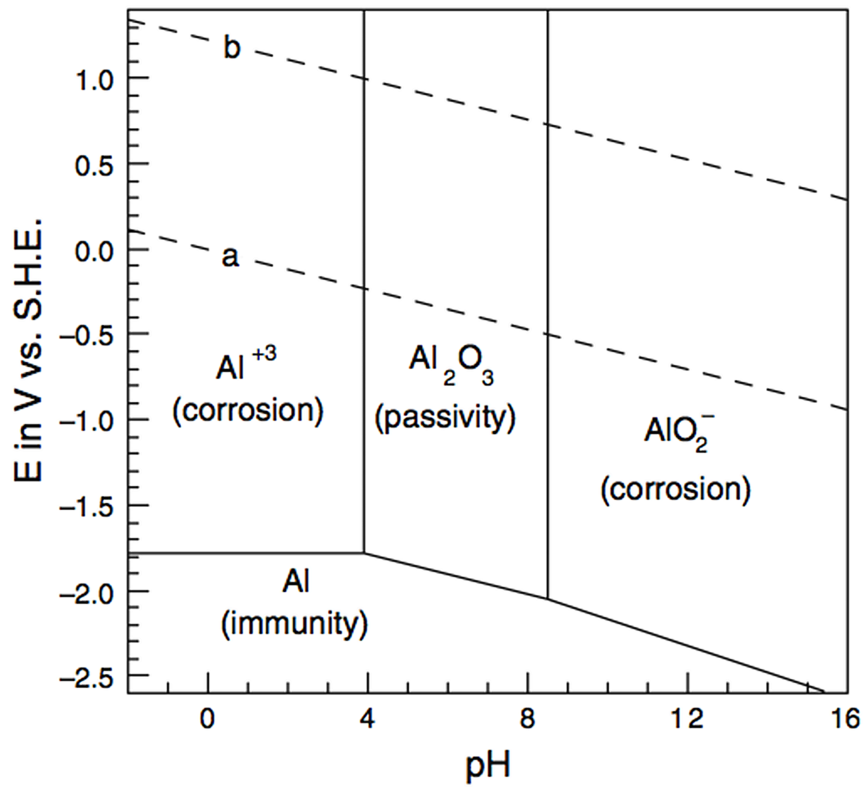
FIGURE 1 POURBAIX DIAGRAM FOR PURE ALUMINIUM AT 25°C [3]
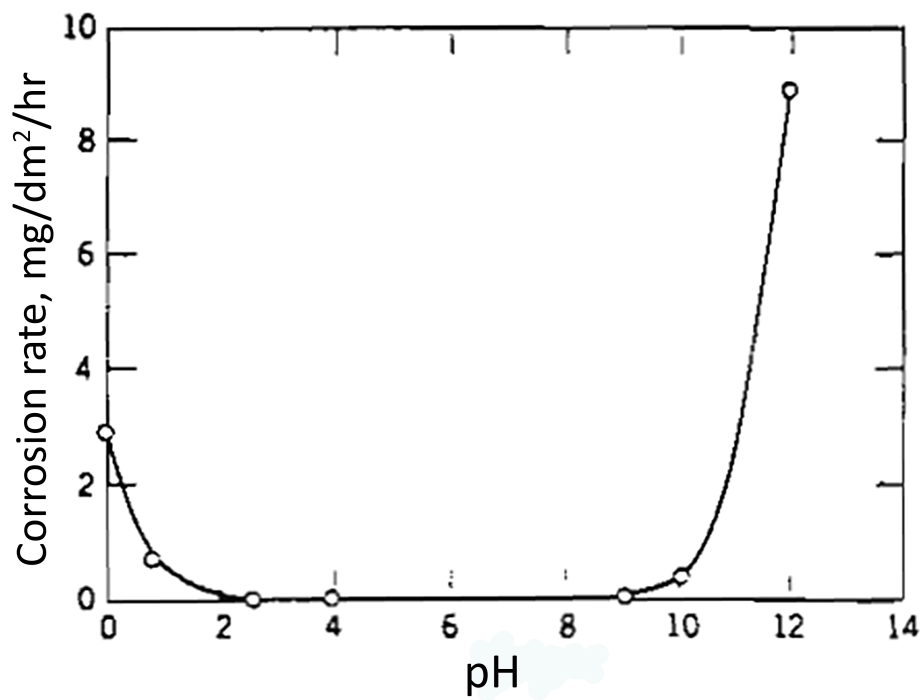
FIGURE 2 CORROSION RATE FOR ALUMINIUM AS A FUNCTION OF PH [4]

4

Temperature is another factor that is important to consider regarding the environment. Most metals will experience an increased corrosion rate as the temperature increases. The reason for this is increased speed of the corrosion reactions, as the temperature gets higher. For aluminium this phenomenon exists, hence there is an additional effect that can increase the corrosion rate.

When doing corrosion design there is a great importance in considering all the factors of the environment. Many of the factors will influence each other, and contribute to a harsher service environment for the selected solution. Such an effect can be seen on the pH range which aluminium oxide is stable within. The range is dependent on the temperature of the electrolyte. There is not done a lot of research on this topic, however some studies have been carried out.

Theoretically it has been proven that the pH range where aluminium oxide is stable within will get narrower as the temperature increases. [4] See the Pourbaix diagrams in Figure 3. From the diagrams can the highest pH were the oxide still is stable be found for the temperatures 25°C, 60° C, 100°C and 200°C. At 60°C is the maximum pH for aluminium to still be passive around 8.5 and at 100°C it is around 7,0. By doing an interpolation can the maximum pH value at 80°C be assumed to under 8,0. This means that from a theoretical point of view aluminium oxide should be unstable in seawater at 80°C, even under cathodic protection. Regarding aluminium under cathodic protection should it be noted that aluminium is not immune but passive, according to the Pourbaix diagram in Figure 1.

Compered with observations from experiments, the theory does not fit well to what is observed. At a temperature of 80°C there is observed an increase of the corrosion rate, but at higher pH values than 8.0 as the theory suggest. The increased corrosion rate is not mainly from the effect of a narrower pH range where the aluminium oxide is stable, but from the know fact that the corrosion reactions will speed up at higher temperatures.[5] Fischer et al. monitored the corrosion potential and current demand at different temperatures as a function of time in a study of flame sprayed aluminium coatings in seawater.[6] The results showed that there was an increased corrosion rate the first ten days in seawater with a temperature of 60°C compered to seawater with 20°C. Afterwards the current demand was about the same for 60°C and 20°C indicating that the corrosion rate nearly is the same for the two temperatures over a long time period.
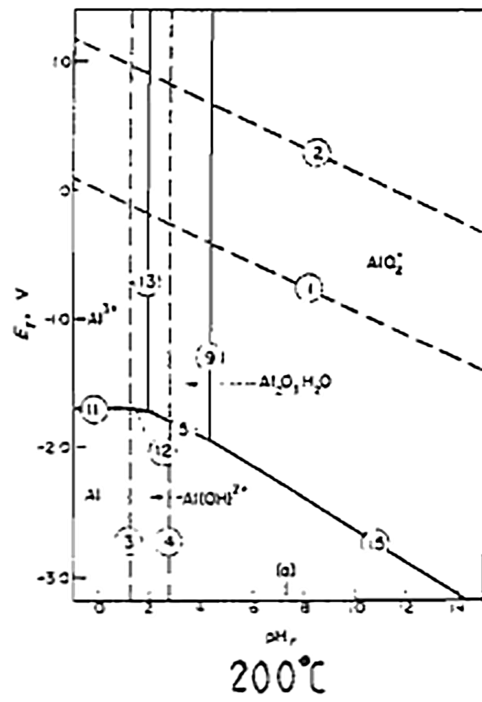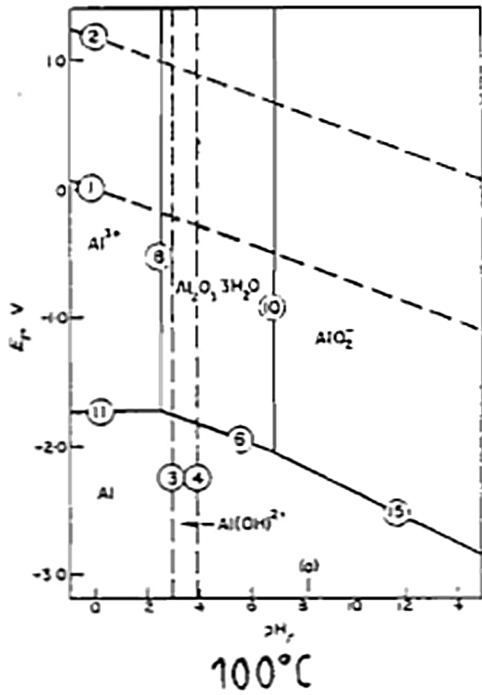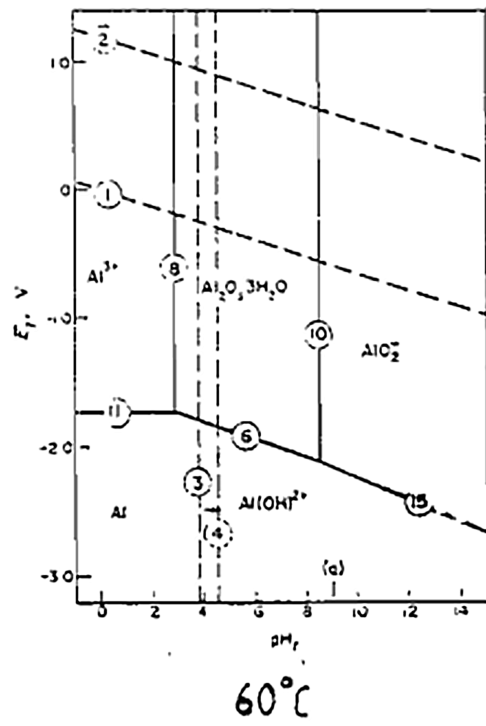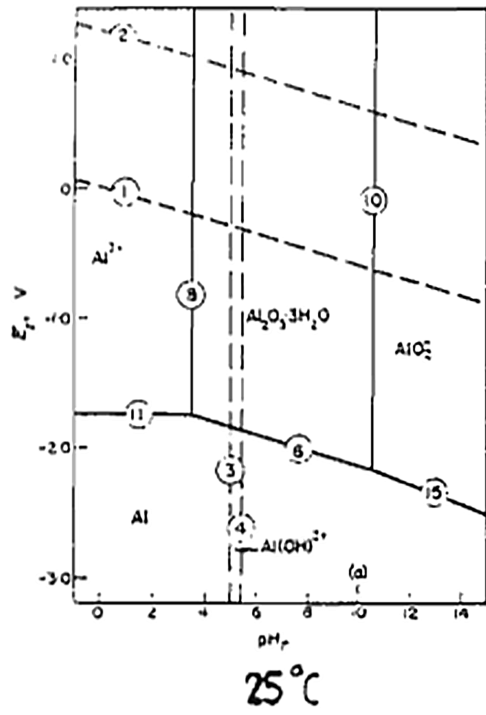
FIGURE 3 PORBAIX DIAGRAM FOR ALUMINIUM AT HIGH TEMPERATURES[7]

2.1.2.   INFLUENCE OF CATHODIC PROTECTION

To protect metals against corrosion is cathodic protection a much-used method. Cathodic protection is lowering the potential of the metal, and ensures that the metal to be protected serves as cathode. Cathodic protection in general will be discussed further later on. In this chapter will there be focus on what the influence of cathodic protection is and what to be aware of when utilizing such systems.

When lowering the potential of a metal is there an increase of the pH at the surface.[5] On a cathode in water will there be either reduction of water or oxygen, or a combination according to the equations (2) and (3). Both reactions results in produced hydroxide ions. This will lead to an increase in pH near the surface of the cathode, in this case the aluminum surface.

$$O_2 + 2H_2O + 4e^- = 4OH^- \tag{2}$$

$$2H_2O + 2e^- = H_2 + 2OH^- \tag{3}$$

The pH will decrease when the distance to the surface gets larger. Figure 4 is an illustration of how the pH at the metal surface can be determined by the production rate of hydroxide and the removal of hydroxide trough diffusion and convection, or both.
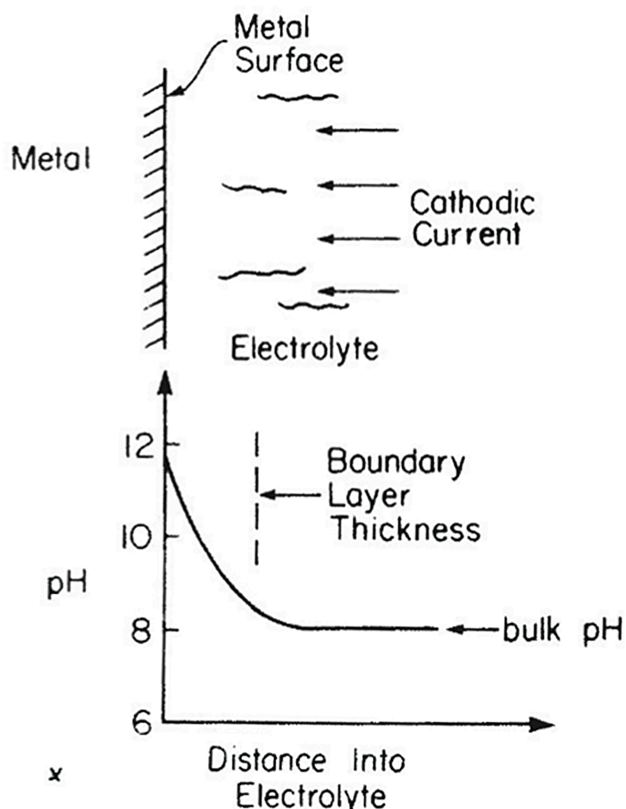
FIGURE 4 PH AS FUNCTION OF DISTANCE[8]

The equation presented under (4) can be utilized for doing a quantitative estimate of the pH at the surface of the catholically protected metal.[5] The basis for equation lays in that it is assumed that the pH would drop linearly with the distance from the metal within the diffusion layer.[5] The diffusion layer is described in Figure 4 as the distance from the metal to the dashed line marked Boundary Layer Thickness.

$$i = zFD\frac{C-C_o}{d}$$ (4)

Where:

i = cathodic current density

z = charge of the species

F = Faradays constant

D = diffusion constant for OH^-

C_0 = OH^- concentration in the bulk

C = OH^- concentration at the surface

d = diffusion layer thickness

The diffusion layer thickness is a function of the water flow rate and the geometry of the specimen. With this equation Gartland estimated that current densities of 1 µA/cm^2 and 10 µA/cm^2 gave a pH at the surface of 9.0 and 10.0 respectively.

2.1.3. INFLUENCE OF ALLOYING ELEMENTS

Even tough pure aluminum has good corrosion properties it is necessary to introduce alloying elements in order to utilize aluminum as a material in many applications. Alloying elements is a small amount of one or a few metals that are mixed into the aluminum molt in order to improve the mechanical properties of aluminum. By adding different metals it is possible to create a wide range of different aluminum alloys for many different applications. When these particles are present in the aluminum alloy they are named intermetallic particles. The most common metals to use as alloying elements are silicon, manganese, copper and zinc.[9] From a corrosion property point of view are the alloying elements very important because they have influence on the corrosion properties of aluminum. The various metals have different effect according to if the metal added is more noble or not than aluminum. Metals that is nobler than aluminum acts as a cathode, and creates a site for reduction reactions on the aluminum matrix. The reactions are triggered because of the potential different between the aluminum matrix and intermetallic particle. For Iron the potential difference is in the order of 1,2V[10]. Copper and Iron are considered to be the most

important alloying elements regarding the corrosion properties of the alloy, as the potential difference are huge for these metals. [11, 12]

If a large intermetallic particle is located at the aluminum surface such that the aluminum oxide don`t cover the particle, intermetallic corrosion can occur. In that case must the intermetallic particle be of a metal with a higher potential than aluminum. When these criteria are fulfilled, a site for reduction reactions is created and a corrosion process can start. While the corrosion process develops there is a change in the local environment around the intermetallic particle. The reduction process leads to a local alkalization around the particle. As described earlier will a pH change have an effect on the protecting aluminum oxide. The elevated pH leads to a depassivation of the aluminum oxide and an increased corrosion rate of the aluminum matrix around the intermetallic particle. In some cases can the intermetallic corrosion lead to pitting corrosion around the intermetallic particle, as a result of the crevices created around the particle.

The corrosion around the particle will proceed until all of the aluminum around the intermetallic particle is corroded away and the particle will fall out, or that the particle is covered in calcareous deposits and corrosion products. See Figure 5. Calcareous deposits are formed when there is a pH increase on the metal surface in addition to that calcium and magnesium is present in the water. Then calcium carbonate CaCO3, magnesium carbonate $MgCO_3$ and $Mg(OH)_2$ is formed. [8] These solid products are named calcareous deposits, they decreases the corrosion rate of the metal by acting as a barrier against oxygen diffusion. [13] This thesis does not have a specific focus on calcareous deposits so no more documentation will be presented.

In the case of that the intermetallic particle unfastens from the aluminum matrix but remains on the surface without being in contact with the matrix. By been separated from the surface from a layer of corrosion products, which has been formed between the particle and the surface. Then the particle will be electrically isolated from the matrix by the corrosion products. The corrosion products will fill the crevice between the particle and the matrix, and lead to a repassivation of the aluminum surface.

9
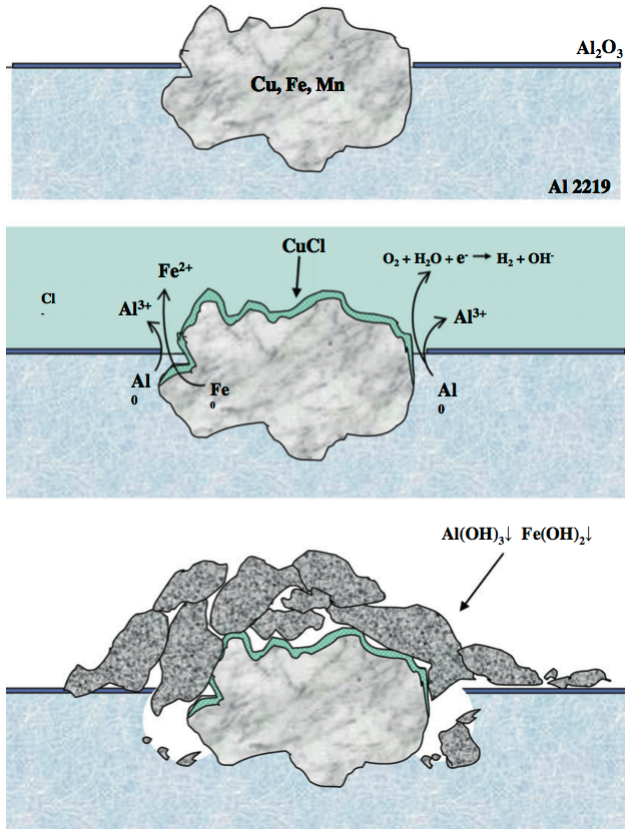
FIGURE 5 INTERMETALLIC CORROSION [14]

In combination with cathodic protection, the described mechanism of alkalization around the cathodic sites will occur with an even faster rate. The repassivation of the surface described above will lead to a quickly protection of the surface, because if the aluminum oxide that forms on the surface. Gundersen and Nisancioglu described this effect and the resulting current time curve in [15]. The corrosion and depassivation around the intermetallic particles will lead to an increase of the current density in the start of the exposure. After a certain period of time, will the current density reach a maximum value and from there decrease exponentially. The decrease is a result of the repassivation of the surface. This mechanism will lead to a current-time curve as shown in Figure 6.
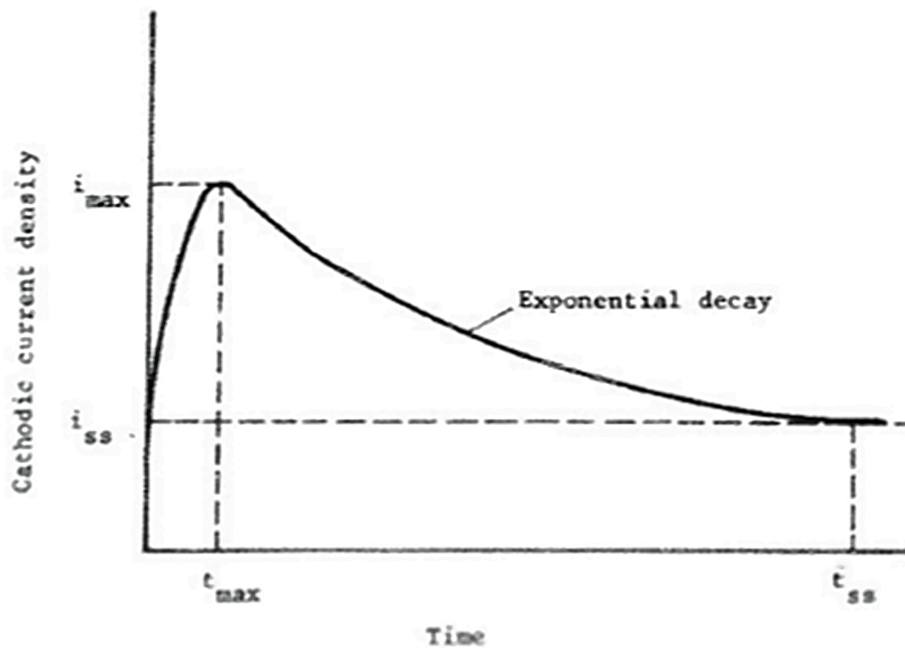
FIGURE 6 CURRENT -TIME CURVE FOR AN ALUMINUM ALLOY UNDER CATHODIC PROTECTION[15]

Metals those are less noble than aluminum will have a positive effect on the corrosion properties. The choice of alloying elements with a lower standard electrode potential than aluminum is small compared to alloying elements with a higher standard electrode potential. Today magnesium is the only commercially used as an alloying element that is less noble than aluminum. [2] Aluminum can hold up to 15% magnesium, but because of the β-phase Mg_5Al_8 that precipitates on the grain boundaries and leads to grain boundary corrosion and brittleness is the amount often less. Normal content is between 1-5% magnesium in solid solution.[16] A great advantage with these alloys is that they are resistant to pitting corrosion in chloride containing environment. In addition magnesium has a lower potential than aluminum, hence it will act as a sacrificial anode and corrode faster than aluminum. As the magnesium corrodes away a surface of purer aluminum will be produced.[2] Because of this aluminum-magnesium is a very popular alloy to utilize in marine environments in addition to silicon containing aluminum alloys. Silicone is resistant to acids and salts. By adding silicone particles to the aluminum alloy the corrosion resistance in alkaline environments increases.[10]

2.2. Corrosion Protection

A metal can be protected from corrosion in many ways. One way is to prevent the corrosive environment to reach the surface of the metal by applying a coating. It is also a common method to supplement the coating protection with anodic and cathodic protection methods as sacrificial anodes and impressed current. Anodic and cathodic protection is both methods that have influence on the potential of the protected metal, but they utilize two different principles.

An example of cathodic protection is impressed current, which is used to lower the potential of the metal being protected to the immune area. The current is obtained from a direct current source that is connected between the metal that shall be protected and an auxiliary anode. Electrons will flow to the metal from the corroding auxiliary anode and protect the metal. Sacrificial anodes can also provide cathodic protection. For them to work must the metal to be protected and the sacrificial anode be immersed in the same electrolyte and be electrically connected. The sacrificial anode has a lower electrode potential than the protected metal. This means that the sacrificial anode will corrode, and as it corrodes it will prevent an anode reaction on the metal by supplying electrodes to the metal.

Protection of aluminum is obtained by being secure of maintaining passivity of the surface. Anodic protection is increasing the potential of the protected metal to the passive area. This type of protection in normally not used for aluminum. The potential needed to keep aluminum in a passive state is very low see Figure 1.

A second common way to do corrosion protection is as mentioned to apply a coating. The choice of coatings for corrosion protection is large, both organic and metallic coatings are used. Both coatings prevent the corrosive media to reach the metal, the difference of the two is that the metal coating is conductive and the organic not. This thesis will not deal with organic coatings so no more attention to that topic will be given. The next chapter will deal with metallic coatings in form of thermal sprayed coatings.

2.3. THERMAL SPRAYED COATING

By utilizing thermal spraying, a selection of metals can be applied as a metal coating. These types of coatings provide a functional surface to protect or modify the behavior of the substrate material. [17] Over the years there has been developed many techniques for applying thermal sprayed coatings, giving a range of techniques to utilize. The simplest technique is the flame spray technique, which was invented by Dr. Max Ulrich Schoop in 1910. [18] Newer techniques as vacuum plasma spraying, high velocity oxy-fuel and high frequency pulse detonation are all methods that are improving the qualities of the coating compered to flame spray, making thermal sprayed coatings even better. Common for all the techniques is the basic principle of thermal spraying. The coating material is fed into a spraying gun, in form of powder or wire, heated to a molten or semi molten state and accelerated towards the substrate by air or gas. The material hits the substrate in form of splats and cools down and coagulates. Each splat bonds to the previous, forming a lamellar structure. Inclusions, oxides and pores will be present in the structure. The bonding mechanism is primarily mechanical, not metallurgical.

Thermal sprayed coatings (TSC) are a very applicable alternative for corrosion protection. It has many advantages because of its unique technique of spraying metal onto the surface. The coating is easy to apply, especially on long structures as pipes, inexpensive to operate compared to welding, and the coating can be sprayed on site with special transportable equipment. Compered to organic coatings is the lifetime the of TSC superior. According to Fischer, a 200 μm thermal sprayed aluminum (TSA) coating can achieve a lifetime over 30 years in the splash zone of an oil and gas platform. [19]

As mentioned thermal sprayed coatings are a good choice for corrosion protection, and the range of use is large with a wide choice of metals to spray. Thermal sprayed coatings are used in many applications. Examples are: repair and salvage, biomedical coating, wear resistance, thermal barrier coatings and corrosion protection. [18] There are three different groups of corrosion resistant thermal sprayed coatings: neutral-, anodic- and cathodic- coatings. Common for all three groups is that they all act as a barrier against the corrosive environment. The coating prevents the corrosive environment to reach the surface of the protected substrate.

The difference between the three groups is in how they act electrochemically against the substrate that shall be protected. Neutral coatings will not decelerate nor accelerate the corrosion rate in case of damage in the coating, but provides superb corrosion protection in most environment as they act as a barrier. These coatings are often very thick and dense to create a good barrier coating. Chromium oxide ceramics and alumina are examples of materials that are used to form a neutral thermal sprayed coating.[17]

Anodic coatings are anodic relative to the substrate and will act as a sacrificial anode in case of a coating damage. They provide hence excellent corrosion protection. The material for these coatings is very often zinc or aluminum. For protecting steel on offshore structures with metal coatings, aluminum has been found to be most effective, according to[17].

A cathodic coating is cathodic relative to the substrate and will accelerate the corrosions rate of the substrate if a coating damage occurs. These coating does provide good corrosion protection, but it is important to be aware of the consequence of a coating damage. In order to decrease the chance for coating damages that penetrates the coating should these coatings be dense, thick and sealed.

2.4. THERMAL SPRAYED ALUMINIUM

Aluminium is used extensively in corrosion protection applications. The reason for this is as mentioned earlier that aluminium has a low electrode potential compered to the majority of metals. Hence aluminium will act as an anode against carbon steel, which are very much utilized in offshore oil and gas industry.

2.4.1. CORROSION PROTECTION WITH THERMAL SPRAYED ALUMINIUM

Thermal sprayed aluminum has become an efficient and durable solution in corrosion protection of steel structures. And have over many years been utilized by the oil and gas industry.

The porosity of the TSA coating is a vital factor for the corrosion protection properties for the TSA coating as the primary function of the coating is to act as a barrier. To control the porosity it is important to choose the best application technique and parameters. The porosity varies between the different techniques and with the grain size and shape of the feedstock powder. [20, 21]

When used as corrosion protection a sealer should be applied to the TSA coating according to NORSOK standard M-501. The sealer fills the metal pores and shall be applied until the absorption is complete. There shall not be a measurable overlay of sealer on the TSA after application. [22]

The sealer enhances the barrier properties of the TSA significantly by creating an overall denser coating. In comparison to an overcoat that has as function to create a protective layer over the TSA, will a sealer penetrate the TSA and fill the pores inside the TSA. An overcoat adds thickness to the coating system whereas a sealer shall not add any significant thickness. To ensure that the sealer penetrates the TSA and seals of the pores, the sealer shall have a low viscosity. For maximum performance of the sealed TSA the sealer should be applied as soon as possible after application of the TSA. The reason for this is to ensure a smooth surface texture and no contamination on the surface. [5]

There have been done many studies on the effect of sealing TSA. According to [23] the application of a sealer has a significant effect. Over a period of 11 months, in exposure at free corrosion rate or lower it has been proven that there is an 30 to 50% drop in the corrosion rate of the TSA on specimens with sealer compered to unsealed TSA.

Regarding the performance of different sealer types, Fisher et al have done a study to test the performance of vinyl-based sealers and silicone-based sealers. These two types of sealers were the two most common used types of sealers at the time of study. The test was carried out on the risers and tether of a tension leg platform in offshore service. The risers were partially cathodic protected as the upper half were catholically polarized by the cathodic protection of the hull. The tethers received no cathodic protection as they were insulated from the hull. The silicone based sealer showed best performance with no degradation of the coating after 4 years, the vinyl based sealer suffered from blistering on the tethers after the same time period. Aside from the blistering all of the TSA samples were in good shape and there was no corrosion damage on the substrate.

Regarding corrosion of TSA is it commonly expected that TSA corrode in the same way as aluminum. With respect to current densities is it therefore assumed that TSA will experience a development as described in Figure 6, with a rapid increase of the cathodic current in the beginning of exposure followed by a exponentially decrease. The corrosion rate is assumed to follow the same pattern, as long as aluminum is not polarized over the pitting potential of aluminum (about-850 mV vs. Ag/AgCl).[5]

2.4.2. COMBINATION OF TSA AND CATHODIC PROTECTION

TSA is an excellent corrosion protection coating, and can serve as a stand-alone protection system. For additional redundancy and performance cathodic protection is often used in combination with TSA in subsea applications. This creates challenges regarding the design of the corrosion protection system. To prevent a design failure and then failure of the corrosion protection system guidelines have been developed for the design process of the corrosion protection system.

The system that is closest to TSA in combination with cathodic protection, in terms of protection technique, is steel protected with an organic coating in combination with cathodic protection. Unfortunately are these to system too different, so the guidelines for the organic coating based system are not applicable for the TSA based system. The main reasons for this is that TSA will have its own design values in terms of current densities and potential because it is a metal coating. The design values for the TSA will come in addition to the

values required by the bare steel at coating holidays, which for a organic based coating system will act alone. In addition is the durability of the TSA coating much better than for an organic coating so the breakdown figures of the two systems will be entirely different. In the recent years have some organization made guidelines for TSA under cathodic protection. A summary regarding current density on TSA and temperature compensation are given in Table 1

TABLE 1 CURRENT DENSITY AND TEMPRATURE COMPENSATION FROM STANDARDS

Standard	Current density on TSA	Temperature compensation
NORSOK M-503 [24]	10 mA/m^2	0.2 mA/m^2/°C over 25°C
DNV-RP-B401[25]	10 mA/m^2	0.2 mA/m^2/°C over 25°C

There have been performed several experiments regarding this topic by Gartland and Eggen. [5, 23] In [5] suggests Gartland a protection potential for TSA of -900 mV vs. Ag/AgCl, and a design current density of 11mA/m^2 at temperatures from 5 to 15°C and 17mA/m^2 at 40°C. Above temperatures of 10°C should the protection potential be lowered with 1mV for each degree. As pointed out in [5] these values are conservative, the design basis for the current density determined from the experiments done in the mentioned study is at 2mA/m^2. Yet, the values suggested by Gartland and Eggen is in good accordance with the guidelines given in the standards. However, the current density is found to increase with the water depth, based on experiments done at 600m water depth carried out by Veritec is the design value for the current density requirements for a water depth at 300m set to 11mA/m^2.

All the previous mentioned design values are for a TSA coating with zero damage. The amount of bare steel is very important for the corrosion protection system and must be taken into account. To expose steel from under the TSA, a failure has to be introduced to the coating. Such damages are often created under installation and handling of the structure, hence will the coating start it`s service life with a failure. Since this is known to the industry has a design guideline been made for this concern, however only for organic coatings. The guideline suggests 1 % initial coating failure. Since the TSA coating is tougher than organic coatings, is it a good estimate is to say that the initial coating failure for TSA coatings is no more than for organic coatings.

As the time goes by will the amount of exposed steel depend on the durability of the coating. Since TSA is more robust than an organic coating is it estimated a coating failure of only 10% at the end of the lifetime for the TSA coating according to [5]. In [23] has Gartland and Eggen reported a current demand of 1

mA/m^2 for a sprayed AlMg coating with sealer after 1 month until the end of the experiment 16 months after start. This shows that the durability of the TSA coating in an environment with low risk of mechanical impact is excellent.

2.4.3.   HIGH TEMPERATURE

The experience with the use of TSA at higher temperatures (50-120 °C) is not extensive. There are mainly three documented experiences to consider: Risers on the Heidrun platform, risers on the Hutton platform and risers on the Jolliet platform. Reports from the Hutton platform and Jolliet platform has shown good performance of the TSA coating with silicone sealer. [19] The temperatures in these applications were around 60°C and higher. Because of the lack of experience at that time, Frankel et al initiated a project to establish how TSA coating with and without sealer would behave at high temperatures (70 to 100°C) in the splash zone. The samples were freely exposed and with potentiostatic polarization. None of the samples that were sealed and exposed to 70 to 100 °C showed any blistering or coating deterioration after 14 months of exposure. [19] The results were thereby promising for high temperature service with TSA.

The experience from Heidrun is totally different, after less than four years did three export risers suffer from serious coating damage in the splash zone. The coating suffered from blistering. Because of the similarity between the application at Heidrun and in this project, a summary of the investigation project follows.

To determine the reason for the early failure a joint industry project was started. The objective of the project was to do a evaluation of TSA used on hot risers, review the application history of the TSA applied on Heidrun, simulate service conditions and do relevant testing for the Heidrun riser failures. The test revealed three trends:[26]

- The tendency to develop blistering increases with increasing TSA coating thickness.
- The tendency to blistering decreases with increasing the number of silicon sealer coats applied.
- The tendency to blistering increases for the heated samples (Internal pipe temperature 50°C) compared to the ambient samples.

The results regarding the increasing tendency to develop blistering as the TSA coating thickness increases is summarized here: [26]

- All samples with 100 μm coating thickness showed no blistering for any combination of sealer or heating.
- Samples with 200 μm coating thickness showed minor blistering on the heated samples with sealer and high density blistering on the heated samples without sealer. The non-heated samples show good performance.
- A series with 450 μm coating thickness was also tested, the results was more or less the same as the samples with 200 μm coating thickness for the non-heated samples. All the heated samples showed even more blistering that for the samples with 200 μm coating thickness.

These results are more or less in accordance with what Fischer et al. found in [19]. The TSA coating thickness in the experiments done by Fischer et al. was 200 μm and the sealer was applied in two layers.

The reason for the TSA coating failure on Heidrun was suggested to be a combination of wrong thickness of the applied TSA coating, wrong sealer application and intense thermal cycling. The measured coating thickness varied from 210 to 500 μm, while the design specification was 200 μm. The testing done showed that TSA with a coating thickness of 450 μm are very susceptible to blistering when exposed at high temperatures. The replicas of the TSA coating with sealer that was applied on the Heidrun risers showed only minor blistering in the laboratory test. This implies that the sealer was not applied inn accordance with the design requirements for the Heidrun risers.

The thermal cycling was intense on the Heidrun export risers. The reason for more intense thermal cycling on the export risers is that in difference to the production risers was not the export risers equipped with packer fluid. Packer fluid is fluid that remains in the tubing-casing annulus over the packer when a well is completed. The packer fluid acts as a thermal barrier and hinders a large temperature increase on the outside of the riser. Thus, the temperature on the outside on the export risers would be much higher than the temperature on the outside of the production risers. This means that the thermal cycling was more intense on the export risers. Assumed that the outside of the export risers reaches a temperature near the 50°C of the fluid inside, there will be a cyclic temperature swing of about 40 °C. This temperature swing will happen within seconds when a wave strikes the riser.[26]The combination of the to thick TSA coating, which has higher internal stresses than a thinner coating, and the stress from the thermal cycling was therefore believed to be the reason for the coating failure on the exports risers at Heidrun.

What is important to remember is that the splash zone was the most aggressive zone because of the thermal cycling. And that the sealer would be much easier

washed out than in the submerged zone. This implies that TSA under high temperature service is more robust in the submerged zone than in the splash zone.

The failures of the TSA coatings at Heidrun are reflecting the importance of having good control of the application techniques and the application process in general. Such that the installed products coating is in accordance with what's is specified for the product.

2.4.4.   THERMAL SPRAYED ALUMINUM IN SALINE SEABED MUD

The knowledge about how TSA preforms as corrosion protection when covered with saline seabed mud is not great. A concern is that the mud will trap the hydroxide produced by the cathode reaction, and lead to a pH increase near the TSA surface. If this occurs could the result be that the aluminum no longer is passive, but active. This will result in rapid corrosion of the aluminum and a coating failure. Regarding what Gartland stated in [5], which implies that the diffusion of hydroxide is dependent on the flow rate at the surface of aluminum strengthens this concern.

Not much work has been carried out on the performance of TSA in mud, and it is seldom mentioned in standards. S.L. Wolfson started a project to determine the performance of TSA in saline sea mud. TSA coated steel was exposed to saline mud and seawater in 4 and 12 months. The samples consisted of coatings with 0, 3, 5 and 10% coating holiday. Wolfson reported promising results, all of the samples afforded protection to the exposed steel areas, except the 10% coting holiday sample in the 12-month test. He did also state that for no or a very small coating holiday it appears that significantly longer service lives can be obtained in saline mud environments compered to seawater environments. The overall current demand for steel in mud environments was found to be lower than in seawater. The conclusion of the study was that a 254 µm thick TSA coating can provide cathodic protection to approximately 5% steel coating holiday with a lifetime of more than 25 years.[27]

2.4.5.   TSA DUPLEX COATING

TSA gives excellent corrosion protection. Attempts have been done to increase this performance even more by applying a thick organic coating on top of the TSA. The idea is that the coating system will get an increased lifetime, 20 years lifetime for the organic coating and 30 years lifetime for the TSA gives an total lifetime of 50 years. Unfortunately this is not the case, the reality is rather different. The Sleipner Raiser Platform was designed with a lifetime of 50 years. Hence the lifetime for the corrosion protection system was also designed to protect the structure in 50 years. To achieve such relative high lifetime a TSA duplex system was chosen. The platform was put in service in 1992. Already after eight years in service, in year 2000, was it reported that the coating system

suffered from serious degradation. Blisters had developed on the overcoat that was applied to the TSA. The industry wondered what the cause was, and research projects were started.

The reason was found to relate with the galvanic nature of aluminum and steel. Knudsen, Røssland and Rogne suggests a degradation mechanism in [28]: When TSA duplex coatings are coupled galvanic to bare steel, galvanic corrosion of the TSA starts. Cathodic oxygen reduction takes place at the bare steel, while anodic corrosion of the aluminum takes place under the organic coating. In chloride containing environments, like marine atmosphere, will chloride ions migrate under the organic coating to maintain the charge balance. Aluminum chloride is formed. However, aluminum chloride is highly unstable in presence of water, and hydrolyses to form hydrochloric acid. An acidic electrolyte is formed under the organic coating and cathodic hydrogen evolution will start. Aluminum oxide is unstable in acidic electrolytes and the TSA will not be protected by it`s oxide. Hence, aluminum will corrode actively.[28]

2.5.   IRIDIUM ELECTRODES.

Knowledge about the pH is always a deciding factor regarding corrosion protection and how to design the best corrosion protecting system. In order to get knowledge about the pH, pH measurements are needed. Utilizing a glass electrode has traditionally done such measurements. The limitations of the glass electrode are many: manufacturing methods, operation in alkaline or HF solutions and its brittle nature. These restrictions have enhanced the effort the search after alternative pH sensors.

It has been done a lot of research on electrodes made from iridium over the past years see Table 2. Compered to other metal oxides electrodes and glass electrodes have the Iridium electrodes many advantages. They can serve at high temperatures, high pressures and in aggressive environments. Yet a good stability over a wide pH range is maintained. The response of the electrodes had proven to be fast even in non-aqueous solutions. [29] There have been problems with the performance of iridium oxide electrodes regarding potential drift. This makes the pH measurement inaccurate and weakens the iridium electrodes advantage over other electrodes. The problem is found to relate to the fabrication methods and conditions as they have a big influence on the characteristics of the Iridium electrode.

TABLE 2 OVERVIEW OF RESEARCH DONE ON INRIDIUM ELECTRODES FROM[29]

Table I. Performance of iridium oxide-based pH electrodes made by different methods.

Method	Electrode	Sensitivity (mV/pH)	$E^{\circ\prime}$ (mV, *vs.* SHE)[a]	Total drift[b] (mV)	Authors/Year
Electrochemical growth (AIROF)	IrO_2/Ir Wire (0.5 mm diam)	77.7 (25°C)	1240	-[c]	Burke *et al.*[10] 1984
	IrO_2/Ir wire (0.6 mm diam)	71.2	714	-	Kinoshita, E. *et al.*[11] 1986
	IrO_2/Ir wire (1 mm diam)	75 (25°C)	925	35	Hitchman *et al.*[12] 1988
	IrO_2/Ir wire (0.15 mm diam)	62-74 (21°C)	734-1066	15-130	Olthuis *et al.*[13] 1990
	IrO_x/Ir wire (0.5 mm diam) (deeper purple tint)	74-78	909-934	-	Song *et al.*[14] 1998
Electrodeposition	(Pd-Ir)O_x/glassy carbon (3 mm diam)	62 (pH <6, 21°C) 83 (pH >6)	910 ± 6 (pH < 6) 1020 ± 20 (pH >6)	-	Jaworski *et al.*[15] 1992
	IrO_x/glassy carbon (1.5 mm diam) (bright blue)	63-82	940-1120	25	Baur *et al.*[16] 1998
	Nafion/IrO_2/Pt/Kaption film	61-65(22°C)	~810	-	Marzouk *et al.*[17] 1998
Sputtered coating (SIROF)	IrO_x/Ta or stainless steel (1500Å, dark blue)	59.5 (19°C) 68.8 (80°C)	1042	220	Katsube *et al.*[18] 1982
	IrOx /alumina (1500-7500Å)	55-60(22°C)	995 ± 35	200	Tarlov *et al.*[20] 1990
	IrO_2/sapphire sheet (1000Å, dark blue)	59 (25°C)	880	10	Kato *et al.*[21] 1991
	IrO_x/alumina or silicon wafer	54-49 (22°C)	1016	150-200	Kreider *et al.*[23] 1995
Thermal method	IrO_2/Ir wire (blue black)	62.8 (4°C)	930 ± 5	-	Papeschi *et al.*[25] 1976
	IrO_2/Ti ($IrCl_3$ decomposition)	59	950	-	Ardizzone *et al.*[26] 1981
	IrO_2/Ti ($IrCl_3$ decomposition)	59 (25°C)	982 (fresh)	80	Kinoshita, K. *et al.*[27] 1984
	IrO_x/Ir wire (blue-black)	59 (25°C) 59 (25°C)	1000-1172 870 (after pretreatment)	200 10	Hitchman *et al.*[28] 1992
	Nafion/IrO_2/Ti $IrCl_3$ decomposition, blue-black)	51-56 (22°C)	850-856	-	Kinlen *et al.*[30] 1994
Printing method	IrO_2/inert matrix	59.8 (25°C)	~900	-	Fog *et al.*[7] 1984
Current method (Thermal method)	IrO_x/Ir wire (deep black)	58.9 (22°C)	923	0.2	Current paper

[a] Some data is calculated by assuming that Ag/AgCl reference electrode potential is 197 mV *vs.* SHE.
[b] Different papers report drift data over varying periods of time.
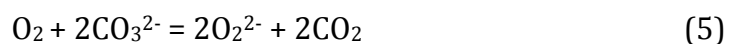[c] (-) indicates that the data is unclear.

Wang et al. have developed a new method based on carbonate melt oxidation of iridium that don`t suffers form the potential drifts problems. The new approach shows very promising pH sensing results with good potential stability over a wide pH range and an ideal Nernstian pH response. [29] Wang et al reported in [29] that the OCP drift over a period of two days only was in the order of 0.2 mV. The cause of the drift was suggested to be temperature changes in the room as the test was performed at room temperature. The long-term stability of one electrode is presented in [30]. In a 2.5 years long period ten calibration curves was measured for the same electrode, the variation is presented in Table 3

TABLE 3 LONG-TERM STABILITY FOR ONE IRIDIUM ELECTRODE FROM [30]

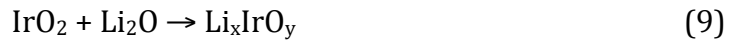| Average variation in E°′[mV]	Average variation in the slope [mV/pH]
E°′= 705.4±2.5	S= -58.4±0.2

The electrodes are made by placing the iridium wires in the bottom of an alumina crucible lined with gold foil and cover the wires with lithium carbonate. Lining with gold foil is necessary for preventing a meta-aluminate reaction that can possibly occur between lithium and alumina forming lithium alumina.[31] The oxidation are done at 870°C for 5 h under air atmosphere. Cooling down to room temperature is done at a rate of 1°C/min before dissolving the solid carbonate with diluted HCl and the oxidized iridium wires are picked out and rinsed properly with deionised water so dried at 120°C overnight. In order to make the electrode the oxide is scraped of for about 1 mm at one end of the oxidized wire, so that the bare iridium wire is exposed to make electrical contact. Then a wire is connected, and the whole oxidized wire is coated with a adhesive except for a small area for minimize the pH sensing area[29]

Iridium is a very noble metal and belongs to the platinum metal group. The resistance to aggressive chemicals is remarkable, and at room temperature it is unaffected by all acids including aqua regia. To produce a stable iridium oxide by conventional chemical method is very difficult, however the carbonate melt oxidation method have been proved to be an effective way to oxidize Iridium. [30, 31]Following is the proposed oxidation mechanism described by Wang et.al.[29] The O_2 from the air dissolves into the melt and reacts with carbonate ions to form O_2^{2-} (5), at high temperatures O_2^{2-} acts as a strong oxidant, this leads to oxidation of the metal and reduction of O_2^{2-} to O^{2-} (6). The O^{2-} reacts with the CO_2 from (5) and forms CO_3^{2-} (7). The overall reaction is showed in (8).

$$O_2 + 2CO_3^{2-} = 2O_2^{2-} + 2CO_2 \tag{5}$$

$$Ir + 2O_2^{2-} = IrO_2 + 2O^{2-} \tag{6}$$

$$O^{2-} + CO_2 = CO_3^{2-} \tag{7}$$

$$Ir + O_2 = IrO_2 \tag{8}$$

Lithium is also present in the oxidation process. The presence of Lithium leads to a lithiation of the iridium oxide (10). As the oxide is exposed to an aqueous solution, hydration occurs (11). The reported composition of the oxide is $Li_{0.86}IrO_{2.34}(OH)_{0.76} \cdot 0.39H_2O$.

$$IrO_2 + Li_2O \rightarrow Li_xIrO_y \tag{9}$$

$$Li_xIrO_y + nH_2O \rightarrow Li_xIrO_y \cdot nH_2O \text{ or } Li_xIrO_p(OH)_q \cdot mH_2O \tag{10}$$

How the pH sensing mechanism is for the iridium oxide electrode has not been confirmed, but Wang et.al. suggested that the oxygen intercalation mechanism could describe the pH sensing. This theory suggests that the iridium oxide forms a higher and lower valence couple (12), equilibrium potential is then pH dependent with a Nernstian slope -59,16/pH at 25°C (13).

$$Li_xIrO_y + 2\delta H^+ + 2\delta e^- \leftrightarrow Li_xIrO_{y-\delta} + \delta H_2O \tag{11}$$
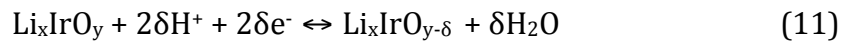
$$E = E° + \frac{2,303RT}{2\delta F}\log\frac{[Li_xIrO_y] \cdot [H^+]^{2\delta}}{[Li_xIrO_{y-\delta}]} = E° + \frac{2,303RT}{2\delta F}\log\frac{[Li_xIrO_y]}{[Li_xIrO_{y-\delta}]} + \frac{2,303RT}{F}\log[H^+] =$$
$$E°' - \frac{2,303RT}{F}pH = E°' - 59.16pH \tag{12}$$

The thickness of the iridium oxide is about 25-30 μm [29, 31] the oxide is growing outwards perpendicular to the surface of the iridium wire with a columnar structure. The grains are well defined and have a size from one to several microns. [29] Santi reported a two-layered structure with a dense inner layer and porous outer layers see Figure 7. [31]
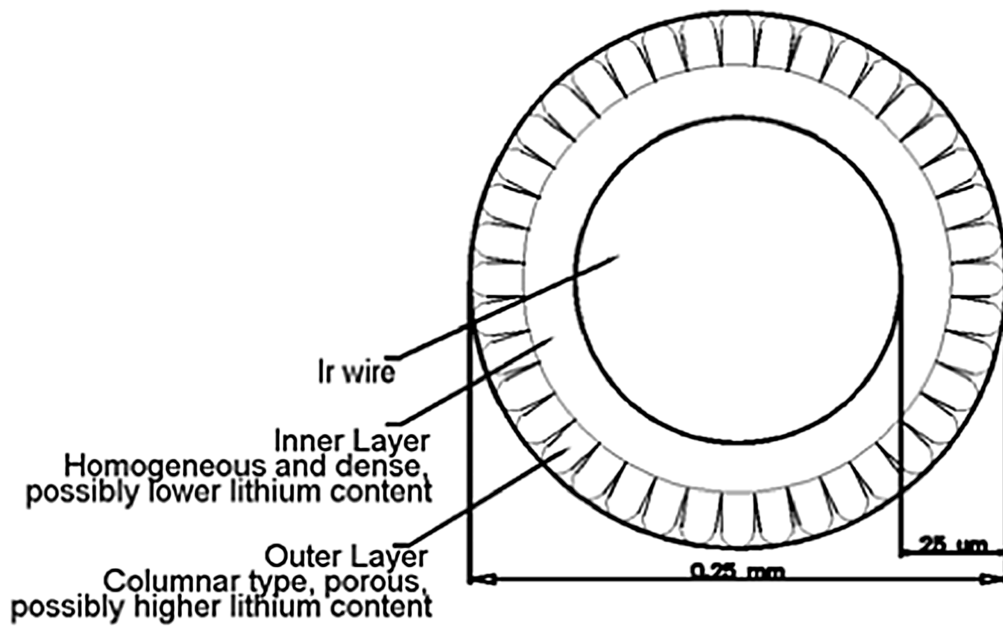
FIGURE 7 SCHEMATIC STRUCTURE OF THE IRODIUM OXIDE ELECTRODE[31]

Measuring the potential between a reference electrode and the iridium electrode in the electrolyte is the method for doing the pH measuring. Note that a measurement of the pH response of the electrode is needed in advance. The pH response is measured by measuring the potential between the iridium electrode and the reference electrode at different pH, in that way can a pH-response curve be obtained. Such curve can be seen in Figure 8. From such measurement can a calibration curve be made, an example is presented in Figure 9.
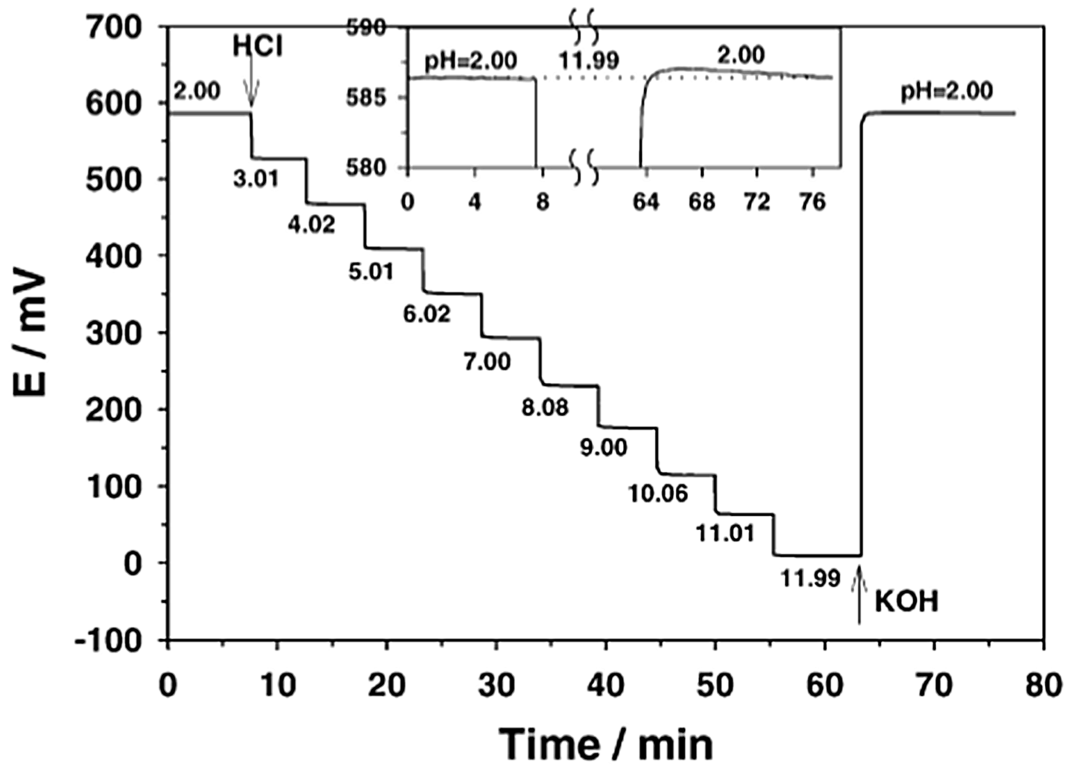
FIGURE 8 PH RESPONSE CURVE FOR IRIDIUM ELECTRODES FROM [30]
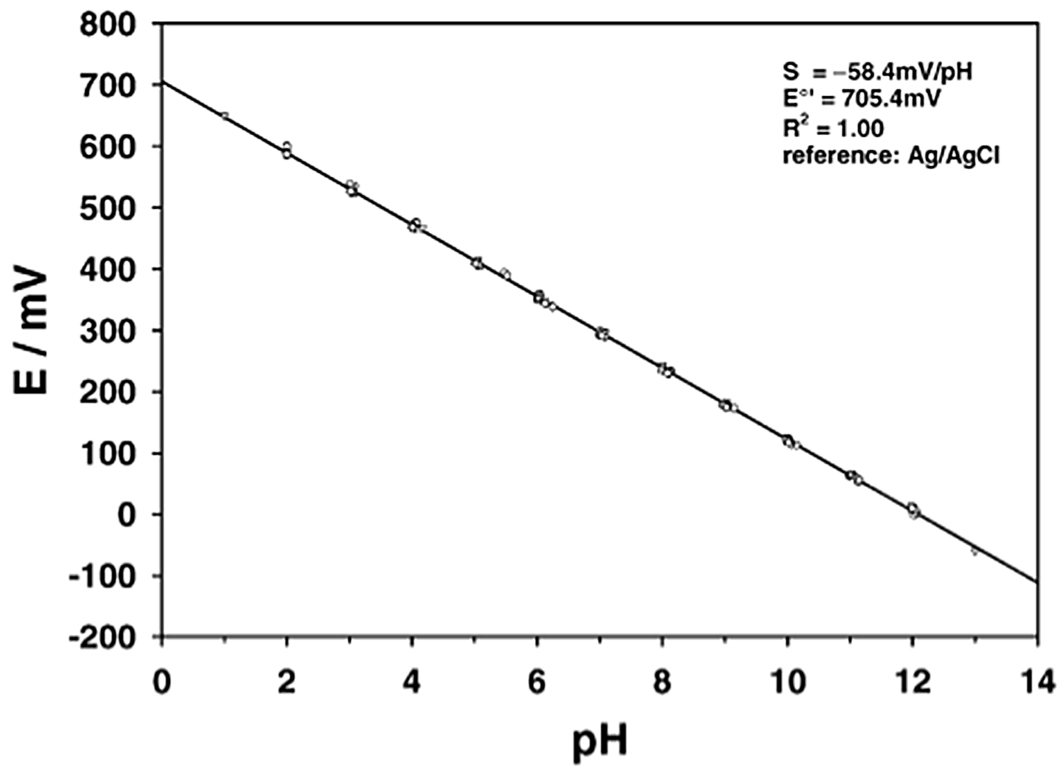
FIGURE 9 EXAMPLE ON CALIBRATION CURVE FOR IRIDIUM OXIDE ELECTRODE [30]

3. EXPERIMENTAL WORK

3.1. pH ELECTRODES

The electrodes used for pH sensing were made from an Iridium wire with 99,8% purity, 0,5mm diameter and 5 cm length obtained from VWR international. The wire was cut in 7 pieces of 7 mm each.

3.1.1. FABRICATION THE IRIDIUM ELECTRODES

After the cutting the manufacturing procedure of the electrodes started on, see Table 4 for working procedure. The wires were first ultrasonic cleaned with 6M HCl, and rinsed in deionized water. To oxidize the wires they were placed in a platinum crucible without lid covered with Li_2CO_3. See Figure 10. A platinum crucible was used, instead of gold foiling a alumina crucible that was described in [32]. The crucible was placed in a furnace and heated at 870°C for 5 hours in ambient atmosphere.
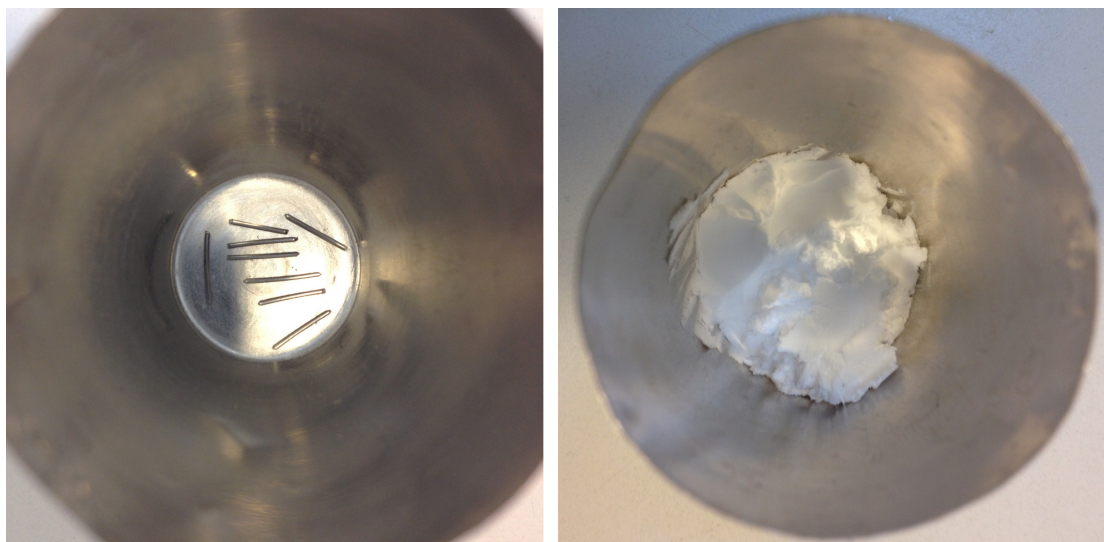

FIGURE 10 IRIDIUM WIRES BEFORE OXIDATION

After oxidation was the crucible cooled down to room temperature at a speed about 1°C/min. To separate the oxidised wires from the solid carbonate diluted HCl was used. The wires was picked out from the crucible and rinsed with deionized water several times to remove any attached soluble components. To dry the oxidized wires they were placed in an oven at 120°C over night. The procedure is also presented in Table 4.

Finally to make an electrode the oxidation product was scraped of a small area at one end of the oxidized wire (see Figure 11), and a copper wire was attached. In order minimize the sensing area of the electrode; the electrode was covered with blue silicone (Loctite 5926) except 2-3 mm at the end. The blue silicone served

also as adhesive to mount the electrode in a plastic pipe, see Figure 12. A schematic drawing of the assembly is presented in Figure 13. The plastic pipe served as housing for the sensor, and provided some protection in addition to make it possible to stick the sensor through the mud down to the TSA surface.
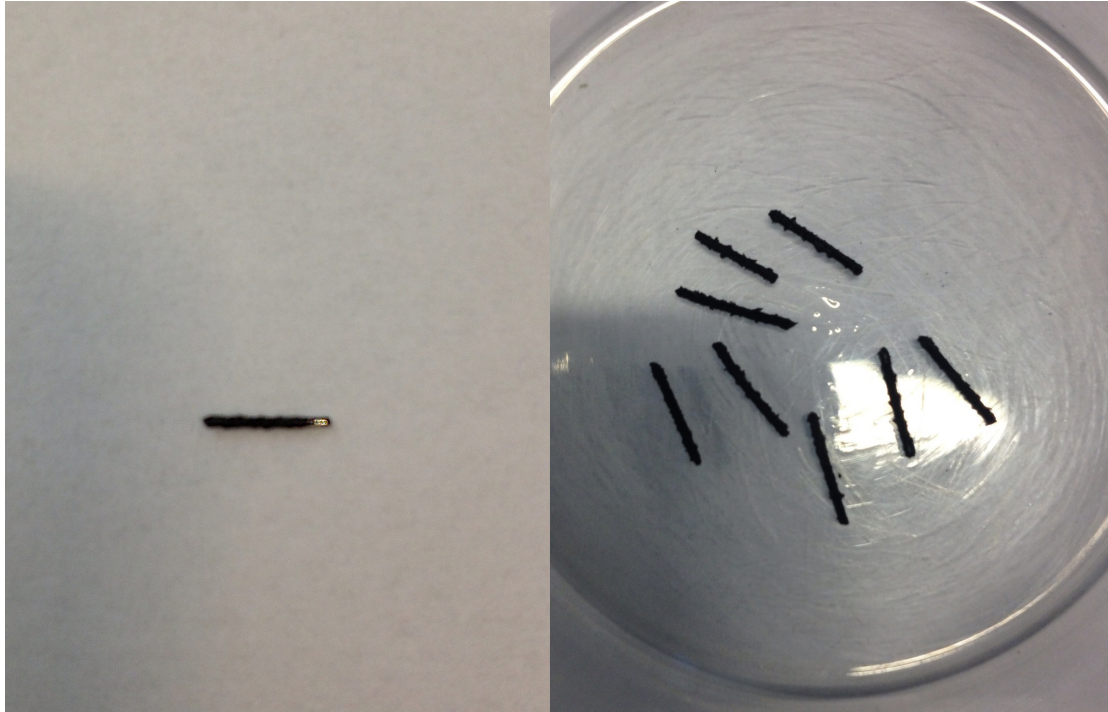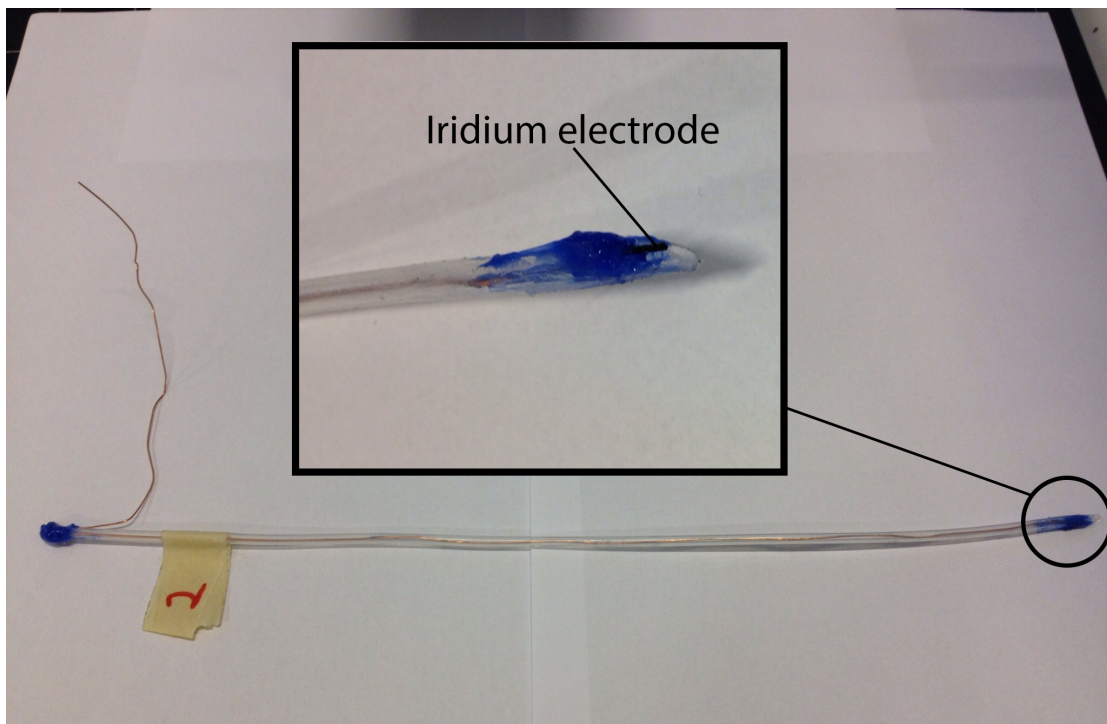

FIGURE 11 IRIDIUM WIRES AFTER OXIDATION

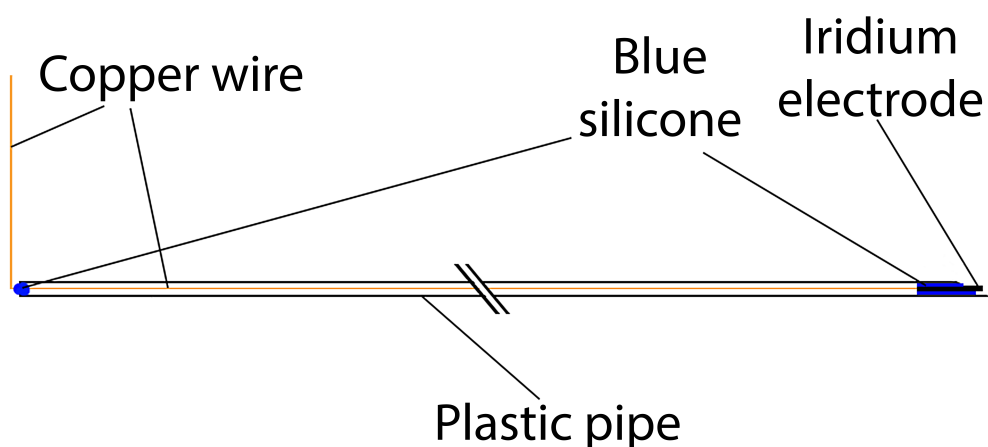

FIGURE 12 IRIDUM ELECTRODES READY FOR USE

FIGURE 13 SCHEMATIC DRAWING OF THE IR ELECTRODE ASSEMBLY

TABLE 4 PROCEDURE FOR FABRICATION OF IR ELECTRODES

Process	Time	Temperature	Chemicals
Ultrasonic cleaning	2 min	Room temperature	6M HCl
Rinsing	-	Room temperature	Deionized water
Oxidation	5h	870°C	Li_2CO_3
Cooling to room temperature	Ca.14,5 h	1°C/min	-
Dissolving	-	-	0.001M HCl
Rinsing	-	Room temperature	Deionized water
Drying	12 h	120°C	-

3.1.2. MEASUREMENT OF THE PH RESPONSE

To map the pH response of the electrodes the open circuit potential (OCP) was measured as a function of pH against an Ag/AgCl reference electrode with a multimeter. The method used was to immerse the electrode into four different pH buffer solutions with exact known pH. The buffer solutions were obtained from Radiometer Analytical; the pH values used are presented in Table 5. The results were then used to make a calibration curve for each of the seven electrodes. The results were compared to the calibration curve from the literature. The curve from the literature can be seen in Figure 9. The test setup is presented in Figure 14

3.1.3. MEASUREMENT OF THE STABILITY

Stability is crucial for pH measurements; hence a stability test of the fabricated sensors was needed. One of the electrodes was placed in a pH 7.000 buffer solution for two weeks. The OCP between the iridium oxide electrode and an Ag/AgCl reference electrode was logged every hour throughout the two weeks. An Agilent 34970A data acquisition connected to a pc was used to log the potential. The test setup is presented in Figure 14

TABLE 5 PH VALUES USED FOR CALIBRATION OF THE IRIDIUM ELECTRODES

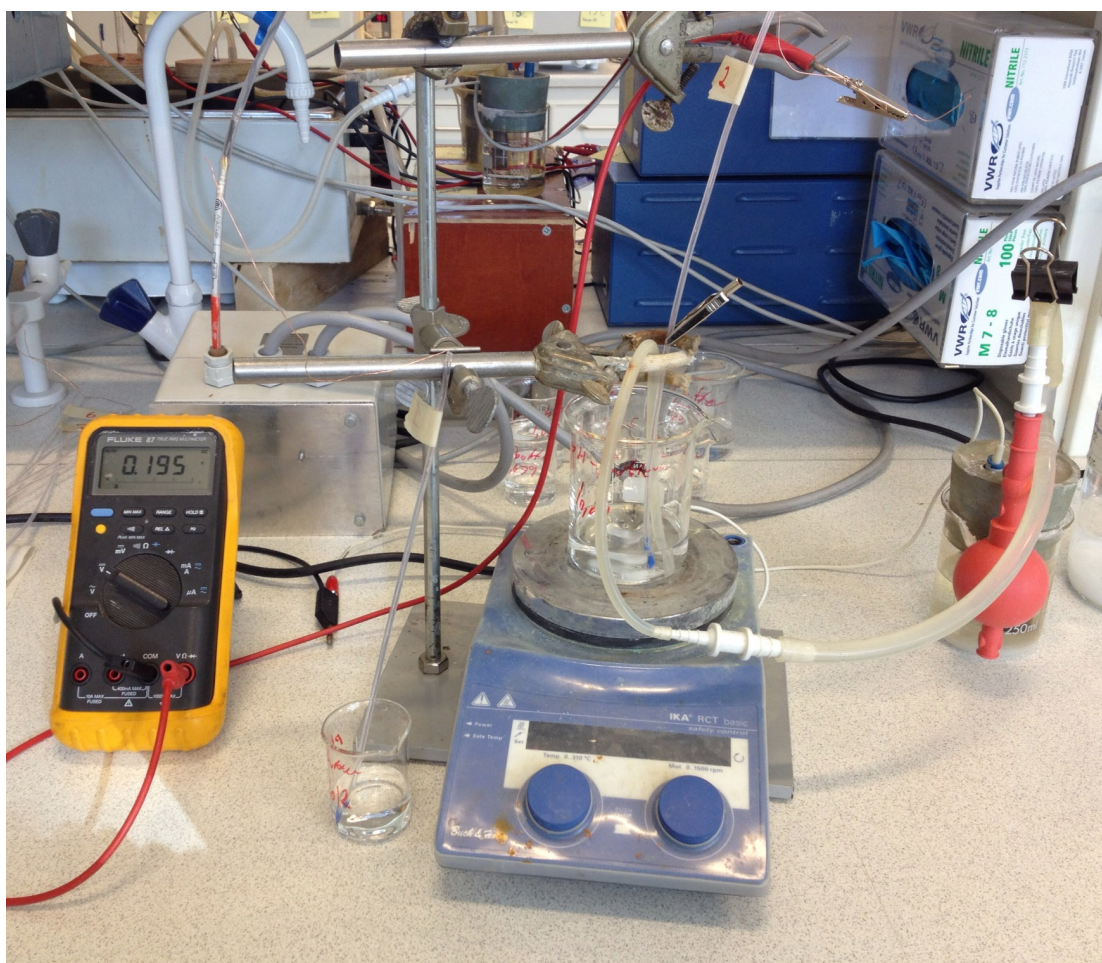| pH values used for calibration of the iridium electrodes			
Value 1 [pH]	Value 2 [pH]	Value 3 [pH]	Value 4 [pH]
1.679	4.005	7.000	10.012

FIGURE 14 TEST SETUP FOR STABILITY AND PH RESPONSE MEASUREMENTS

3.2. Mud for the Corrosion Test

To ensure that the mud should represent seabed mud as good as possible the mud used for the experiment was collected from the Trondheims fjord at low tide. To match the conductivity of the mud used in previously performed experiments at SINTEF Materials and Chemistry synthetic seawater and salt was added to the mud. 2,3 L of synthetic seawater and 70 g of NaCl was added to about 10 L of mud. The change in conductivity was from 12,7 mS/cm to 26,9 mS/cm, the target value was 27,4 mS/cm.

3.3. Sample Plates for the Corrosion Test

Five sample plates were made from a steel panel with thickness 5mm that were coated with thermal sprayed aluminum. The steel grade used is carbon steel with similar properties as X65 steel pipes. Before coating the steel was grit blasted with Garnet to a roughness 70 – 110 μm and a Sa 2,5 quality. Coating was applied the same day. Keafer Energy AS performed the thermal spraying. The TSA type used was arc sprayed aluminum ISO Grade 1100 with 250 μm thicknesses. After coating the steel panel was cut to 150mm x 150mm test plates.

3.4. SEALER AND SEALER APPLICATION

A sealer was applied to all the samples in the corrosion test. The sealer is based on pure silicone with small aluminum flakes. The brand name of the sealer is Intertherm 179 produced by International. The sealer was diluted with Xylene. The ratio was 60% Xylene and 40% Intertherm 179. Application was done with a brush, ensuring that the whole surface was wetted with the sealer. One layer was applied. To ensure that the aluminum flakes did not sink to the bottom of the diluted sealer a magnetic stirrer was used to have continues motion in the sealer before application. The Aluminum flakes would have fallen to the bottom of the vessel and hence not be applied to the TSA surface if stirring of the sealer not was done under application. After application the samples were left to air dry for 24 hours. Note that in the product data sheet for Intertherm 179 it is stated that for optimum performance as a sealer the application should be within 8 hours after application of the TSA. This was not possible to do in this case because the thermal spraying and sealer application was done at two different locations.

3.5. MAKING OF THE MUD CELL

In order to isolate a certain area of the TSA surface that should be exposed to the saline mud a plastic pipe was mounted on the surface. The inner diameter of pipe was 71 mm and height 150 mm. The pipe was glued to the TSA surface with blue silicon of the make Loctite 5926 see Figure 15.1. The cell was left to dry for 24 hours before anything more was done with the cell. When the silicone had dried the cell was filled with mud until the mud was about 10 cm deep. See Figure 15.2. Because of the consistence of the mud it was difficult to make sure that there was no air trapped inside or between the mud and the TSA surface. To be sure of that there was no air trapped the samples were placed in an autoclave and a small vacuum (0,2 bar) was applied for about three minutes. After this the rest of the plastic pipe was filled with synthetic seawater. The synthetic seawater hinders the mud to dry out. A lid was put on the cell to limit evaporation.
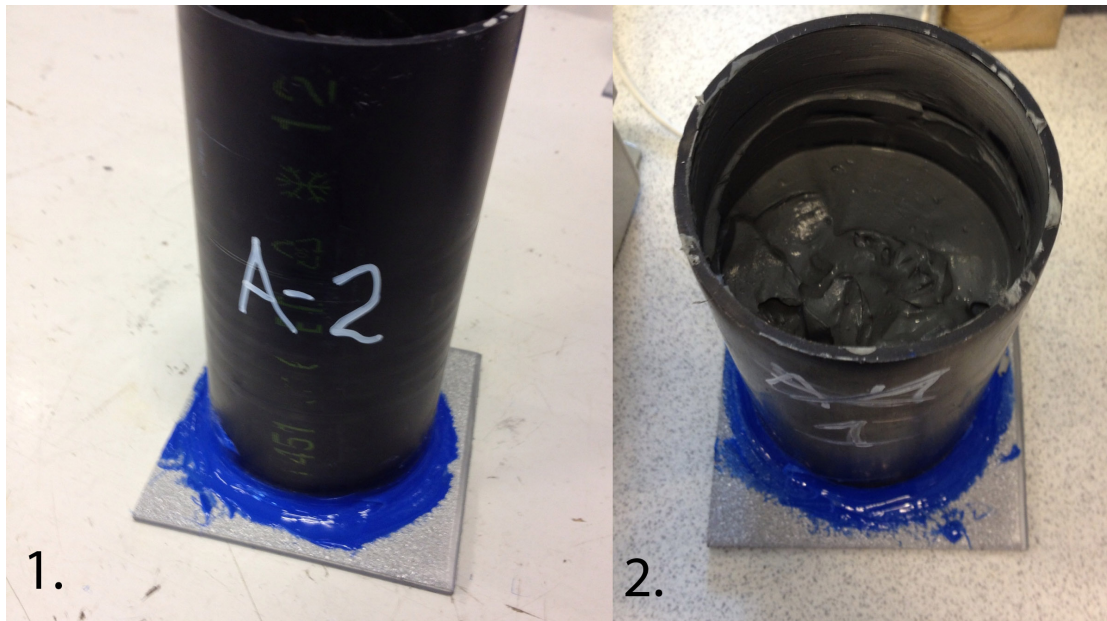
FIGURE 15 1. GLUING OF THE MUD CELL 2. MUD

3.6.   TEST SETUP FOR THE CORROSION TEST

The samples were put in an isolated steel vessel containing oil such that the steel plate was covered in oil. The oil was heated to 95°C by a hotplate placed under the steel vessel, see Figure 16 for a schematic illustration of the test setup. The hotplate was connected to a thermostat that measured the temperature in the oil and thereby controlled the hot plate. The iridium oxide electrodes, for pH measurements, were pushed through the mud until the plastic pipe hit the TSA surface. A temperature sensor was placed on the inside off a glass pipe, which were sealed in the lower end to not expose the metal temperature sensor to the electrolyte. The samples were polarized by an individual potentiostat using a platinum wire as counter electrode, the TSA coated steel plate as working electrode and a Ag/AgCl reference electrode. See Table 6 for test matrix and for Figure 17 test setup.

TABLE 6 TEST MATRIX FOR THE CORROSION TEST

Sample	Temperature [°C]	Potential [mV]	Sealer
1	95	-1150	Yes
2	95	-1000	Yes
3	95	-850	Yes
4	95	-1050	Yes
5	95	-1100	Yes

During the experiment these measurements were logged:

- pH near the TSA surface by placing the iridium pH-electrode near the mud-TSA interface. Logged by measuring the potential between the Iridium oxide electrode and the reference electrode
- Temperature near the TSA surface with a thermo element. Logged by using a thermometer that converts the temperature to a potential.
- Cathodic current over a 10 ohm resistor on the counter electrode.
- Potential between the reference electrode and the working electrode (steel plate)
- Linear polarization resistance (LPR) to measurements the corrosion rate.

Measurements and logging frequency during the test period is presented in Table 7. To log the values was an Agilent 34970A data acquisition used in combination with a personal computer. And the program KorrosjonsLogger© was used for collecting the data.

TABLE 7 MEASURMENT AND LOGGING FREQUENCY

Parameter	Frequency	Location	Description
Potential	Every hour	TSA surface	Used by the potentiostat
Cathodic current	Every hour	Counter electrode	Potential drop over 10 ohm resistor
pH in mud	Every hour	TSA surface	Iridium electrode
Temperature	Every hour	TSA surface	Glass tube with a thermo element inside
LPR	Weekly	TSA	Corrosion rate
Tafel curve	At termination	TSA	

The samples were watched after every day (week days), and the evaporated synthetic seawater was replaced with synthetic seawater as the level in the mud cell decreased.

The test period was 5 weeks. Tafel curves were obtained at termination of the experiment. After termination of the experiment was the mud cell detached from the steel plate and the TSA surface and the cross section of the samples was examined.
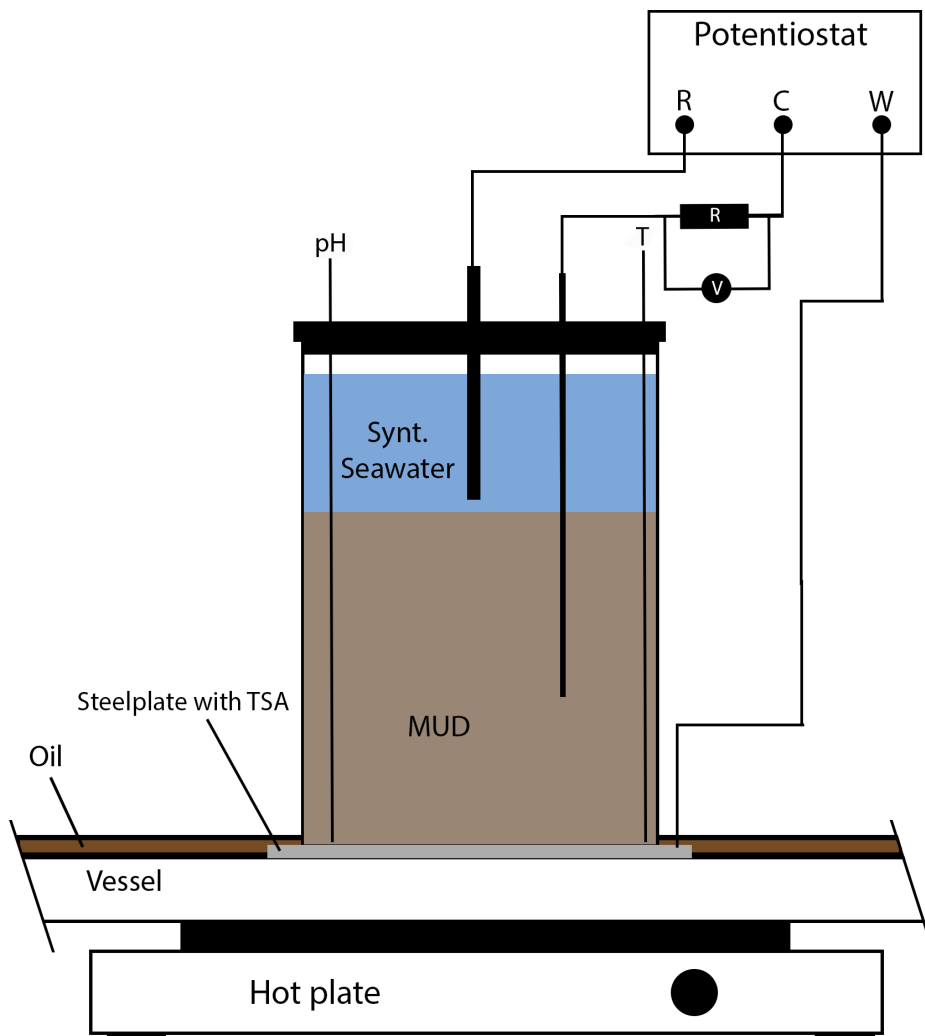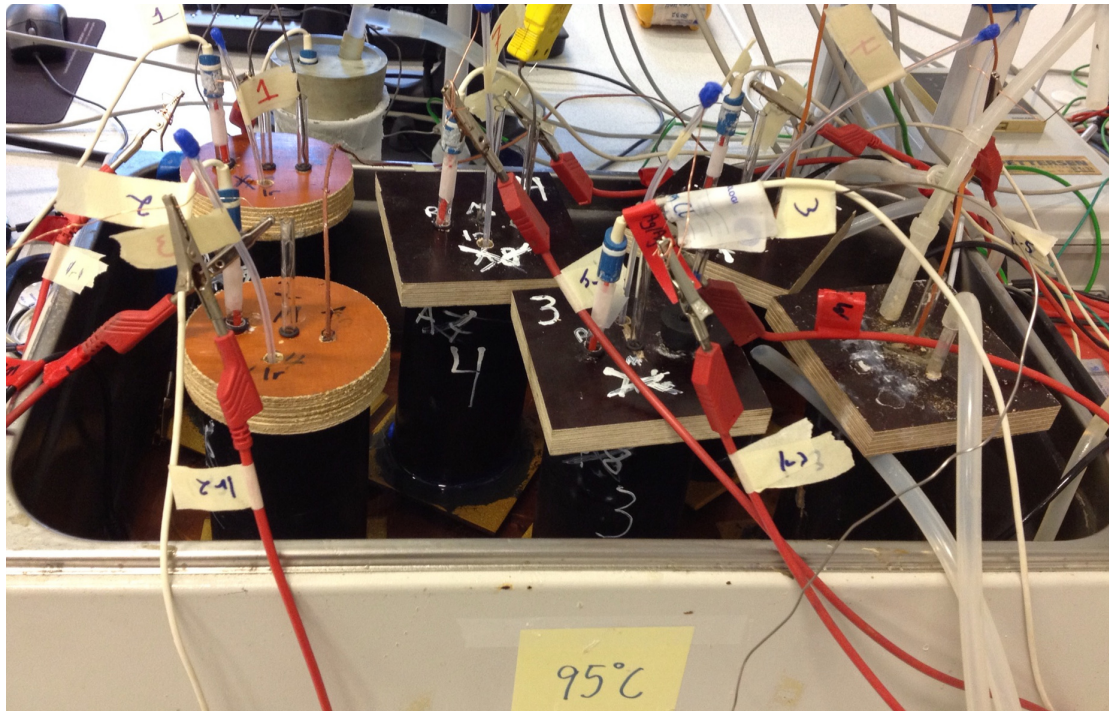
FIGURE 16 TEST SET-UP SCHEMATIC

FIGURE 17 TEST SETUP

3.7. RECORDING OF TAFEL CURVES

At test termination recording of Tafel curves was performed. The recording of
Tafel curves was only done at the end of the test period, as the process can be
destructive for the samples. To record the Tafel curves was a Gamry Reference
600 potentiostat controlled by a personal computer used. The Tafel curves were
recorded by using the Gamry Framework computer program. See Figure 18 for
explanation of the setup. The settings for the recordings are presented in Table 8.

TABLE 8 SETTINGS FOR THE TAFEL CURVE RECORDINGS

Start potential [mV]	End potential [mV]	Scan rate [mV/s]	Sample period [s]
-300	300	0,5	1

3.8. CATHODIC TAFEL CURVES FOR UNSEALED TSA

Tafel curves for TSA in mud at temperature of ambient room temperature, 60°C
and at 95 °C was made in order to investigate the effect of temperature and
sealer application to the TSA.

3.8.1. SAMPLES FOR RECORDING TAFEL CURVES OF UNSEALED TSA
Three plates with same specifications and TSA application as in the corrosion
test was used. The only difference with the plates in this test and the corrosion

test was that the plates used in this test were not sealed. The mud cells were made in the same way.

3.8.2. RECORDING OF CATHODIC TAFEL CURVES ON UNSEALED SAMPLES

The recording was done in room temperature, at 60°C and at 95°C. The samples that required heating were placed in a vessel containing oil at 60°C and 95°C i.e. the same method as used in the corrosion test. To record the Tafel curves a reference and a counter electrode were put into the cell. A clamp with a wire was mounted to the steel plate in order to connect the steel plate as working electrode. These three electrodes were coupled to a Gamry Reference 600 potentiostat that was controlled by a personal computer. See Figure 18. The Tafel curves were recorded by using the Gamry Framework computer program. See Table 9 for the settings for the record.

TABLE 9 SETTINGS FOR THE CATHODIC TAFEL CURVE RECORDINGS FOR THE UNSEALED SAMPLES

Start potential [mV]	End potential [mV]	Scan rate [mV/s]	Sample period [s]
0 (OCP)	-300	0,5	1
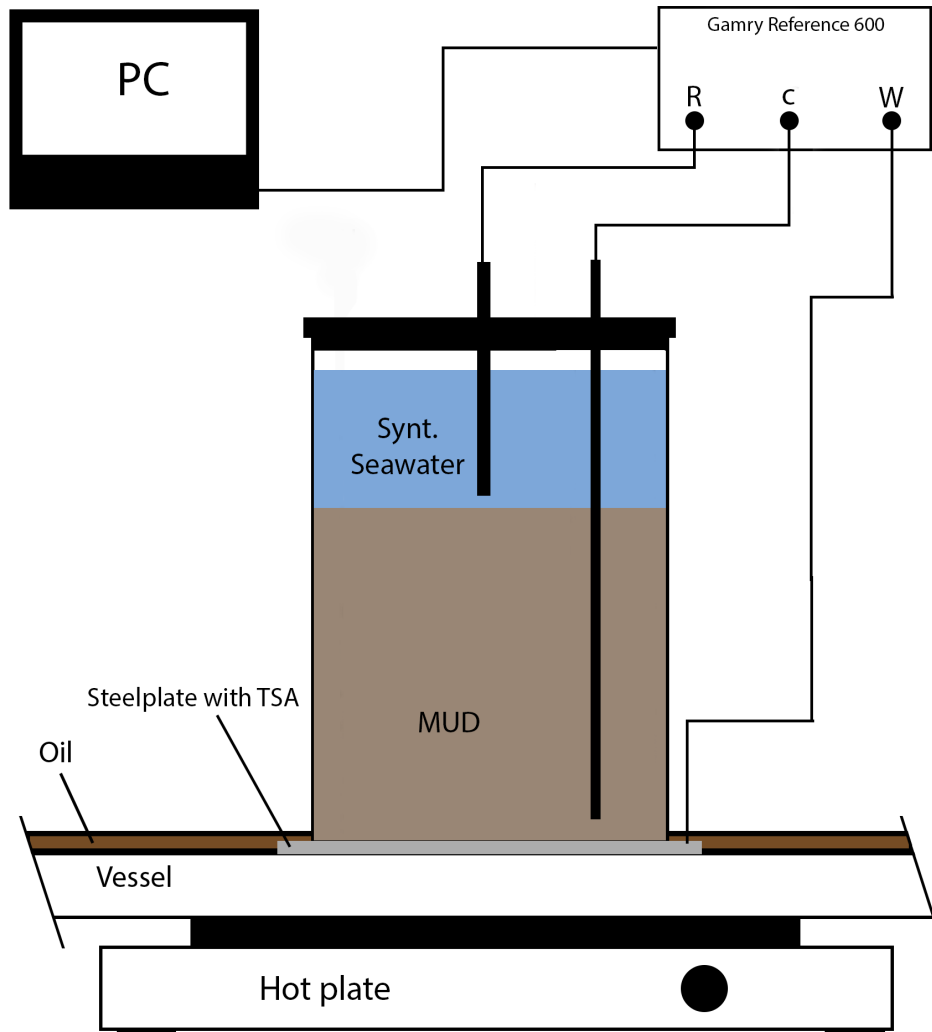
FIGURE 18 SET-UP FOR THE TAFEL CURVE RECORDING

The recording was done at all of the three temperatures with same settings. To ensure that the temperature was 60°C and 95°C at the two hot samples they were put in the vessel the day before the recordings were done.

3.9. VISUAL EXAMINATION OF THE SAMPLES

After test termination the remaining samples plates were examined visual. In order to examine the samples was the mud cell removed and the TSA surface cleaned. To clean the surface was a brush used with frequently flushing of water. The surface was taken picture of by using a normal camera.

To examine the cross section of the samples was the LVSEM (Low vacuum field emission scanning electron microscope) Hitachi S-3400N used. The samples were cut using a Struers Discotom-5 with Struers High Quality Cut off Wheels number 50A25. After the cutting was the cross section grinded using SiC paper from 320 grit to 4000 grit. The SEM pictures were taken at 10-15 kV and at

varying working distance and magnification. It was a special focus on the outer interface of the TSA.

3.10. TSA Duplex

In order to investigate and confirm the TSA duplex problem a sample was coated with an epoxy coating. Simply drilling a 6mm hole in the epoxy and TSA coating made a coating failure, such that bare steel was exposed see Figure 19. A plastic pipe was glued onto the sample with blue silicone (Loctite 5926) in order to make a cell. After 24 hours of drying was the cell was filled up with synthetic seawater.

FIGURE 19 TSA WITH EPOXY COATING AND COATING AND MANUFACTURED COATING FAILURE.

The experiment was carried out in room temperature and with no polarization. The duration was until there was sings of coating degradation on the sample.

4. Results

4.1. Iridium pH Electrodes

The results presented in this chapter are from the testing of the iridium oxide electrodes, before they were utilized in the corrosion test. The pH measurements from the corrosion test will be presented later in the thesis.

4.1.1. Calibration Curves

Seven iridium oxide electrodes for pH measuring were made. The electrodes were organized with numbers, one to seven. In order to get as good measurements as possible was the pH response of each electrode mapped. The pH response was mapped by measuring the OCP of the electrodes in four different pH buffer solutions obtained from Radiometer Analytical. The pH value of the buffer solutions is presented in Table 5. The pH response curve, which was made by linear regression of the four measured point, was compered to the calibration curve found in the literature see Figure 9. The curve for electrode 1 is shown in Figure 20, the curves for rest of the electrodes are to be found in appendix A. The blue line in the charts represents the calibration curve for the pH sensors made in this project, the red line represents the calibration curve presented in the literature and is obtained from [32].
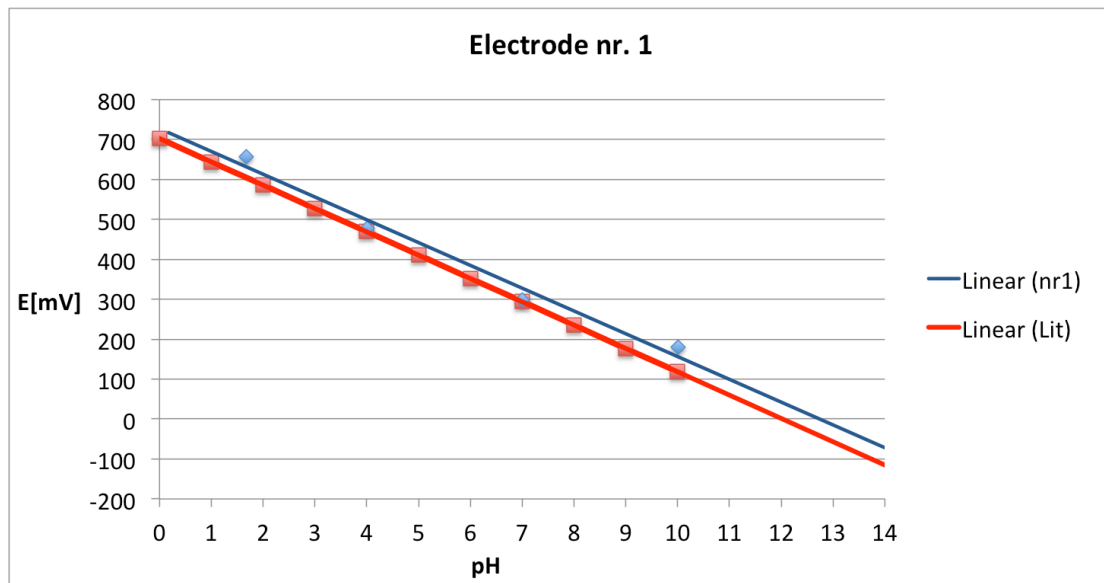
FIGURE 20 CALIBRATION CURVE ELECTRODE 1

Electrode 1, 3, 4, 6 & 7 showed a pH response close to the calibration curve from the studies done by Wang et.al. Since only five electrodes were needed in the corrosion test those five electrodes was preferred for the corrosion test.

E°´values and the sensors sensitivity in mV/pH for each electrode are presented in Table 10. They are derived from the equation representing the linear regression line for each sample.

TABLE 10 E°´VALUES AND SENSOR SENITIVITY IN MV/PH

Electrode number	E°´ [mV]	Sensor sensitivity [mV/pH]
1	726.98	-57.005
2	596.78	-45.432
3	735.88	-57.61
4	715.85	-56.635
5	554.39	-40.473
6	717.27	-55.036
7	698.21	-52.778

The pH is calculated by measuring the potential between the iridium oxide electrode and the Ag/AgCl reference electrode and applying the measured potential into the equations presented in as x.

TABLE 11 CONVERION EQUATIONS FROM POTENTIAL TO PH

Electrode number	Conversion equation from potential to pH
1	$pH = \dfrac{x - 726.98}{-57.005}$
2	$pH = \dfrac{x - 596.78}{-45.432}$
3	$pH = \dfrac{x - 735.88}{-57.610}$
4	$pH = \dfrac{x - 715.85}{-56.635}$
5	$pH = \dfrac{x - 554.39}{-40.473}$
6	$pH = \dfrac{x - 717.27}{-55.036}$
7	$pH = \dfrac{x - 698.21}{-52.778}$

The standard deviation values for the E°´values and the sensor sensitivity, compered to what Wang et al reported in [30] is presented in Appendix J.

4.1.2. STABILITY OF THE pH ELECTRODES

A stability test was carried out to document the stability of the fabricated electrodes. Electrode number 3 was used for measuring the OCP between an iridium oxide electrode and an Ag/AgCl reference electrode in a buffer solution of pH 7,000 (obtained from Radiometer Analytical) over two weeks. The result is presented in Figure 21 with respect to the potential and in Figure 22 with respect to the pH.
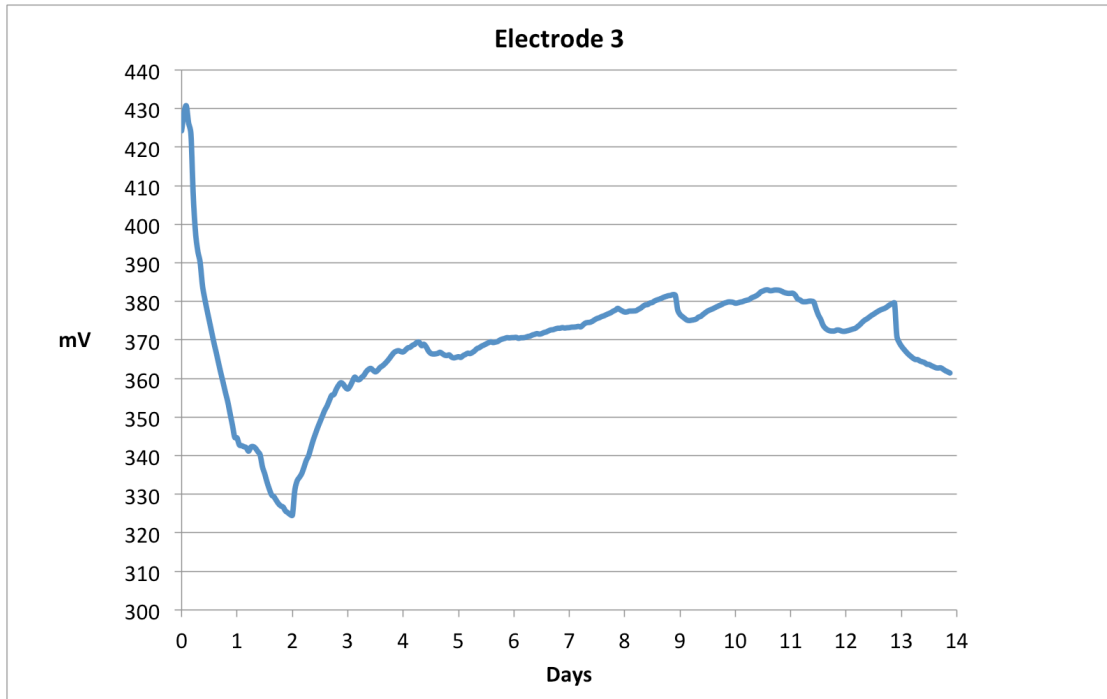
FIGURE 21 STABILITY OF IRIDIUM ELECTROE
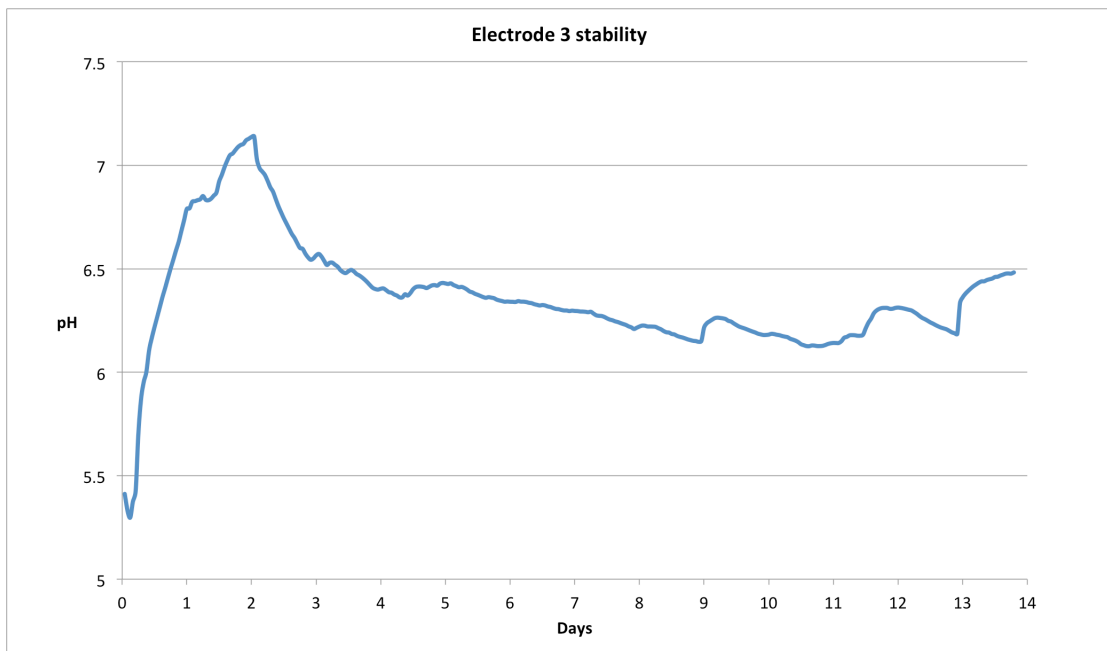
FIGURE 22 STABILITY OF IRIDIUM ELECTRODE IN 7.000 PH BUFFER SOLUTION

The result showed a significant drift, in the order of about 2 pH values the first 3 days, and about 0.5 pH values the rest of the period.

4.2.   RESULTS FROM THE CORROSION TEST

During the test period sample 3 suffered from a leakage in the silicone sealing between the steel plate and the mud cell. Two attempts were done to reseal the

42

mud cell, but without success. Sample 3 was therefore removed from the test after 14 days.

4.2.1. Visual Inspection of the TSA Surfaces
After the corrosion test the mud cells were removed from the samples, and the TSA surfaces were cleaned. The mud had attached surprisingly well to the TSA, and hard surface scrubbing with a brush was needed to get a clean surface. Still then was some of the mud stuck on the TSA surface.

Neither of the samples showed any signs of coating degradation, except for sample 3. Sample 1 and 3 is shown in Figure 23 and Figure 24 respectively, pictures of the other samples can be found in appendix B. The dark and gray spots on the surface are mud remnants. The mud had attached itself very hard to the TSA and was nearly integrated to the TSA surface. It was impossible to remove all of the mud by brushing.
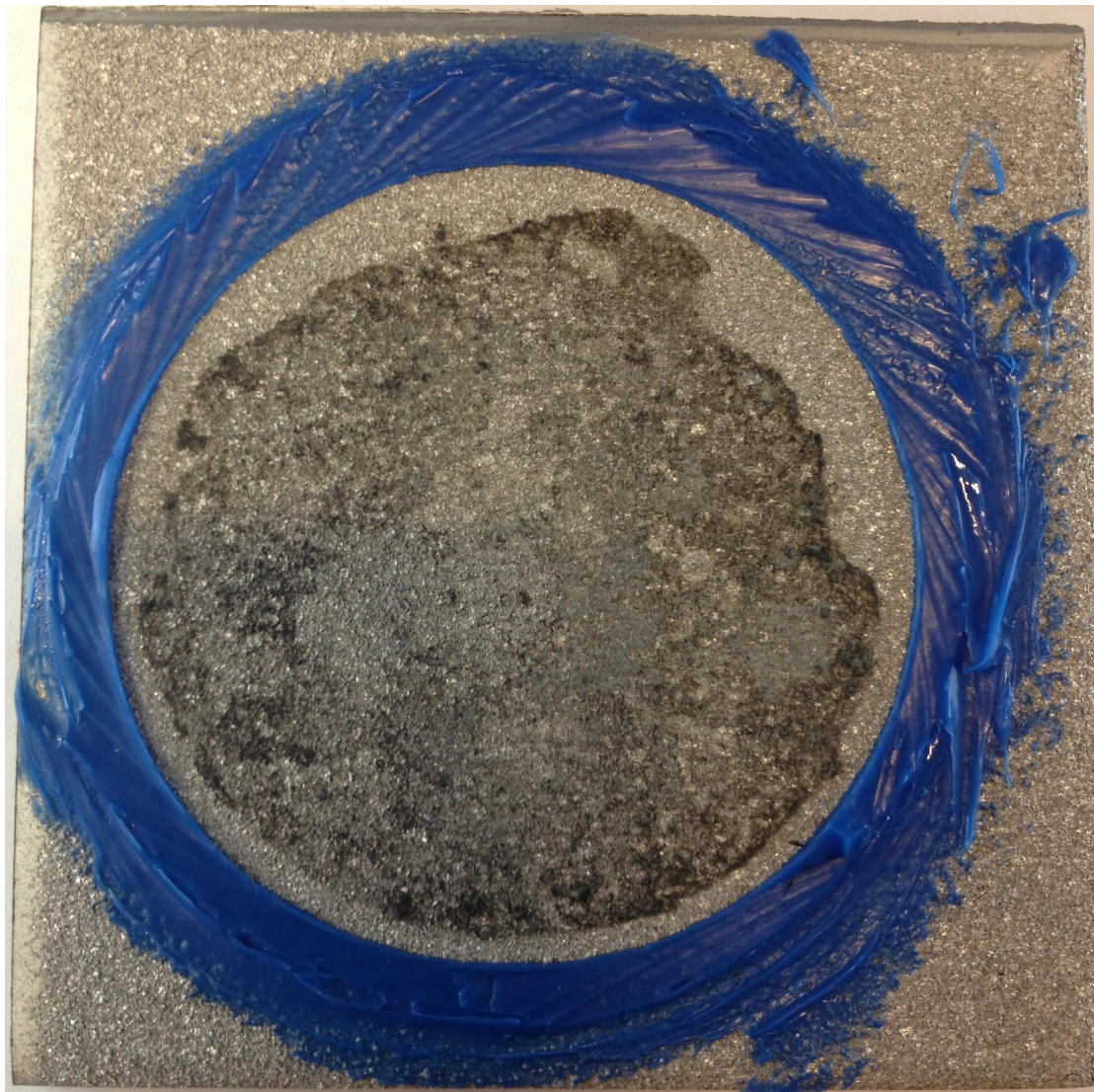
FIGURE 23 SAMPLE 1 AFTER THE CORROSION TEST
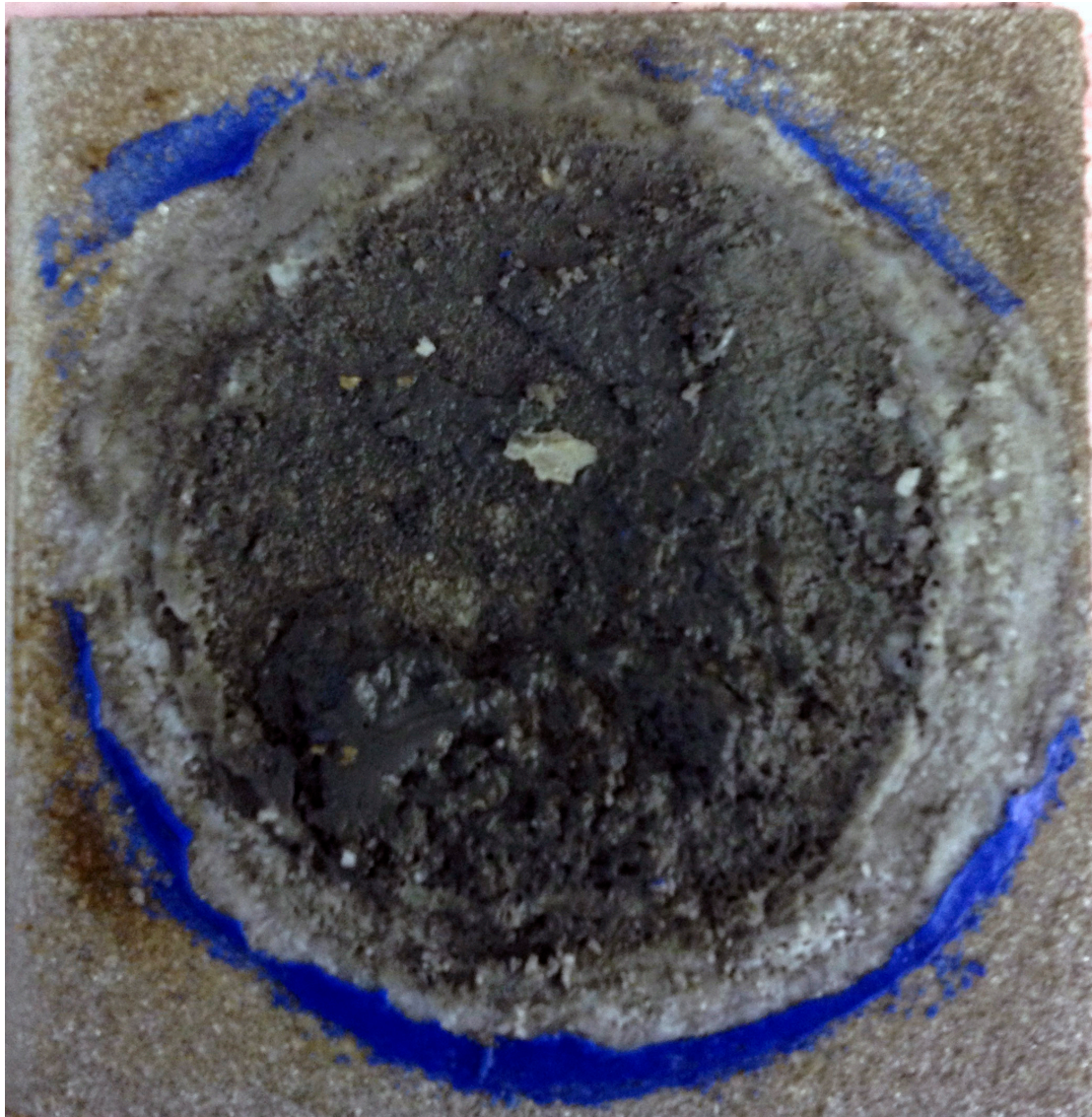
FIGURE 24 SAMPLE 3 AFTER THE CORROSION TEST

4.2.2. POTENTIOSTATIC POLARIZATION

The potentiostatic polarization curves displays the current density needed to hold the potential of the samples at the given potentials. The cathodic current densities for sample 1,2 4, and 5 are presented in Figure 25. The anodic current density for sample 3 is shown in Figure 26. The individual charts for each sample can be found in Appendix C. The potential and the temperature logging curves are also to be found in the appendix, respectively in Appendix E and Appendix F. The temperature and potential was stable through the whole test period.
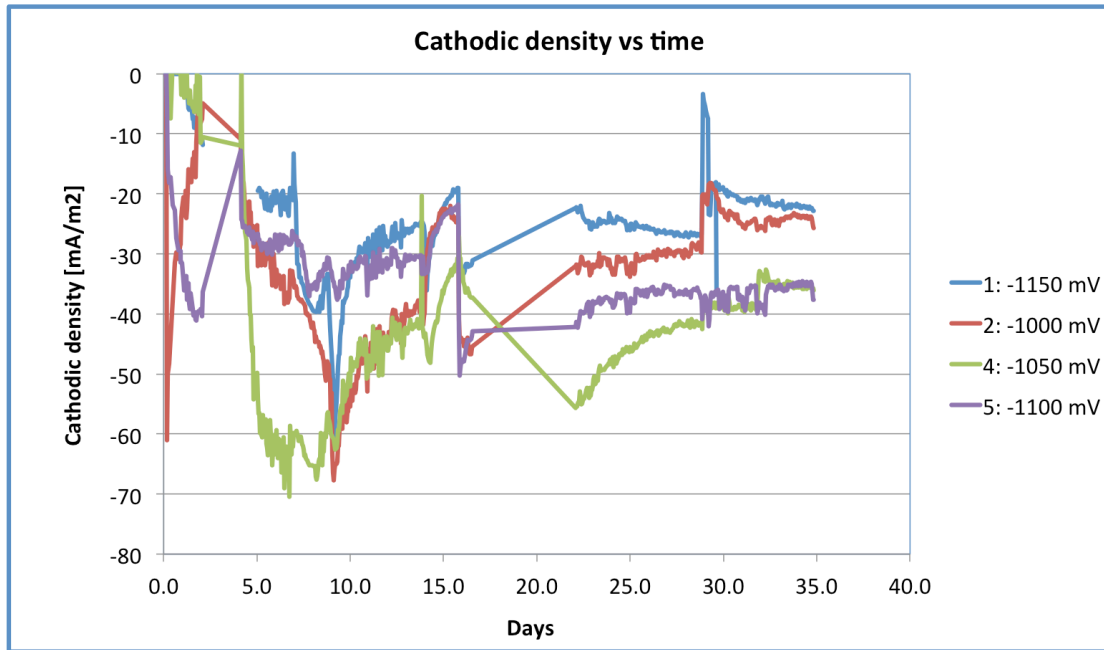
FIGURE 25 CATHODIC DENSITY VS TIME

The figure shows an initial increase in the current density the first ten days, and stabilization occurs after about 20 days of exposure.

Note that the logging equipment stopped between day 2 and 4, and stop breakdown between day 16 and 22 of the test period. The current density values in those periods are therefore not obtained. In the graphs are these periods shown as straight lines. However, the polarization was stable these periods as well.
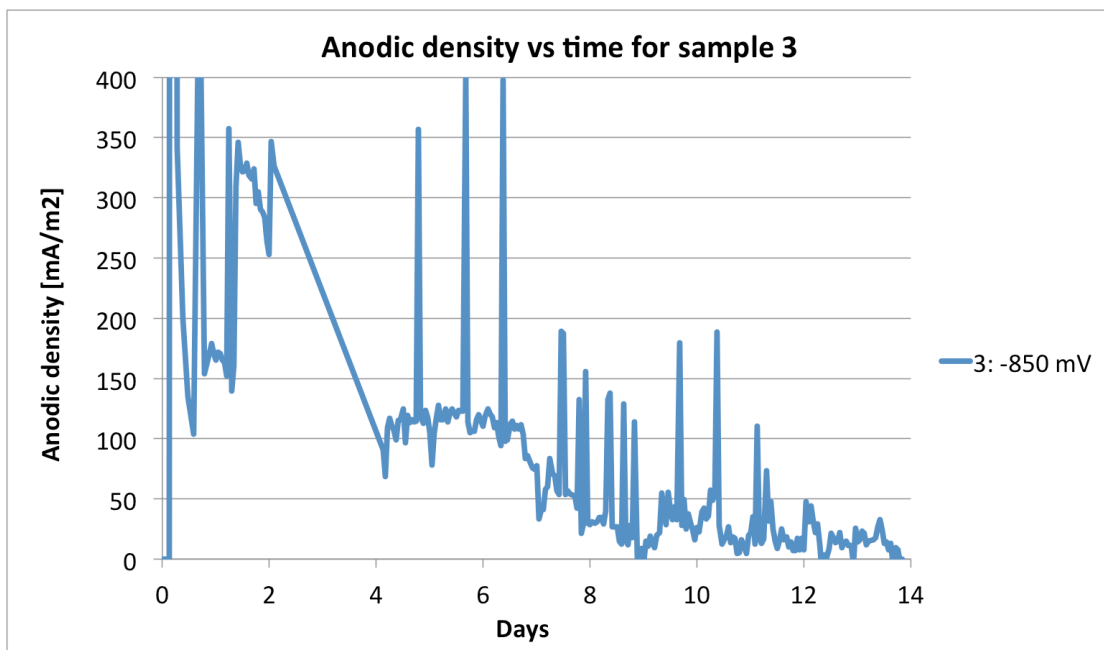
FIGURE 26 ANODIC DENSITY VS TIME

Sample 3 was the only sample that was polarized anodic, as can be seen from the chart is the initial current large with a decreasing trend.

4.2.3. LINEAR POLARIZATION RESISTANCE CURVES

The corrosion rate was logged during the test period by doing linear polarization resistance (LPR) measurements. Measurements were done weekly. The result is presented in Figure 27.
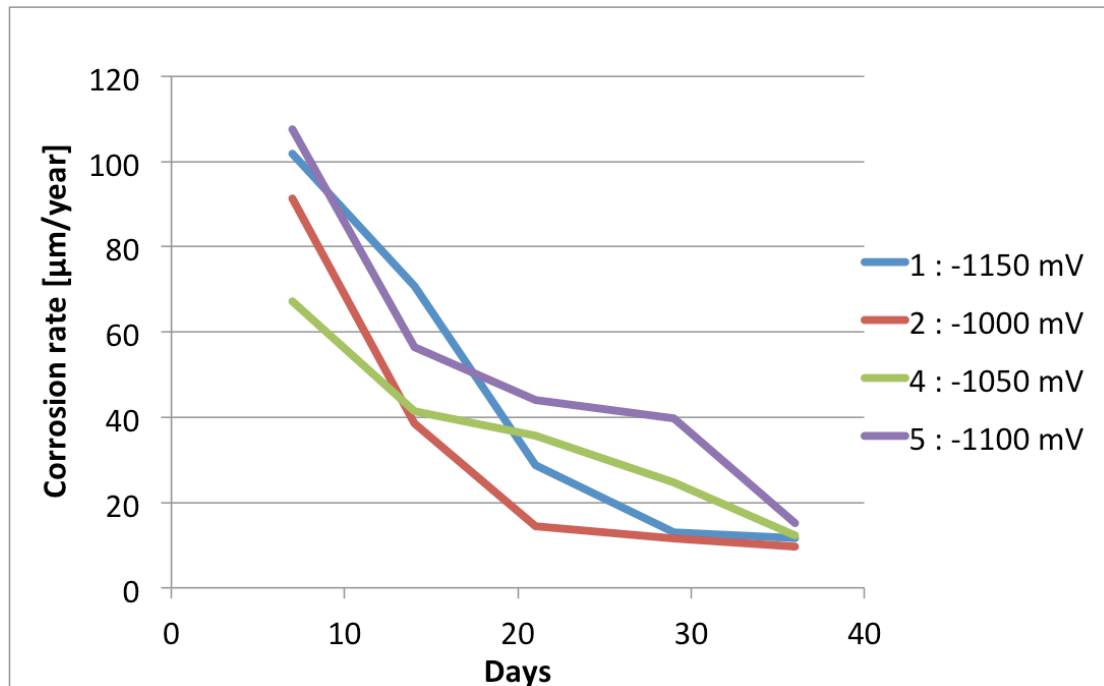
FIGURE 27 LPR MEASUREMENTS

The corrosion rate showed a similar trend as for the current densities, as described by Gundersen and Nisancioglu.[15] The corrosion rate is initially very high, but decreased throughout the experiment. A tendency to stabilization can be seen after 20 days. The exact corrosion rates are presented in Table 12. For calculation of the corrosion rate individual Tafel constants for each sample were used. The Tafel constants were calculated from cathodic and anodic polarization curves obtained at the end of the tests, shown in the next section.

4.2.4. TAFEL CURVES

Tafel curves were recorded for each sample at test termination. The curves were recorded using a Gamry reference 600 potentiostat controlled by a personal computer. The settings for the potentiostat are presented in Table 8. All the curves were recorded at 95°C.
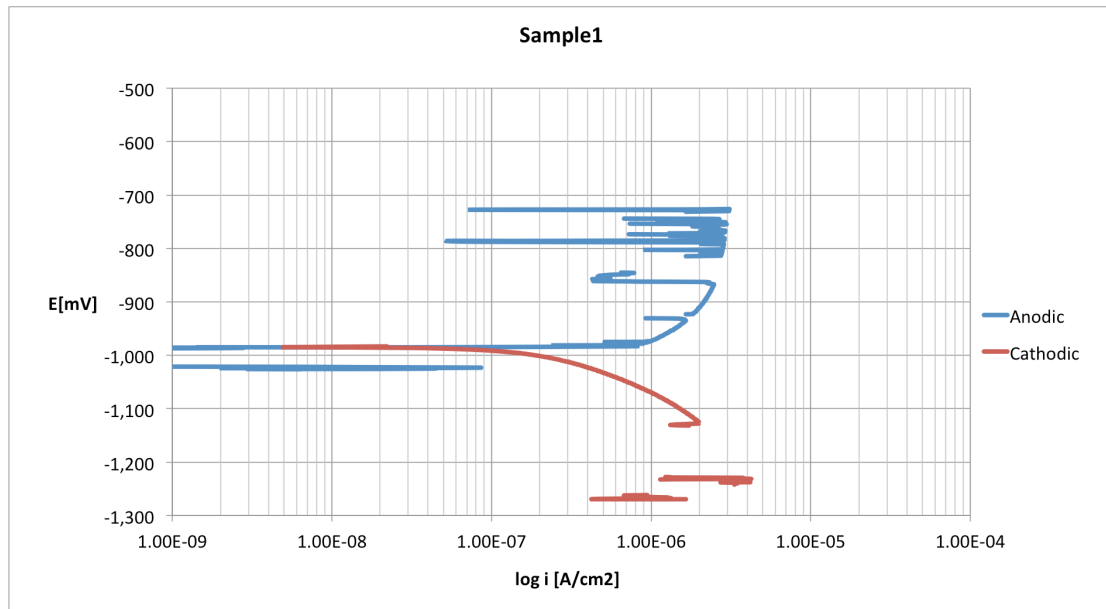
FIGURE 28 TAFEL CURVE FOR SAMPLE 1
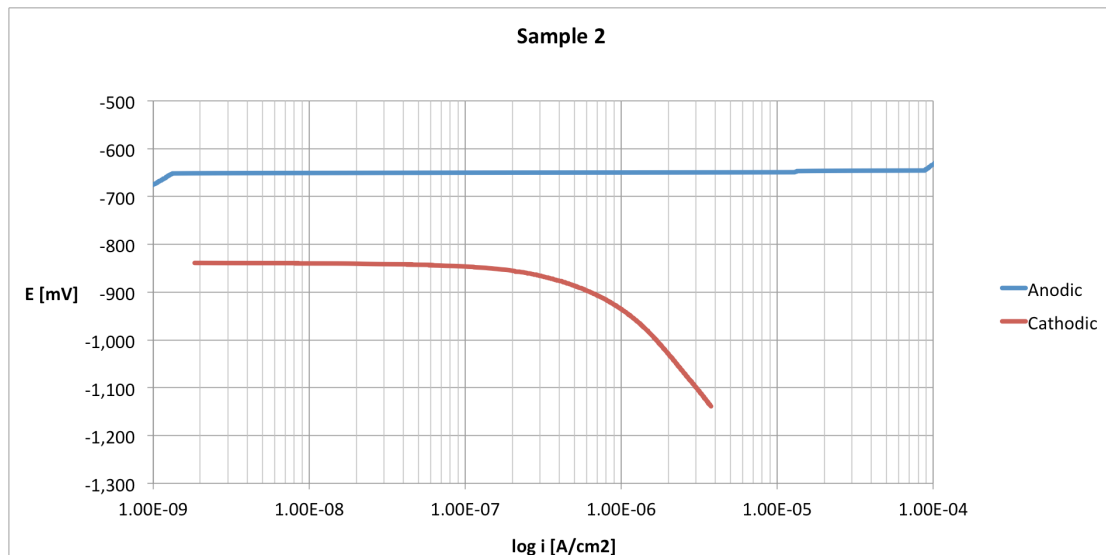
FIGURE 29 TAFEL CURVE FOR SAMPLE 2

As can be seen the anodic curve for sample 2 is useless for doing corrosion rate measurements, hence the corrosion rate estimated with tafel extrapolation for sample 2 is only based on the cathodic curve. The reason for this shape of the anodic curve is probably the sealer. The sealer has probably limited the current demand for some time, before it suddenly broke down resulting in a straight line

47

on the Tafel curve. A chart where the whole anodic curve can be seen is to be found in appendix K.
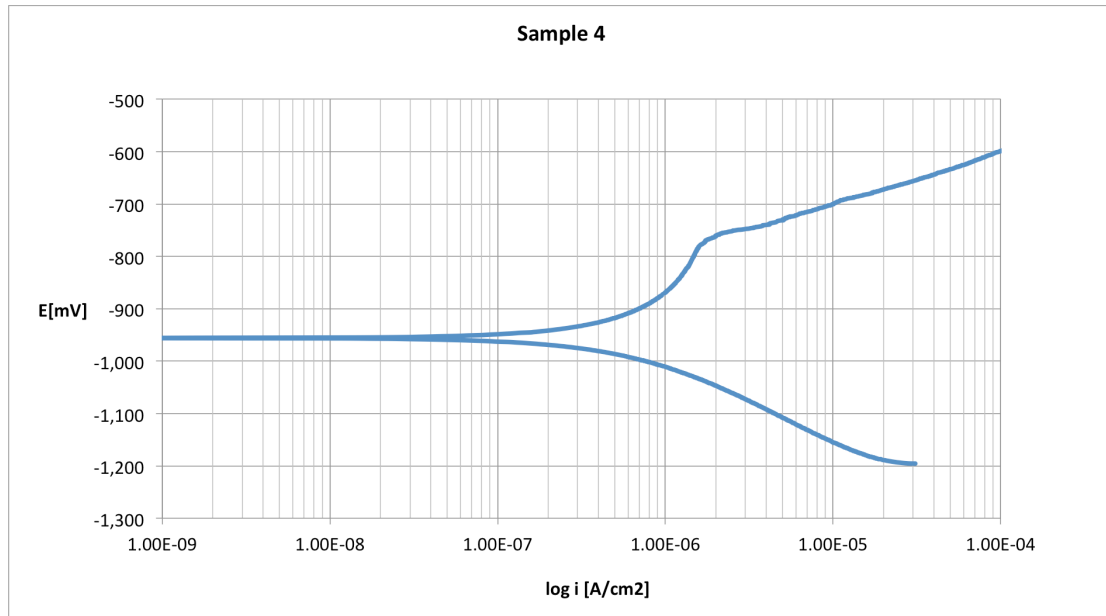
FIGURE 30 TAFEL CURVE FOR SAMPLE 4
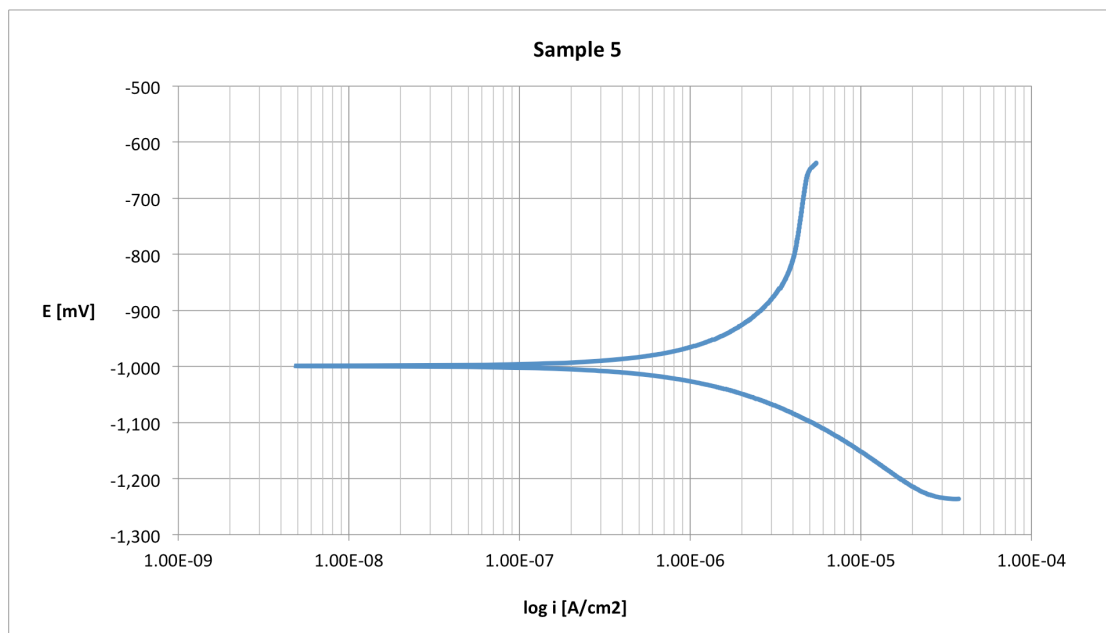
FIGURE 31 TAFEL CURVE FOR SAMPLE 5

For the first two samples (1 and 2) the anodic and cathodic curves were recorded separately, with about 30 minutes time between the cathodic and the anodic recording. The cathodic curves were recorded first, as the anodic polarization is believed to have a more destructive influence than the cathodic curve recording. The two last curves for sample 4 and 5 were recorded in one sweep, from -300 mV vs. OCP to + 300 mV vs. OCP. From the curves can it be seen that this method gave better curves.

48

4.2.5. CORROSION RATES ESTIMATED BY TAFEL EXTRAPOLATION COMPERED WITH CORROSION RATES FROM LPR MEASUREMENTS

Corrosion rates were estimated by Tafel extrapolation from the obtained Tafel curves. In Table 12 is the corrosion rates estimated with Tafel extrapolation compared to the corrosion rates estimated by LPR. All the corrosion rate estimates shown in table 12 are done at test termination.

TABLE 12 COMPERIASON OF CORROSION RATES

Sample	LPR [μm/year]	Tafel extrapolation [μm/year]
1	12	7
2	10	6
4	12	5
5	15	14

4.2.6. pH MEASUREMENTS

The pH was logged using self-fabricated iridium oxide electrodes. The result shows the change in pH near the TSA surface. Unfortunately the electrodes did not function as planned, none one was functioning properly the whole test period. Most of the electrode suffered from malfunction after short time in service. The results are therefore not presented in this chapter, but are found in appendix B.

4.3. CATHODIC TAFEL CURVES FOR UNSEALED TSA SAMPLES

Tafel curves for the unsealed TSA samples were recorded at ambient room temperature, 60°C and 95°C. Settings for the recordings are presented in Table 9, a Gamry Reference 600 potentiostat was used to do the recordings.
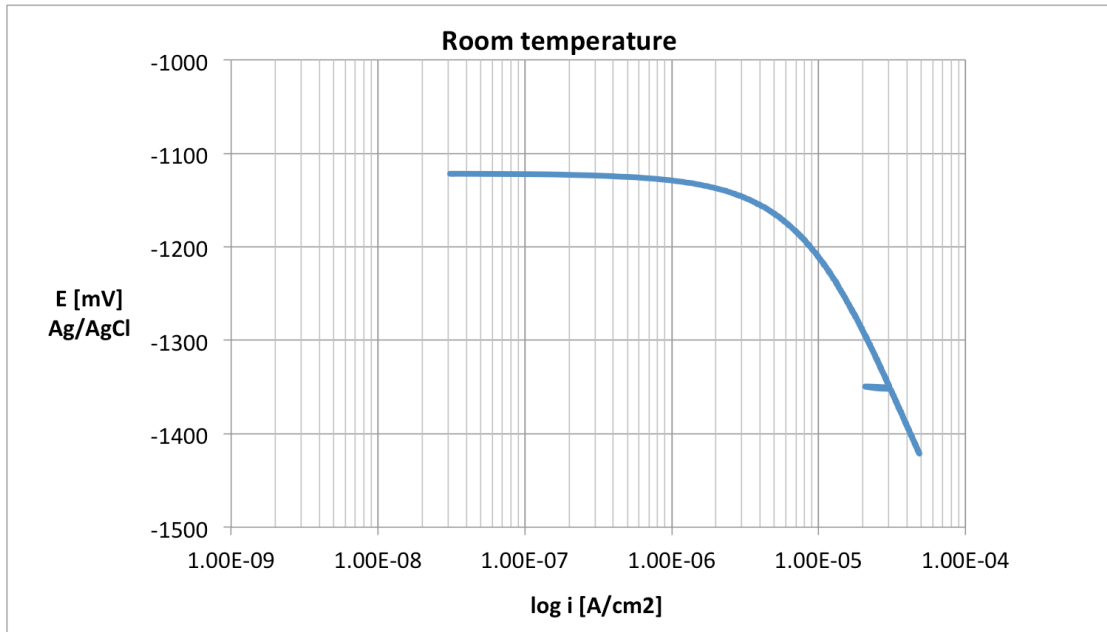
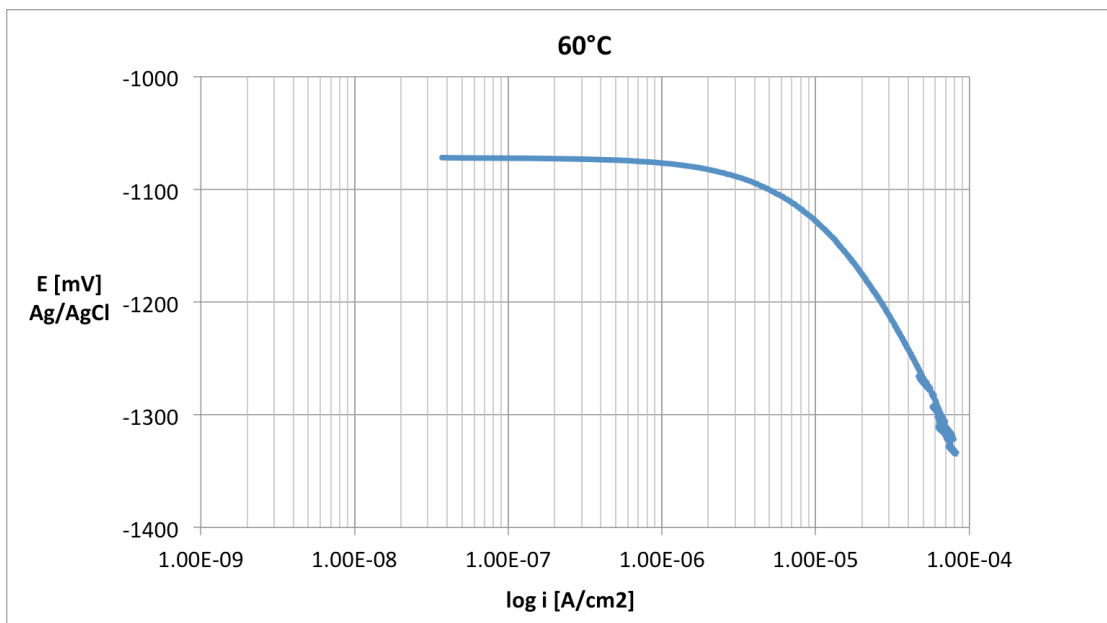**FIGURE 32 CATHODIC TAFEL CURVE AT ROOM TEMPRATURE**

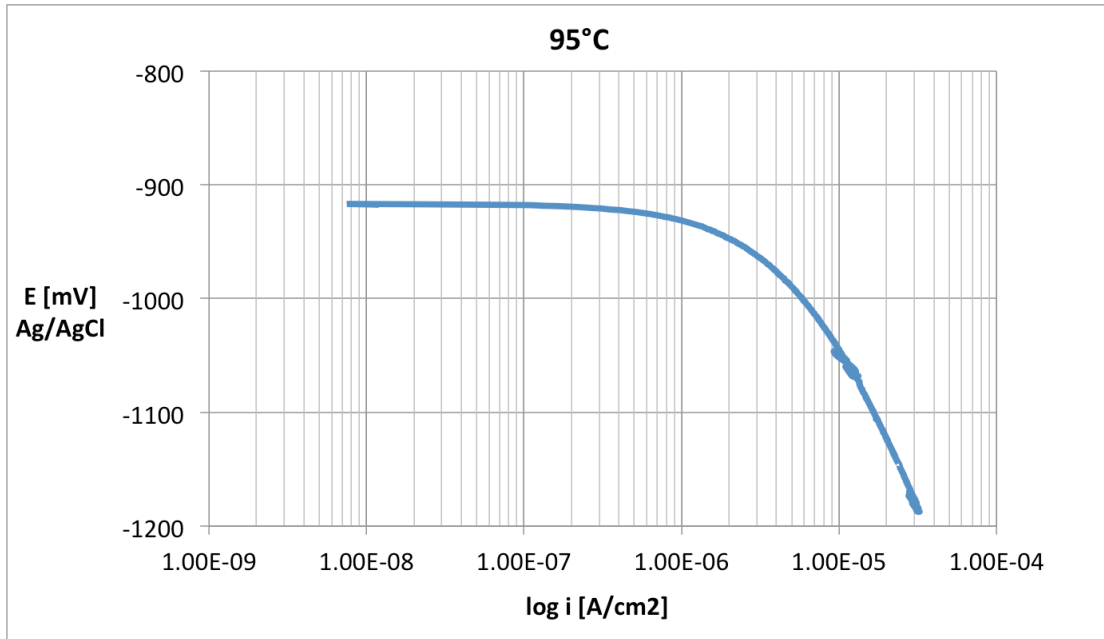**FIGURE 33 CATHODIC TAFEL CURVE AT 60°C**

50

FIGURE 34 CATHODIC TAFEL CURVE AT 95°C

Surprisingly did the sample exposed at 95°C shows lowest current demand at -300 mV vs. OCP.

4.3.1. CORROSION RATES FOR THE UNSEALED SAMPLES

As for the Tafel curves from the corrosion test, the corrosion rate was estimated by Tafel extrapolation. As seen in the figures, only cathodic tafel curves were obtained for these samples, hence the Tafel extrapolation is done on only cathodic Tafel curves. Note that these tafel curves were obtained after 1 day of exposure.

TABLE 13 CORROSION RATE FOR UNSEALED SAMPLES ESTIMATED BY TAFLE EXTRAPOLATION

Temp [°C]	Corrosion rate [μm/year]
Room (20)	57
60	109
95	44

4.4. SEM IMAGES

The SEM pictures revealed that there are pores, as expected, in the TSA. Whether the sealer has penetrated the TSA and filled the pores is difficult to see because the sealer may have detached from the TSA under grinding of the samples. No signs of sealer within the TSA were seen in the SEM. The sealer only contained 15% solids (85% solvent), which left a very thin film of sealer on the surface. At the outer interface of the TSA can a small area of sealer be seen in Figure 35 and

Figure 36. On sample 4, shown in Figure 39, Figure 40 and Figure 41, can a thick layer on the outside of the TSA be seen. The layer is mud that has attached itself to the TSA surface.
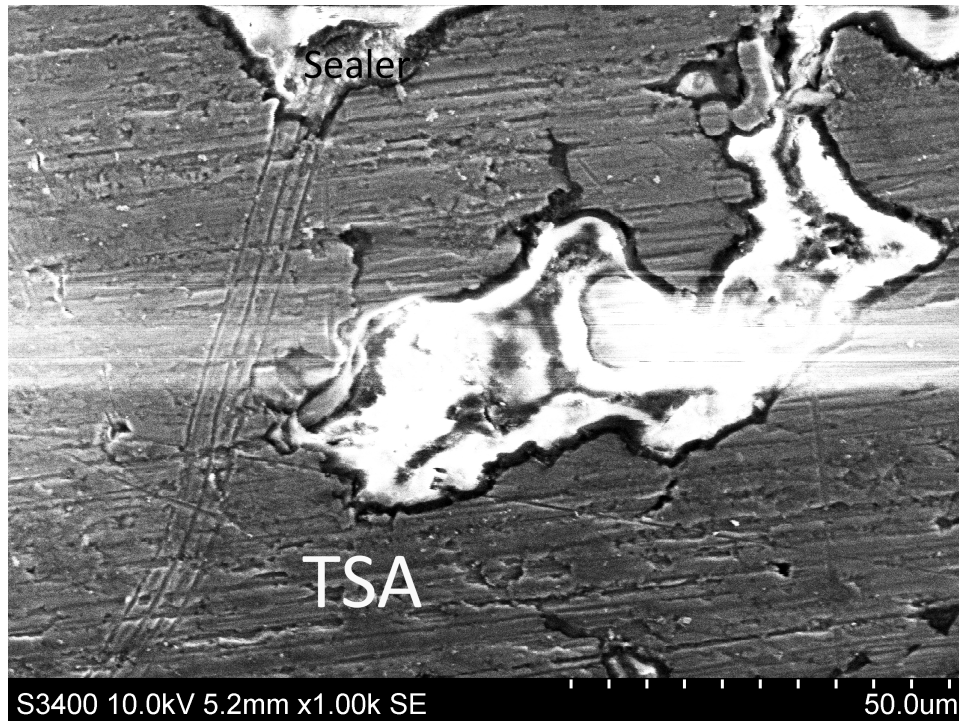
4.4.1. SAMPLE 1

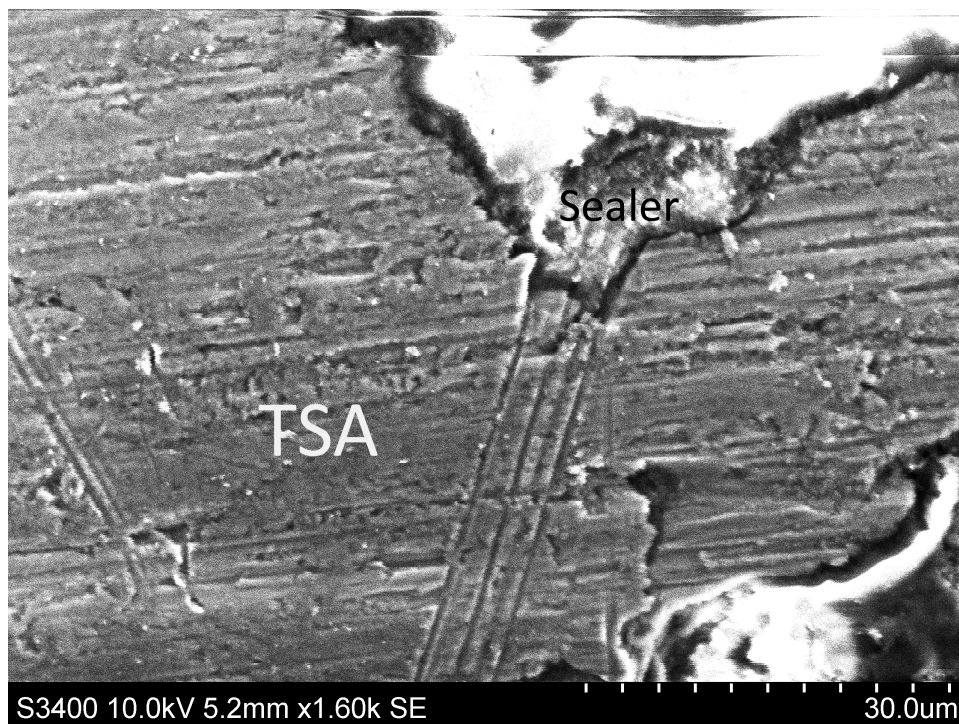**FIGURE 35 CROSS SECTION OF SAMPLE 1 1000X AT MAGNIFICATION**

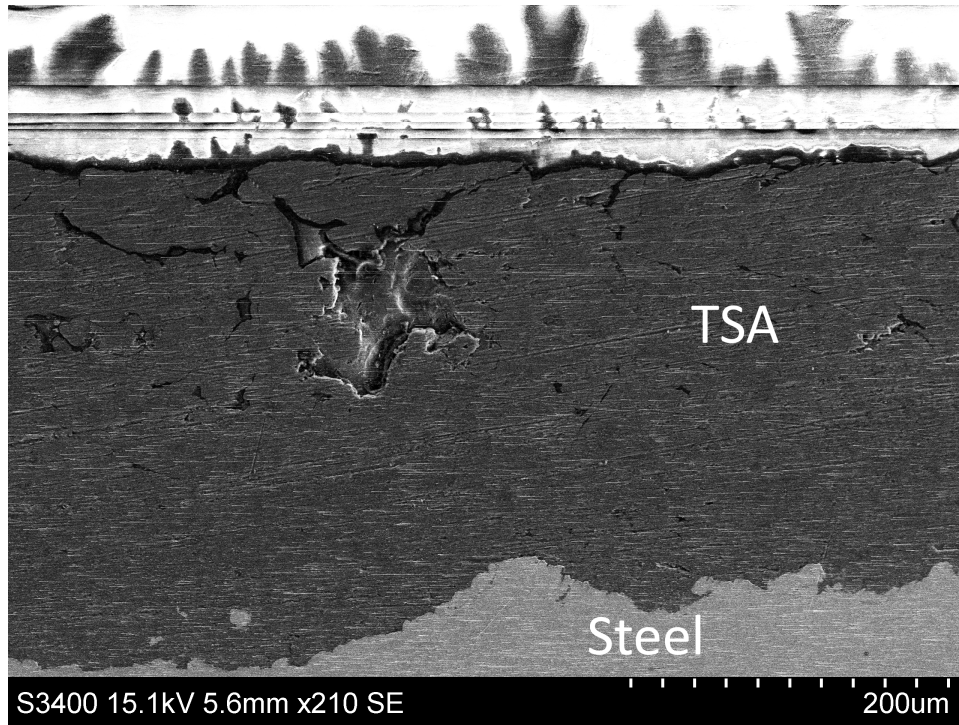**FIGURE 36 CROSS SECTION OF SAMPLE 1 AT 1600X MAGNIFICATION**

S3400 15.1kV 5.6mm x210 SE 200um

FIGURE 37 CROSS SECTION OF SAMPLE 2 AT 210X MAGNIFICATION

S3400 15.1kV 5.6mm x950 SE 50.0um
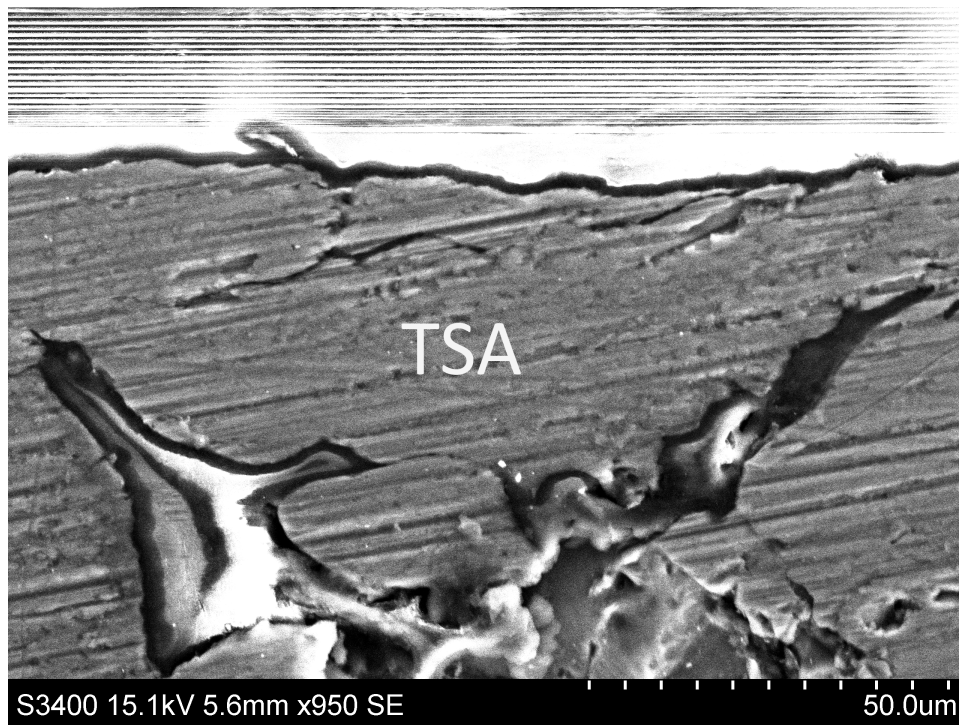
FIGURE 38 CROSS SECTION OF SAMPLE 2 AT 950X MAGNIFICATION

4.4.3. SAMPLE 4
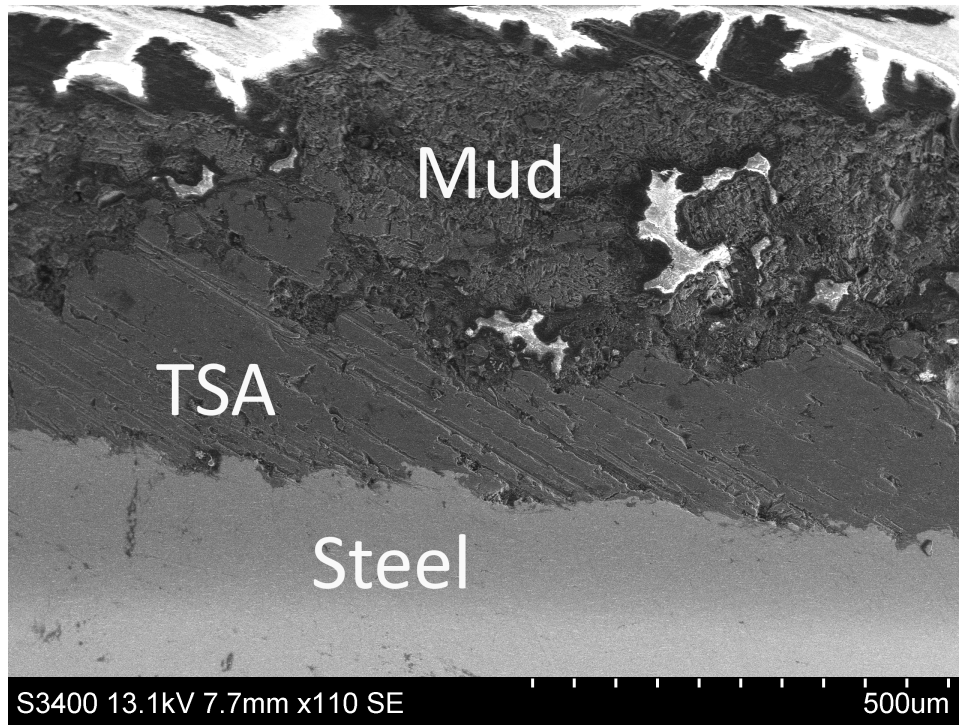
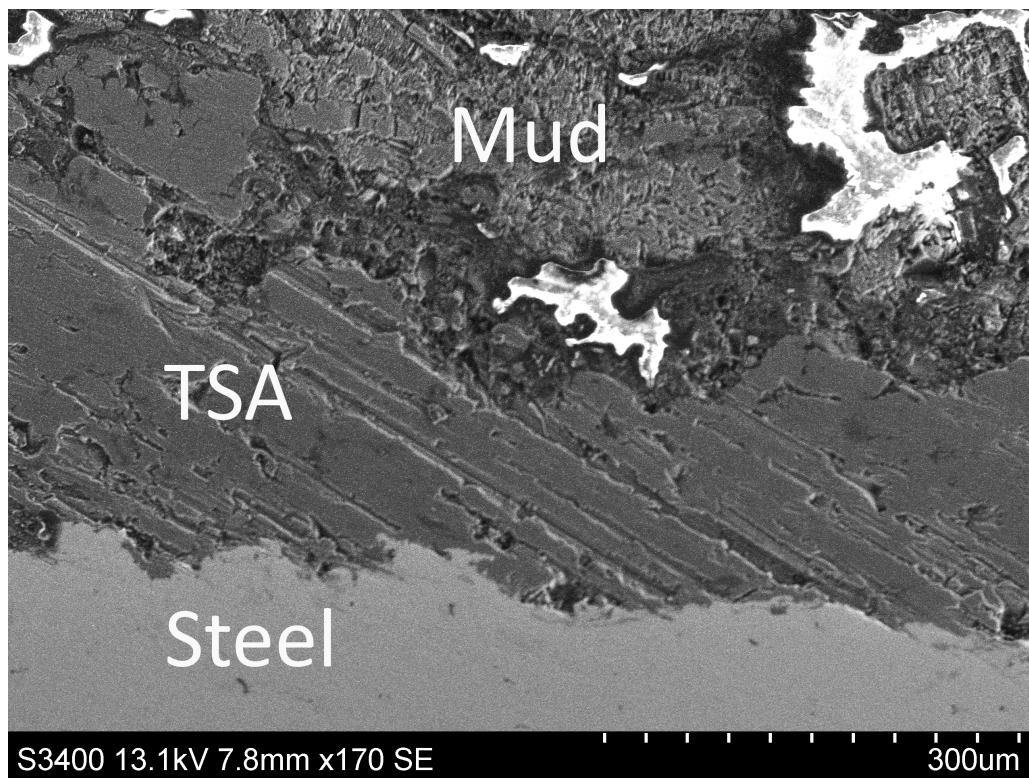**FIGURE 39 CROSS SECTION OF SAMPLE 4 AT 110X MAGNIFICATION**

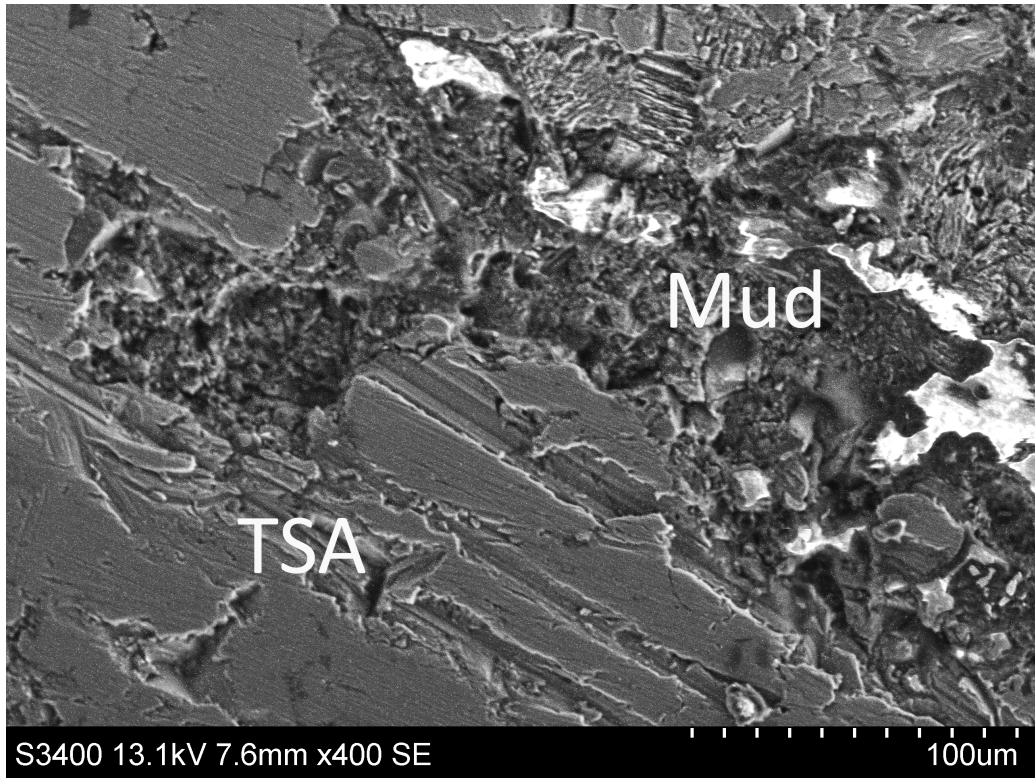
FIGURE 40 CROSS SECTION OF SAMPLE 4 AT 170X MAGNIFICATION

FIGURE 41 CROSS SECTION OF SAMPLE 4 AT 400X MAGNIFICATION
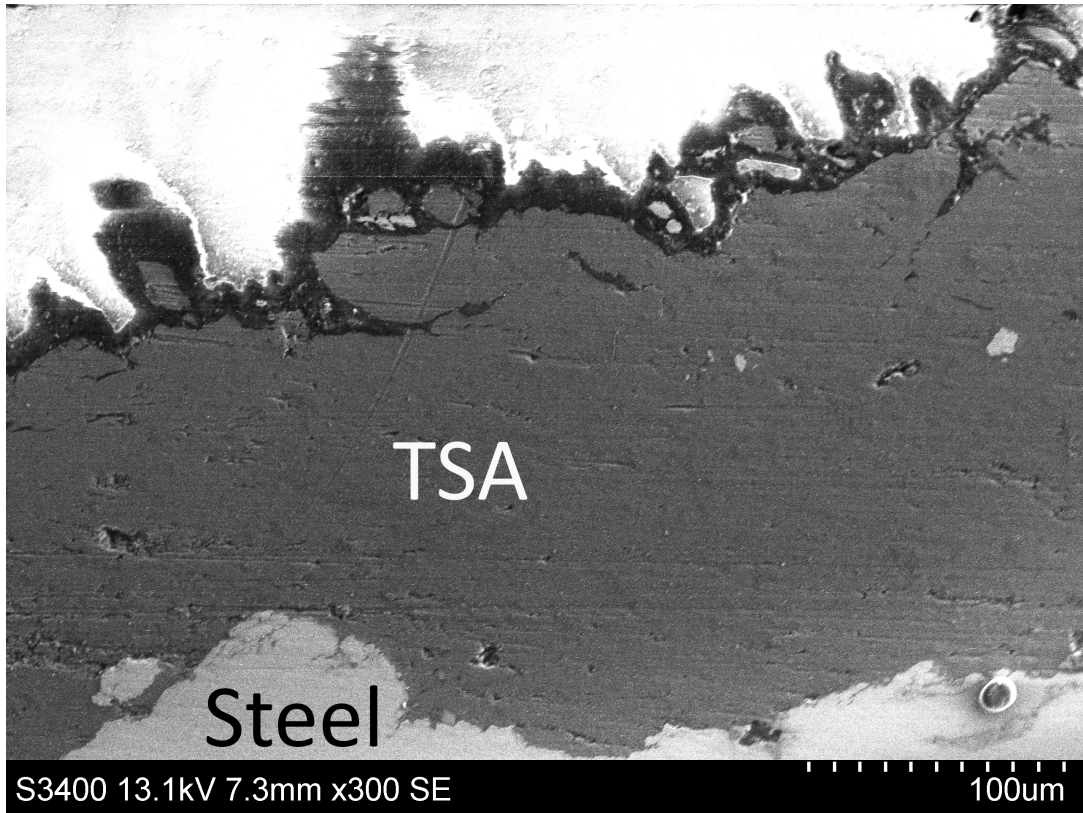
4.4.4. SAMPLE 5

FIGURE 42 CROSS SECTION OF SAMPLE 5 AT 300X MAGNIFICATION

4.5. TSA DUPLEX

The epoxy coated TSA sample was exposed to an environment that replicated submerged service in seawater. After two week was there clear signs of coating degradation at the surface see Figure 43. Three blisters had developed around the constructed coating holiday.
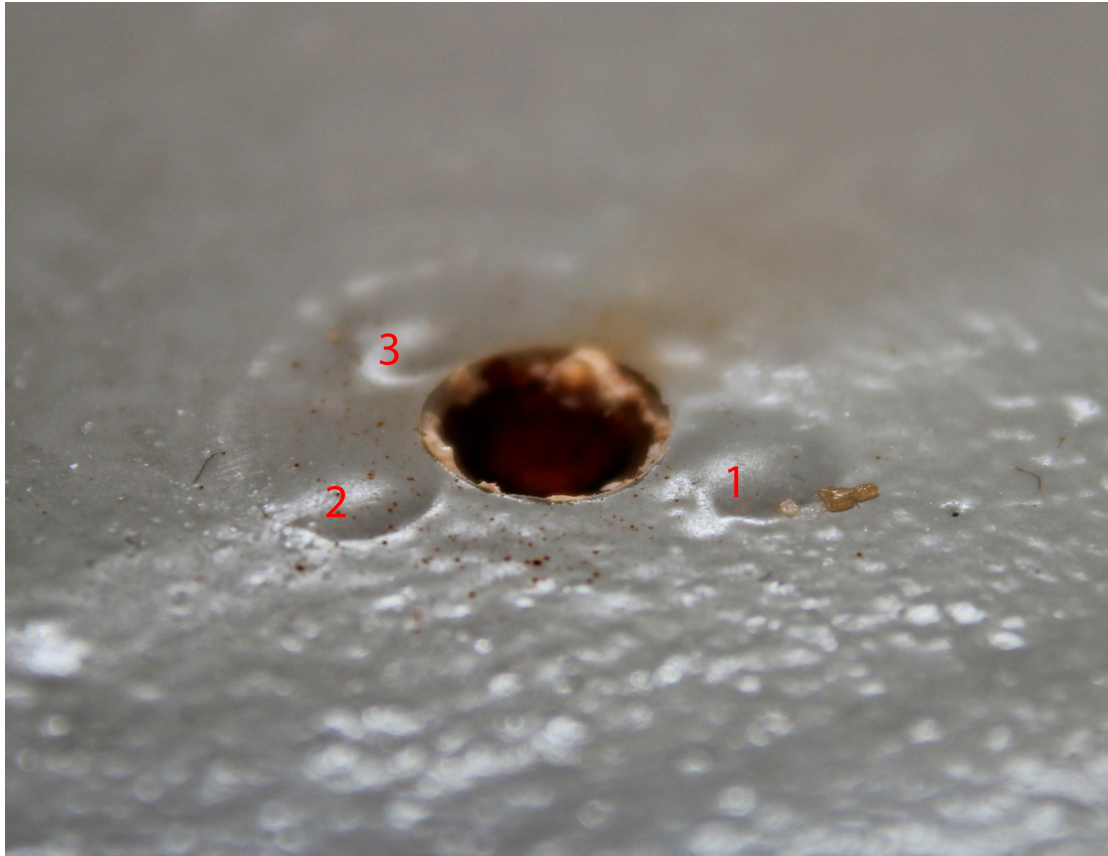

FIGURE 43 TSA DUPLEX COATING FAILURES

The combination of TSA with a tick overcoat was confirmed to have a very harmfully influence on the corrosion protection qualities of TSA. The initiation of the blisters will create an acidic environment under the epoxy coating, which will lead to rapid corrosion of the TSA.

5. DISCUSSION

5.1. IRIDIUM OXIDE ELECTRODES

The iridium electrodes fabricated in this project showed poor performance. Wang et.al stated that the manufacturing process is crucial for the performance of the electrodes. The iridium electrodes used were manufactured after a procedure Wang et. al described in several publications.[29, 30, 32]. The procedure was an exact replica of the one described in the literature, except that a platinum crucible was used instead of a gold lined alumina crucible. The role of the gold lining used in Wang et.als procedure is not know to be anything other than hindering lithium aluminate to form. Lithium aluminate may be formed in a reaction between lithium carbonate and alumina. Santi Chrisanti did an experiment in[31] regarding the role of gold in the oxidation process. He found that the iridium oxide sensors produced without gold lining also were pH-sensitive, but got a different pH response regarding mV/pH. This proved that there is an effect of lining the alumina crucible, however if this is crucial for the performance of the iridium oxide electrode or not cannot be proven with the current data.

What can be said is that the gold lining is utilized by Wang et.al to ensure that any unwanted reactions shall occur. Nevertheless, to use a platinum crucible instead of an gold lined alumina crucible should not result in any problems regarding the pH-sensitivity of the electrodes, since platinum is even less reactive than gold.

Apart from the use of the platinum crucible there are not any differences in the procedure described by Wang et.al and the one used in this project. Faults in the manufacturing method are not believed to be reason for the poor performance of the electrodes.

5.1.1. STABILITY OF THE pH MEASUREMENTS

Wang et al stated in [32] that the stability of the carbonated melt produced iridium oxide electrodes was excellent with only ±0.2mV potential drift in a period of ten days. The stability of the electrodes manufactured in this project was not excellent. In the two week stability test was a potential drift of 106 mV observed. Such large potential drifts will clearly inflict the pH measurements, as the drift covers more than one step in pH. The drift was worst the first four days. Afterwards there was a tendency to stabilization; in the last ten days was the drift of 21 mV.

In the period were a stabilization trend was observed, the measured pH value in the 7.000 pH buffer solution was wrong with between 0.5 and 1 pH value. This implies that the pH response of the electrode had changed.

Santi Chrisanti did also experience problems regarding the stability of the carbonate melt produced iridium oxide electrodes in hers study [31]. She observed a potential drift of around 50 mV over two days, with a tendency of potential stabilization to the end of the test.

The reason for the potential drift seen in the stability test can relate to many factors, what the root cause is hard to tell. Three factors that has influence on the potential drift are discussed under:

- *Stability of the reference electrode.* The reference electrode will always have influence on the measured potential; the potential of the reference electrode will change over time. This will lead to a small drift of the measured potential. Santi Chrisanti carried out a test to document the drift caused by the reference electrode in her study regarding the iridium oxide electrode.[31]. She tested two Ag/AgCl reference electrodes against one another in pH buffer solutions. Fluctuations in the range of 0.6 to -1,5 mV in a short period of 10 minutes were reported. With basis in these finding can the reference electrode be looked away from regarding main source for the drift. The drift caused by a reference electrode alone is certainly not in the order of 100 mV.

- *Hydration of the iridium oxide electrode.* Santi Chrisanti found that the calibration curve for an individual electrode changes if the electrode is stored in an aqueous solution, as an effect of hydration of the oxide. The change in pH response was varying from electrode to electrode; the largest change was in the order of 5mV/pH. She did also observe a potential drift of around 5 mV in a period of 20 minutes when the electrodes were exposed to a pH 4 buffer solution after hydration. Santi Chrisanti suggested therefore that a new calibration curve have to be made each time a pH measurements shall be done after storage in aqueous solution.[31] These findings are in accordance with what was observed in the stability test of the iridium oxide electrodes in this project. The pH response changed as the electrode was expose in aqueous solution over a long time period. Wang et al. reported good long term stability, and that the high stability of the iridium electrode makes it suitable for long term continuous pH monitoring without frequent calibration. The difference in these three experiences is clear, yet it is important to mention that Santi Chrisanti was also trying to reproduce the electrodes after Wang et.als procedures. With the results obtained by Santi Chrisanti and the author of this thesis can the reproducibility of the iridium oxide electrode made by carbonate melt method be questioned. The results described by Santi Chrisanti and in this project imply that the iridium oxide electrode is not very good suited for doing long-term measurements in aqueous solutions since the pH-response will deviate

from the premade calibration curve because of hydration of the oxide. The measured pH will, as a result of the deviation from the calibration curve, be inaccurate. However, the drift caused by the hydration is not big enough to cause such drifts experienced in this project, but it will contribute to making the measurements vague.

- *Transformation of the oxide layer.* By doing Raman and XRD spectra Santi Chrisanti observed transformation of the iridium oxide when the electrodes aged in water or in air. This will have an influence on the sensing mechanism of the electrode and thereby causing a potential drift. The transformation will also have influence on the time the iridium oxide electrode can be in operation. Santi Chrisanti suggested that the transformation of the oxide layer was the cause of the potential drift observed in her study. Such analysis has not been done in this project, however the similarities of the results are large so transformation of the oxide layer is suggested to cause the drift in the stability test.

The big drifts in the corrosion test are not the result of any of the previous mentioned factors. A leakage in the seal that should separate the copper wires from the electrolyte is the reason for the big drifts in the corrosion test. When the copper gets in contact with the electrolyte will the measured potential not be measured only between the iridium oxide electrode and the reference electrode, hence the measurements gets incorrect.

5.1.2.   REPRODUCIBILITY OF THE IRIDIUM ELECTRODES

The excellent stability of the iridium oxide pH electrode that Wang et.al reported in [32] was not obtained in this project, neither was the good reproducibility of the electrodes described in the same article. Wang et.al reported very small standard deviation values for the OCP and sensor sensitivity regarding electrodes fabricated in the same batch. The standard deviation values for the electrodes fabricated in this project indicate a much larger variation between the electrodes. For comparison of the two data sets see Appendix I. Santi Chrisanti did also observe larger variation than Wang et.al described in her study. Why there is a so big difference is hard to tell. The fabrication method is described to be critical for the performance of the iridium electrodes. Small differences in the fabrication method could then lead to unexpected results. If the use of the platinum crucible, and not alumina crucible lined with gold foil, had any influence on the produced electrodes is unknown, as the scope of this thesis is not to characterize the produced electrodes. Most likely was not the use of the platinum crucible the reason for the large variation in pH-sensing performance as platinum is less reactive than gold. Santi Chrisanti, who did use gold foiling, reported also variations larger than described than Wang et.al. Two independent studies have tried to reproduce the iridium oxide electrode for pH sensing by the

carbonate melt oxide, without success. The electrodes have proven to be irreproducible.

5.1.3. ROBUSTNESS OF THE IRIDIUM OXIDE ELECTRODES

The oxidized iridium wires were connected to a copper wire and mounted in a plastic pipe, blue silicone of the brand Loctite 5926 was used as adhesive. The iridium wire was mounted in a way such that only a small part of the oxidized area was exposed and the copper wire was sealed off inside the plastic pipe. The adhesive was chosen because it can function in temperatures up to 200 °C. Unfortunately did not the adhesive maintain sealing the whole test period. The result was that the copper wire was exposed to the electrolyte. This led to interference in the measured potential between the iridium oxide and the reference electrode, thus was the pH measurement system malfunctioning. Most likely has the problem with leakage in the silicon been initiated when the electrodes were pushed into the mud and down to the TSA surface. This can be seen from the charts presented in appendix D, big drifts are observed already the first days. This resulted in that no logging of the pH development at the TSA surface was obtained.

A surprising discovery was done when the electrodes were washed after the corrosion test. When the electrodes were rinsed in spring water was it reveled that the oxide layer had detached from the iridium wire, see Appendix I. This was unexpected because the oxide layer was hard to scrape off the iridium wire when the electrodes were fabricated. The reason for the detachment of the oxide is unknown and not in the scope of this project. Most likely has the oxide come off when the electrodes were washed, and not during the corrosion test.

5.2. pH MEASUREMENTS

The malfunctioning sealing of the plastic pipe destroyed the pH measurements. The results was so damaged that they are useless. For the first 5 days of the test period for sample 1 is the results fairly stable. A tendency to a stable pH value with a small increasing trend can be observed. However since the fabricated pH sensors in this project have proven to have very poor stability cannot this result be said to represent reality. The uncertainties around the result obtained with the iridium oxide electrodes are to big for calling the result reasonable. All ready before the corrosion test were the iridium oxide electrodes showing poor performance. In the stability test in the 7.000 pH buffer solution showed a maximum drift in measured pH of 1.8, and a drift of about 0,4 pH after stabilization. As a result of this is it impossible to make accurate measurements with the fabricated iridium oxide electrodes.

5.3. CURRENT DENSITIES

All the specimens showed similar behavior as Fisher et al reported in [19] with very big variation in the first week, and a slowly decreasing current density against one-month exposure. This effect of decreasing current density is likely due to a combination of formation of aluminum oxide on the surface, and isolation of the cathodic particles on the TSA surface as described by Gundersen and Nisancioglu. Although there is a significant difference between the results Fisher obtained after testing TSA sealed with silicon sealer and the results obtained in this project. The current densities obtained in this project are much lower than what Fisher reported. After one week reported Fisher maximum current density of 400 mA/m^2 and after one month 165 mA/m^2, for samples polarized to -1100 mV vs. Ag/AgCl. In the experiment carried out in this project, were the maximum values 70 mA/m^2 after one week and 40 mA/m^2 after one month for the samples that were polarized cathodic. The possible reason for this will be discussed later in 5.4.

Compared with the results obtained in the earlier experiments done by SINTEF Material and Chemistry is the current density showing a similar trend in the end of the test period, while in the start is there a difference, this is discussed in 5.6

5.4. EFFECT OF MUD ON THE CURRENT DEMAND

The main objective in this project has been to document what blanketing of TSA by mud does to the corrosion protecting properties of TSA. Wolfson stated in his study of thermal sprayed aluminum in saline mud that TSA could provide the sole source of cathodic protection to approximately 5% steel holiday surfaces in saline mud environments. He estimated the lifetime of a 254 μm thick sealed TSA coating with up to 5% coating holiday factor in saline mud to be greater than 25 years. [27] In the same study suggested Wolfson that the overall current demand for steel is lower in mud environments than in seawater. Wolfson did not include protection by sacrificial anodes and the possible problem with hydroxide enrichment on the TSA surface in his study. All his experiments were conducted at OCP and at much lower temperatures than experienced in this project. However the result he reported are in accordance with the results from this study. The current demand for the cathodic polarized samples in this project is ranging from 20 to 40 mA/m^2 after one moth exposure. Compered to the results Fischer got when he tested sealed TSA at 70-100°C and -1100 mV is the results in this project showing that the mud has not increased the current demand compered to TSA is exposed to seawater. It should be noted that the characteristics of mud would vary from site to site around the world. Especially could the conductivity of the mud have influence on the serving conditions for the TSA.

61

5.5. EFFECT OF THE APPLIED POTENTIALS ON THE CURRENT DEMAND

As for steel has not TSA a protection potential that is practical applicable for corrosion protection. However in [5] does Gartland suggest to use a potential of -900 mV vs. Ag/AgCl for cathodic protection of TSA. For higher temperatures he suggest that the potential should be lowered with 1mV for each degree over 10°C. At 95°C will then the recommended potential by Gartland be at -985 mV vs. Ag/AgCl.

The current density curves from the corrosion test do not show a clear difference between the different applied potentials. Two of the samples show lower current densities, in the order of 10 mA/m^2, than the two other samples at test termination. One of these samples is sample 2, which was polarized to -1000 mV vs. Ag/AgCl. In the LPR measurements is sample 2 showing loves corrosion rate out of all the four different applied potentials. This supports Gartlands suggestion of a practical protection potential for TSA.

The reason for the leakage of sample 3 is related to the applied potential. Since the sample is polarized in the anodic way will the aluminum corrode under the silicone seal. This results in a crevice under the seal and a leakage will occur. Observations done under the experiment is in accordance with this theory, leaks were observed at three different positions around the seal. The probability of three leaks on one sample, whereas the four cathodic polarized samples did not suffer from leakage, is very small; a clear indication of that the anodic polarization is the reason for the leaks on sample 3.

5.6. EFFECT OF SEALER

In comparison with experiments done earlier at SINTEF Material and Chemistry on TSA without sealer, the effect of the sealer is noticeable in the first ten days of exposure. All experiments referred too were done at 95°C, see Appendix G for test results from the experiments done by SINTEF Chemistry and Materials. The samples with no sealer showed a high initial current demand the first days, with a decreasing development afterwards. The sealed samples showed an opposite trend the first days compared to the unsealed samples, with low initial current demand but increasing development. Around day ten did the current densities meet for the unsealed and sealed samples, further was the development almost equal. The measured cathodic current was about the same after 30 days exposure, both close to -20 mA/m^2.

The reason for the lower current demand for the sealed samples the first ten days is simply because the sealer is the working as intended. The sealer is aiding to keep the surface passive. After some days will the sealer get washed out and

worn, hereafter will the current demand of the surface begin to follow a similar trend as a unsealed TSA surface.

The effect of the sealer was anticipated to be more significant and last longer. The reason for the relative short and small effect can relate to the application of the sealer in this project. In accordance with the NORSOK standard shall the sealer be applied as soon as possible after application of the TSA to hinder contamination, and is to be applied until the absorption is complete. There should not be a measureable overlay of sealer on the metallic coating after application. [22] In the datasheet for the sealer is it stated that the application of sealer should take place within 8 hours of the final application of metal coating. Recommended application tool is air spray.

The sealer application was not in accordance to the guidelines given in the NORSOK standard or the datasheet. A brush used as application tool, not air spray, this may result in an uneven layer. Secondly was the time between TSA and sealer application much more than the recommended 8 hours. On the other hand should not contaminations on the surface hinder the sealer in penetrating the TSA coating. The amount of aluminum oxide produced in air is not very big. It should not create any significant dense oxide layer on the TSA surface to hinder the sealer in penetrating the coating.

The SEM pictures didn't show any layer of sealer on top of the TSA. Only one layer was applied to be sure of not creating an overcoat on the TSA surface instead of sealing the surface. In retrospect had the effect of an additional layer been anything but negative. The sealer is not as tough and dense as for example an epoxy coating. A sealer will let the aggressive environment that develops under an epoxy coating on TSA trough. The aggressive environment will be washed away. An additional stroke of sealer would most likely increase the effect of the sealer. However, since the samples have been exposed in a tough environment for five weeks is the possibility of that the sealer have experienced deterioration is large. SEM images don after the exposure are thus not a good indication on whereas the amount of sealers applied was to small to give maximum performance of the sealer.

The Tafel curves for the unsealed samples show a large effect of the sealer. Note that for the three unsealed samples were the Tafel curves obtain after one-day exposure. According to Gundersen and Nisancioglu theory is the corrosion rate much greater in the beginning of the exposure period, hence the comparison of the Tafel curves obtained from samples with different exposure time will result in big differences. The basis for comparison of the two Tafel curve sets is hence poor, and a conclusion regarding sealer effect cannot be taken from these measurements.

5.7.   EFFECT OF TEMPERATURE

The temperature effect was not investigated in great detail in this project. Mostly because this was investigated in an earlier project, regarding the same topic, carried out by SINTEF Chemistry and Materials. The cathodic current log and corrosion rate measurements from SINTEFs project are accessible in the appendix, respectively Appendix G and Appendix H. The cathodic current charts does not show a big difference between the samples exposed at 60°C and 90°C. But compered to the sample exposed at ambient temperature, which is about 20°C, can a difference in the magnitude 10 mA/m^2 be seen. A similar behavior is seen on the corrosion rate measurements in Appendix H. The difference is not large between 60°C and 95°C, but noteworthy between the sample exposed at ambient temperature and the two exposed at high temperature. These observations are in accordance with what has been reported in the literature. [6, 19] The current demand and the corrosion rate will increase as the temperature increases. This is expected to be a result of that the rate of the kinetic reactions will speed up as the temperature increases.

5.8.   CORROSION MEASUREMENTS

Electrochemical corrosion rate measurements done on passive metals such as aluminum are in general showing more distribution in the results compered to what is obtained from metals that have a uniform active dissolution. As Frankel states it in [33] electrochemical techniques works well on metals with uniform active dissolution and are suitable for most need on passive metals. The LPR and Tafel extrapolation methods used in this thesis are well known and widely used to measure corrosion rates for aluminum hence they can be trusted.

The two utilized corrosion rate measurement methods gave some differences in the results see Table 12. An effect that is noteworthy is an overestimation of the corrosion rate when utilizing the LPR method on polarized aluminum. In Figure 44 is the effect illustrated. When doing corrosion rate measurements with LPR is the corrosion rate measured at OCP, i.e. not at the potentials applied in this project. From the figure can it be seen that the measured corrosion rate is depending on the anodic Tafel slope, when the sample is polarized away from OCP. The result is an over measured corrosion rate, how big the error gets, is depending on the Tafel slope. With a high slope is the error small, while as the slopes gets lower will the error increase.
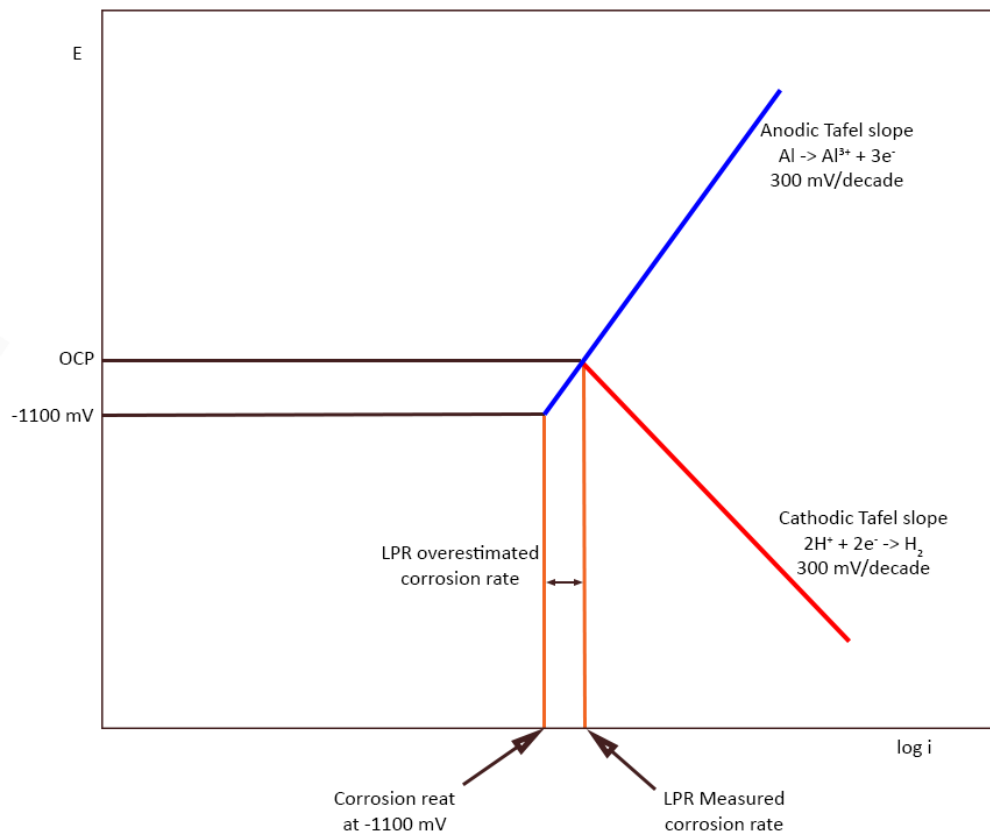
FIGURE 44 LPR OVERESTIMATION

All the samples that completed the corrosion test were polarized to a lower potential than OCP, hence the corrosion rates obtained by LPR is estimated to big. This effect is probably the reason for the differences seen in Table 12. By taking the effect of overestimation into account will the corrosions rates measured by LPR and Tafel extrapolation in good accordance to each other.

6. CONCLUSION

The corrosion protection performance of TSA when covered by mud, exposed at 95 °C and polarized to different potentials have been studied trough litterateur studies and experiments. The corrosion rate was measured weekly during the five-week test period by LPR, and at test termination by recording Tafel curves. The current to the samples was logged hourly during the test period, together with potential and temperature of the samples. An iridium oxide electrode for measuring the pH at the TSA surface has been fabricated and utilized in the experiment. From the results presented in this report can following conclusions be drawn.

- Sealed TSA covered with mud at 95°C has a corrosion rate between 7 μm/year and 15 μm/year after 36 days of exposure, with a decreasing trend.
- Variation in the corrosion rates between the different applied potentials was seen, with -1000 mV vs. Ag/AgCl as the best potential regarding obtaining low corrosion rate of the TSA.
- The sample polarized anodic suffered fast from a leakage in the sealing due to corrosion of the TSA surface under the seal.
- Sealing of the TSA has most effect in the beginning of the exposure period.
- The corrosion rate of TSA is higher at 95°C than ambient room temperature, but the difference from 60°C is not large.
- Mud exposure of TSA did not introduce large corrosion rates, the mentioned possibility of an increased pH at the TSA surface it not a problem.
- The Iridium oxide electrode showed weak stability in the pH measuring compared to what was reported in literature. The electrode has proven to be irreproducible.
- The need for a reliable and tough method for pH measurements in harsh conditions is still present.

7. SUGGESTIONS FOR FURTHER WORK

The work carried out in this study has mainly two main focus areas: feasibility and robustness of TSA when blanketed in mud and long-term continuous pH measurement in harsh conditions. For the sake of simplicity are the suggestions for further work divided in two categories: TSA service in mud and long-term and continuous pH measurement in harsh conditions.

7.1. TSA SERVICE IN MUD:

- Perform a test with sealed TSA, were the sealer is applied according to NORSOK M-501.
- Conduct a long-term (1-year) exposure test with mud blanketed TSA at high temperature to map the performance of TSA at these conditions.

7.2. LONG-TERM CONTINUOUS pH MEASUREMENT IN HARSH CONDITIONS:

- Validate if it is possible to make an iridium oxide electrode that have the same performance that Wang et.al have reported.
- Investigate the production method for the iridium oxide electrode to clarify in which degree the production parameters has influence on the pH sensing properties of the sensor.
- Develop a better housing for the iridium oxide, which enhances the robustness of the sensor.

8. References

1. Fontana, M.G., *Corrosion engineering / Mars G. Fontana, Norbert D. Greene*. McGraw-Hill series in materials science and engineering, ed. N.D. Greene. 1978, New York: McGraw-Hill.
2. Nisancioglu, K. and N.t.h.I.f.t. elektrokjemi, *Corrosion Basics and Engineering: Lecture Notes for the Course 53523 Korrosjonslære*. 1994: Universitetet i Trondheim, Norges tekniske høgskole, Institutt for teknisk elektrokjemi.
3. McCafferty, E., *Thermodynamics of Corrosion: Pourbaix Diagrams*, in *Introduction to Corrosion Science*. 2010, Springer New York. p. 95-117.
4. Gartland, P.O., *Protective properties of Al-based coating in seawater*, 1991, SINTEF: Trondheim. p. 61+2.
5. Gartland, P.O., *Protective properties of Al-based coatings in seawater*, 1991, SINTEF - the corrosion center.
6. Fischer, K.P., W.H. Thomason, and J.E. Finnegan, *Electrochemical performance of flame-sprayed aluminum coatings on steel in seawater*. Journal Name: Mater. Performance; (United States); Journal Volume: 26:9, 1987: p. Medium: X; Size: Pages: 35-41.
7. Nisancioglu, K., *Korrosjonshåndbok for aluminium*. 1987.
8. Hartt, W.H., C.H. Culberson, and S.W. Smith, *Calcareous Deposits on Metal Surfaces in Seawater—A Critical Review*. Corrosion, 1984. **40**(11): p. 609-618.
9. Solberg, J.K. and N.t.-n.u.I.f.m.o. elektrokjemi, *Teknologiske metaller og legeringer*. 2002: Institutt for materialteknologi og elektrokjemi, Norges teknisk-naturvitenskapelige universitet.
10. Mondolfo, L.F., *Aluminum alloys: structure and properties*. 1976: Butterworths.
11. Álvarez, P., et al., *The electrochemical behaviour of sol–gel hybrid coatings applied on AA2024-T3 alloy: Effect of the metallic surface treatment*. Progress in Organic Coatings, 2010. **69**(2): p. 175-183.
12. Szklarska-Smialowska, Z., *Pitting corrosion of aluminum*. Corrosion Science, 1999. **41**(9): p. 1743-1767.
13. Möller, H., *The influence of Mg2+on the formation of calcareous deposits on a freely corroding low carbon steel in seawater*. Corrosion Science, 2007. **49**(4): p. 1992-2001.
14. Grilli, R., et al., *Localized corrosion of a 2219 aluminium alloy exposed to a 3.5% NaCl solution*. Corrosion Science, 2010. **52**(9): p. 2855-2866.
15. Gundersen, R. and K. Nisancioglu, *Cathodic Protection of Aluminum in Seawater*. Corrosion, 1990. **46**(4): p. 279-285.
16. Solberg, J.K., *Teknologiske metaller og legeringer*. 2008, [Trondheim]: Institutt for materialteknologi, Norges teknisk-naturvitenskapelige universitet. III, 316 s. : ill. ; 30 cm.
17. Dorfamn, M.R., *Thermal sprayed coatings*. Handbook of Environmental Degradation of Materials, ed. M. Kutz. 2005: Elsevier Science.
18. Espallargas, N., *Thermal Spary Coatings*, 2010.
19. Fischer, K.P., et al., *Performance history of thermal-sprayed aluminum coatings in offshore service*. Journal Name: Materials Performance; Journal

Volume: 34; Journal Issue: 4; Other Information: PBD: Apr 1995, 1995: p. Medium: X; Size: pp. 27-34.

20. Chow, R., et al., *Characterization of Thermal Sprayed Aluminum and Stainless Steel Coatings for Clean Laser Enclosures*. 2000. Medium: ED; Size: 15p.

21. Deshpande, S., et al., *Application of image analysis for characterization of porosity in thermal spray coatings and correlation with small angle neutron scattering*. Surface and Coatings Technology, 2004. **187**(1): p. 6-16.

22. NORSOK, *M-501*, 2012, standard norge.

23. Gartland, P.O.E.T.G., *Cathodic and anodic properties of thermally sprayed Al- and Zn-based coatings in seawater* in *NACE international*1990: Las Vegas.

24. Norge, S., *NORSOK Standard M-503*, 2007.

25. Veritas, D.N., *DNV-RP-B401*, in *Cathodic Protection Design*2010.

26. William H. Thomason, C.I.S.O., Statoil ASA.; Trond Haugen,Det Norske Veritas.; Karl Petter Fisher, Det Norske Veritas, *Deterioration of Thermal Sprayed Aluminium coatings on Hot Risers Due to Thermal Cycling*, in *CORROSION 2004*2004, NACE International: New Oreleans, La. p. 16.

27. Wolfson, S.L.S.O.C., *Corrosion control of subsea pipings systems using thermal sprayed aluminium*, in *CORROSION 96*1996, NACE International: Denver, Co. p. 9.

28. Knudsen, O.Ø.R., T.; Røssland, T., *Rapid degradation of painted TSA*, in *Corrosion 2004*2004, NACE International: New Orleans. p. 12.

29. Yao, S., M. Wang, and M. Madou, *A pH Electrode Based on Melt-Oxidized Iridium Oxide*. Journal of The Electrochemical Society, 2001. **148**(4): p. H29-H36.

30. Wang, M., S. Yao, and M. Madou, *A long-term stable iridium oxide pH electrode*. Sensors and Actuators B: Chemical, 2002. **81**(2–3): p. 313-315.

31. Santi Chrisanti, B.S., *A pH electrode based on melt-oxidized iridium oxide*, in *Department of Material Science and Engineering*2003, Ohio State University: Ohio p. 101.

32. Wang, M. and S. Yao, *Carbonate-Melt Oxidized Iridium Wire for pH Sensing*. Electroanalysis, 2003. **15**(20): p. 1606-1615.

33. Frankel, G.S., *Electrochemical Techniques in Corrosion: Status, Limitations, and Needs*. Journal of ASTM International 2008. **5**(2): p. 27.

APPENDIX A

PH RESPONSE CURVE FOR THE PRODUCED IRIDIUM OXIDE ELECTRODES

Electrode 1:
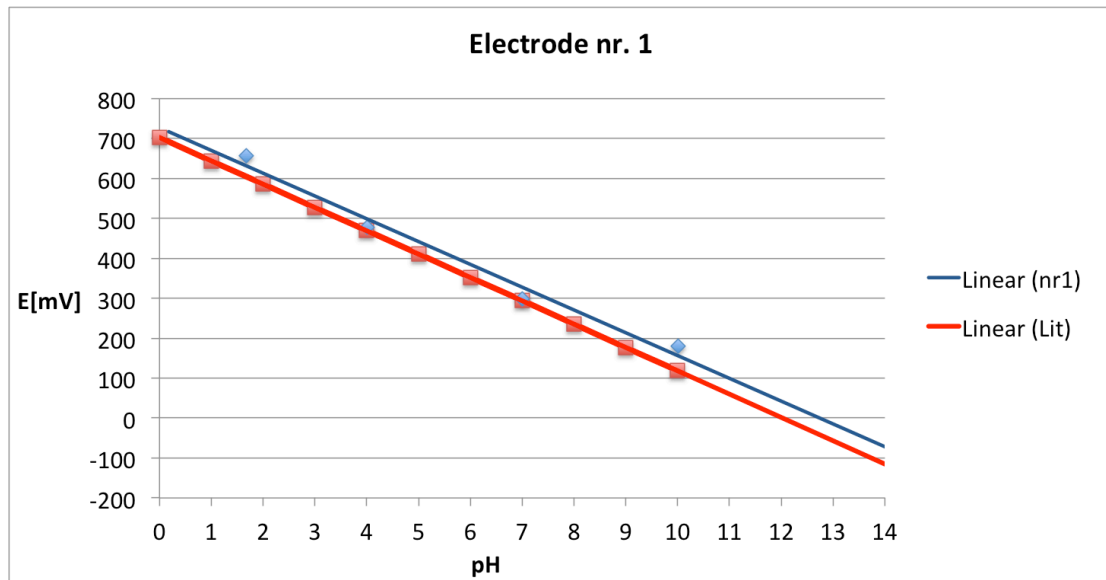
Electrode 2:
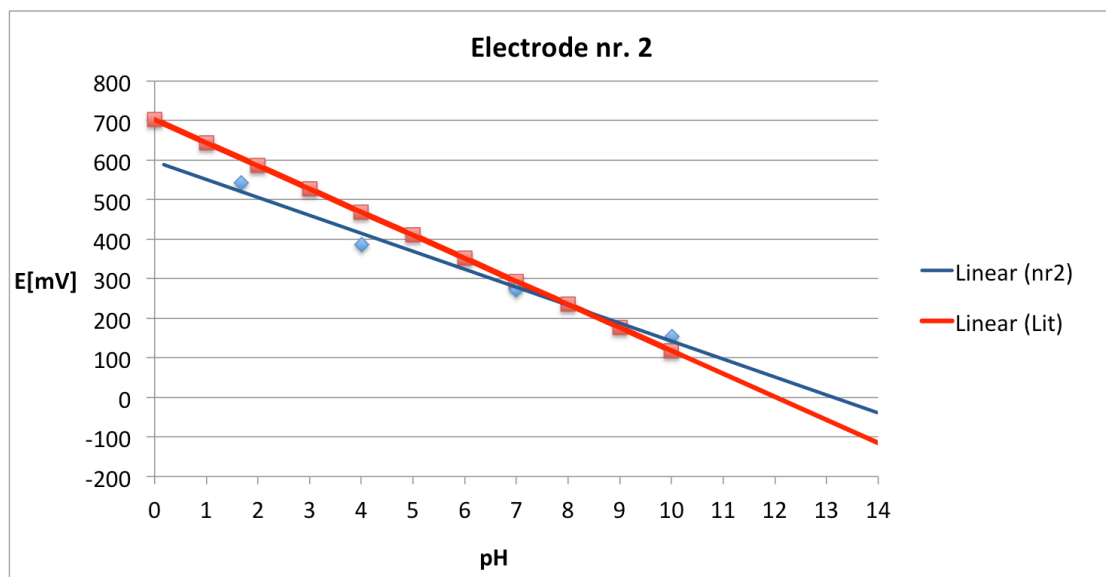
Electrode 3:
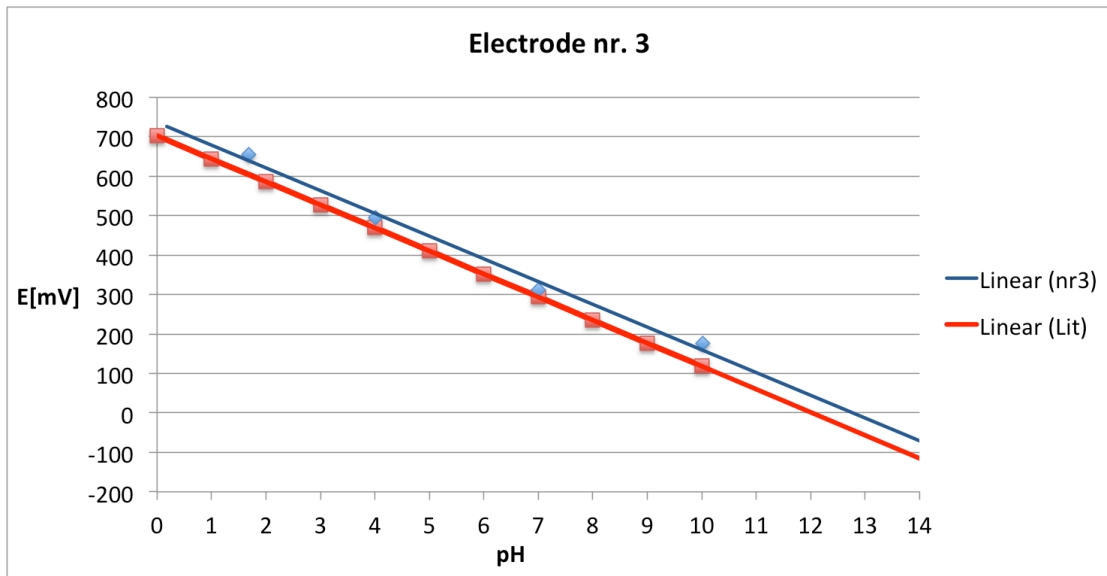
Electrode 4:
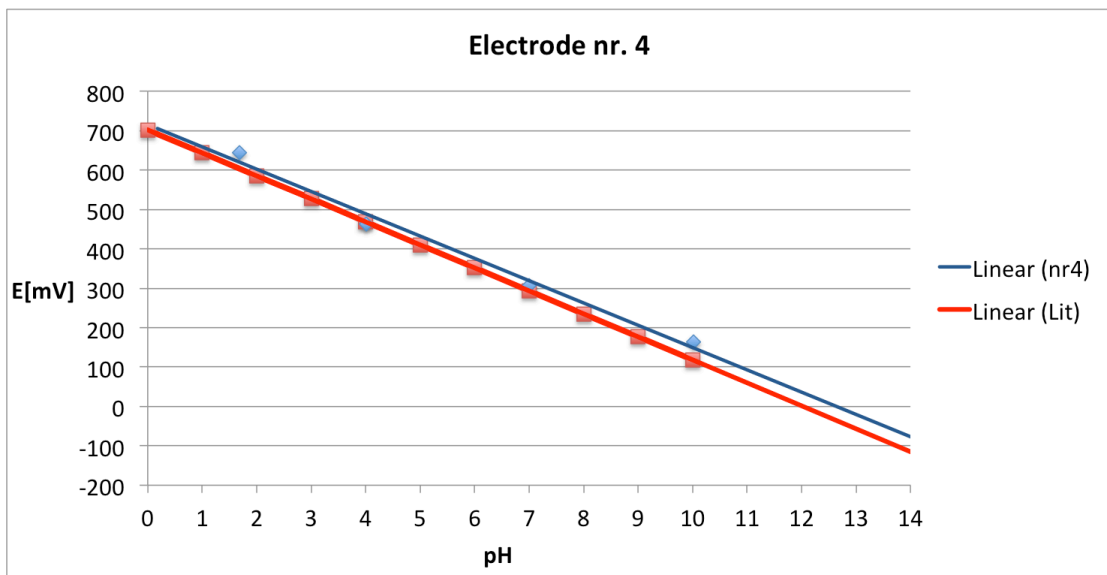
Electrode 5:
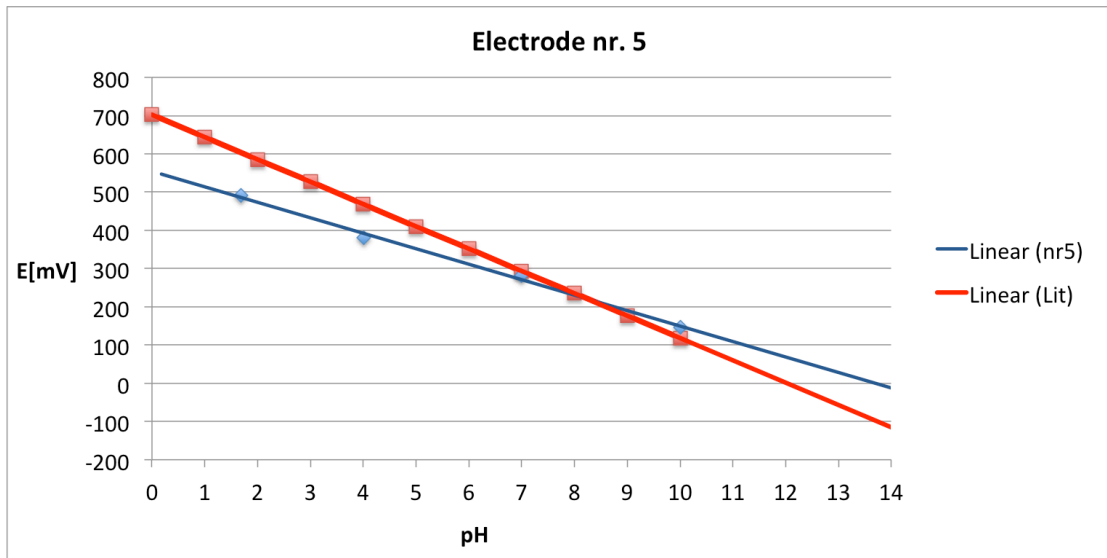
Electrode 6:
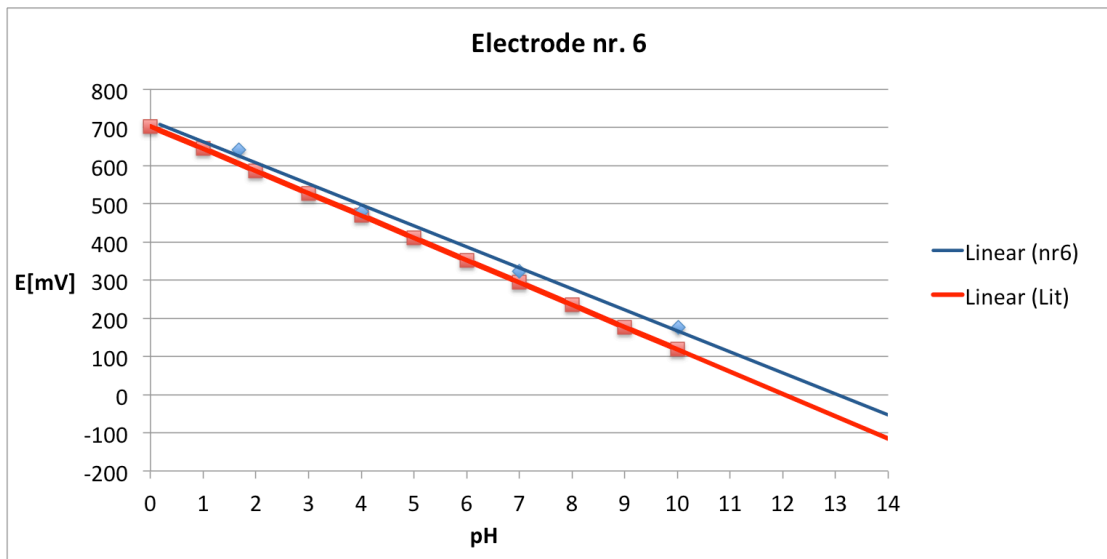
Electrode 7:

Electrode nr. 7
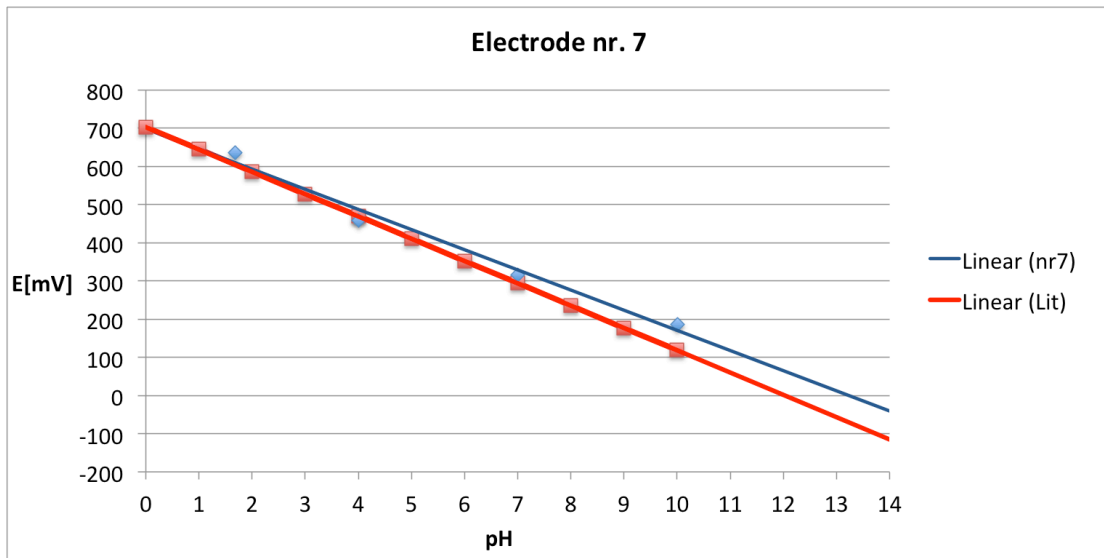
Appendix B

Pictures of the TSA Surfaces After 36 Days Exposure

Sample 1:
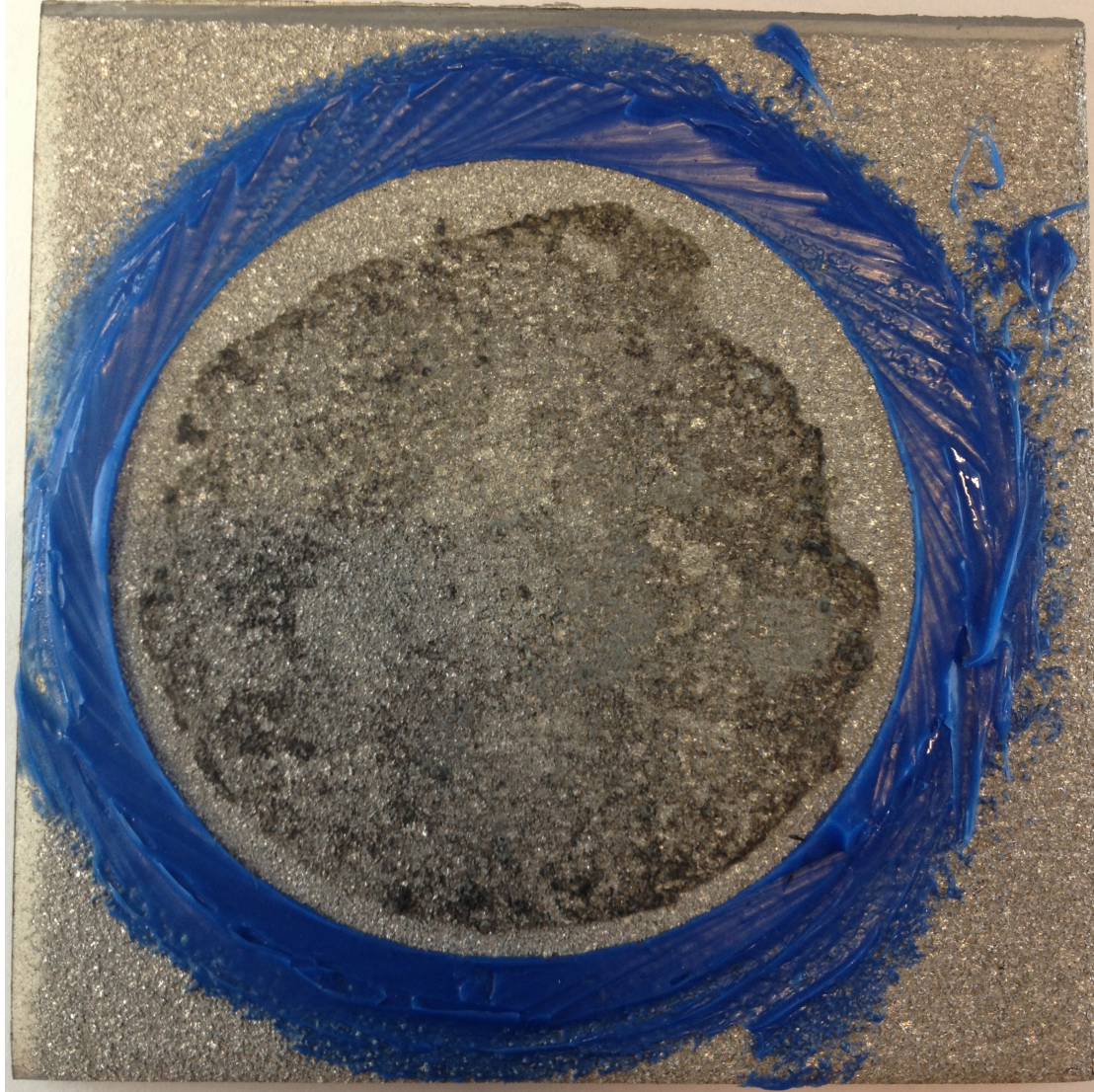
Sample 2:
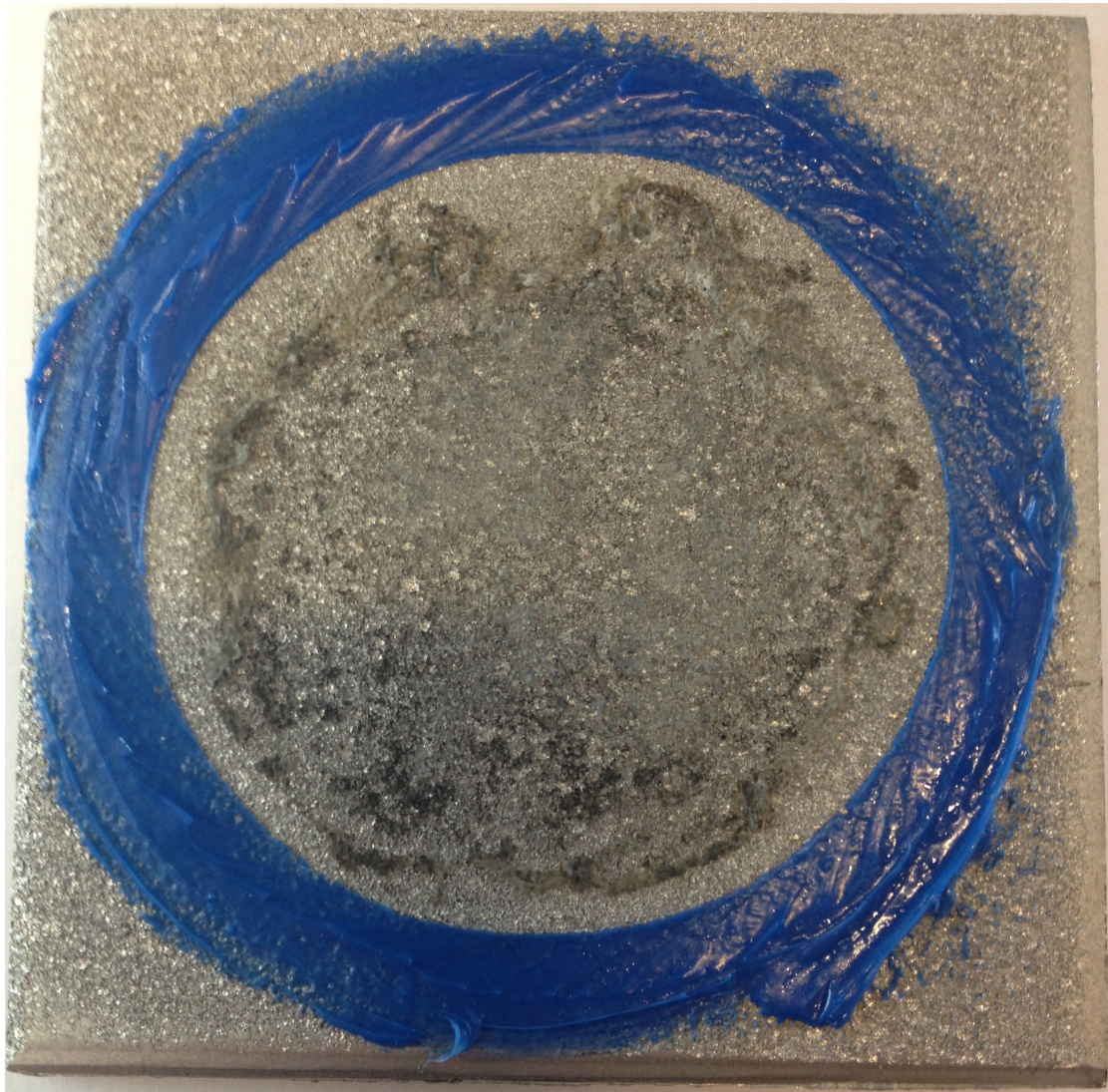
Sample 3:
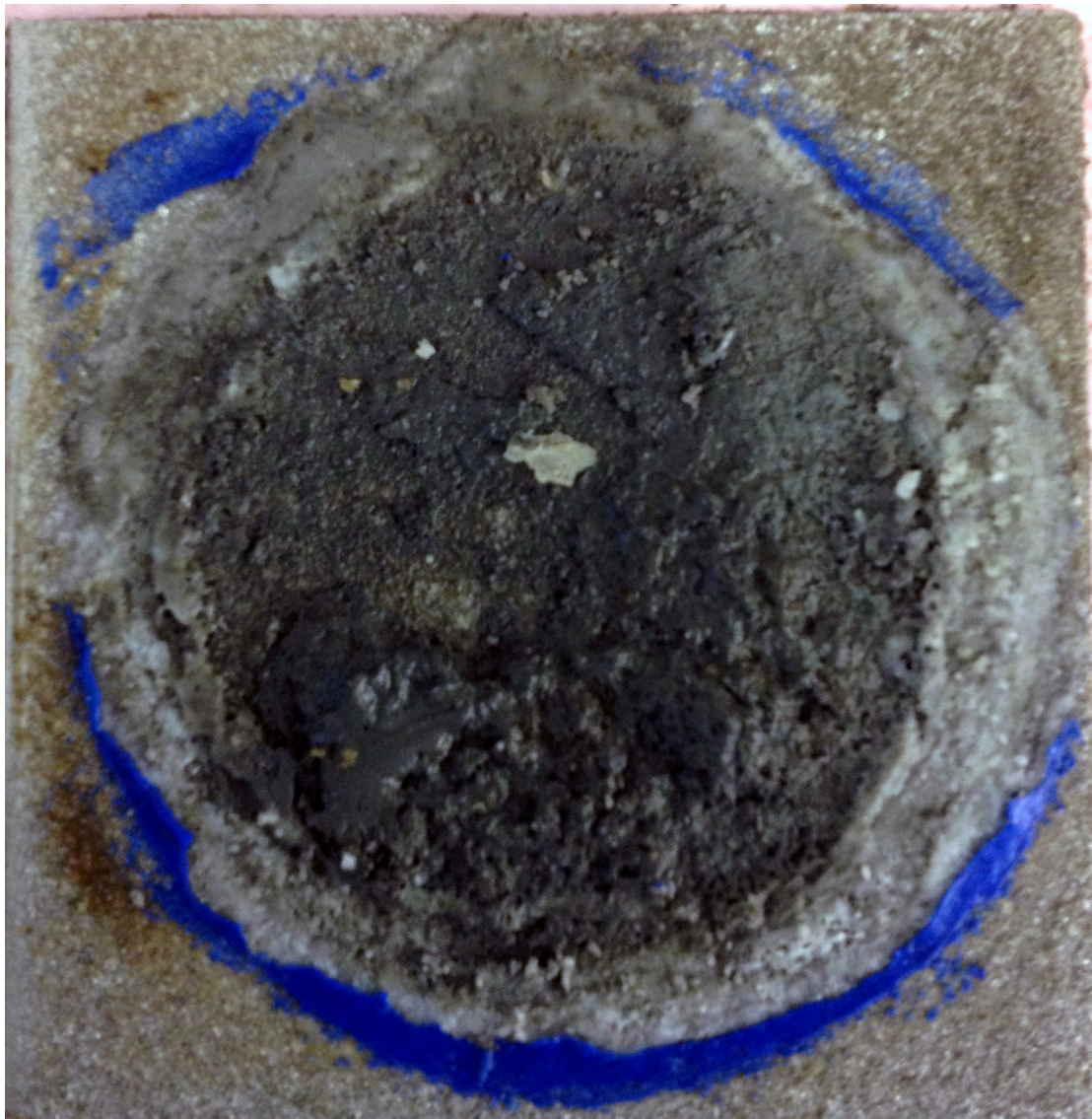
Note: sample 3 suffered from a leakage in the mud cell seal after 14 days of exposure, and was then taken out of the experiment.
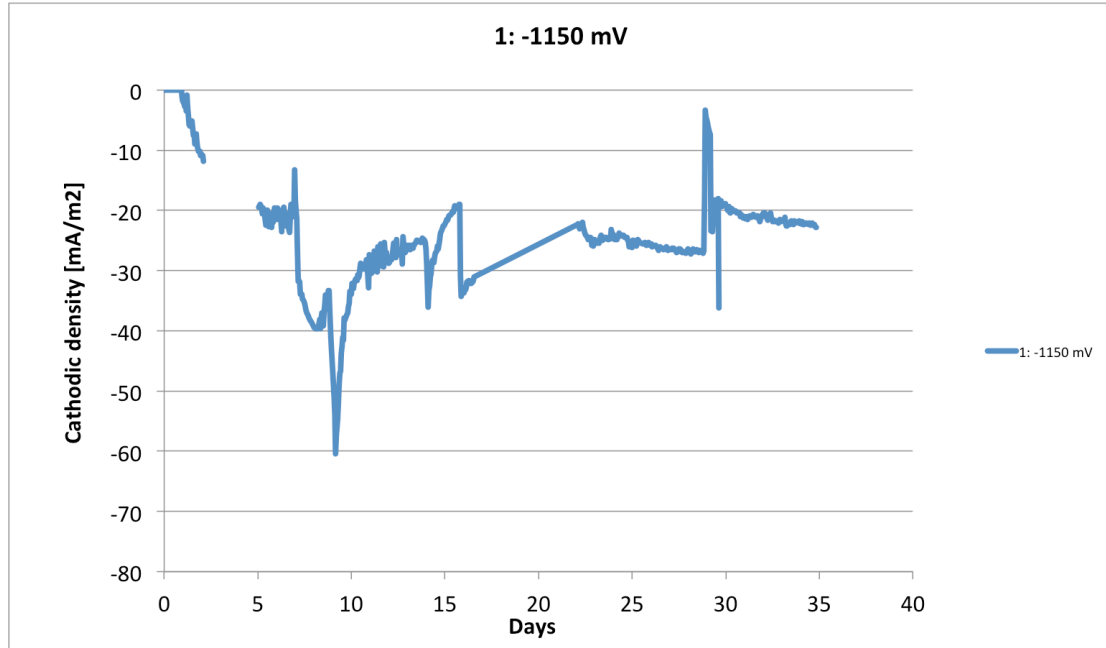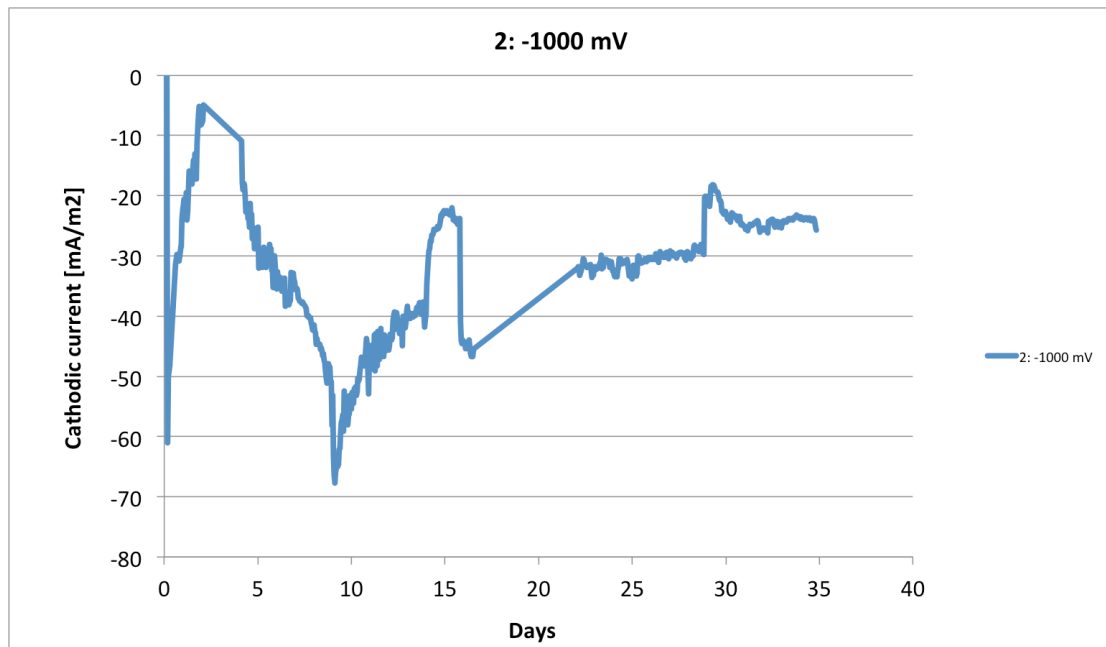
Sample 4:

Sample 5:
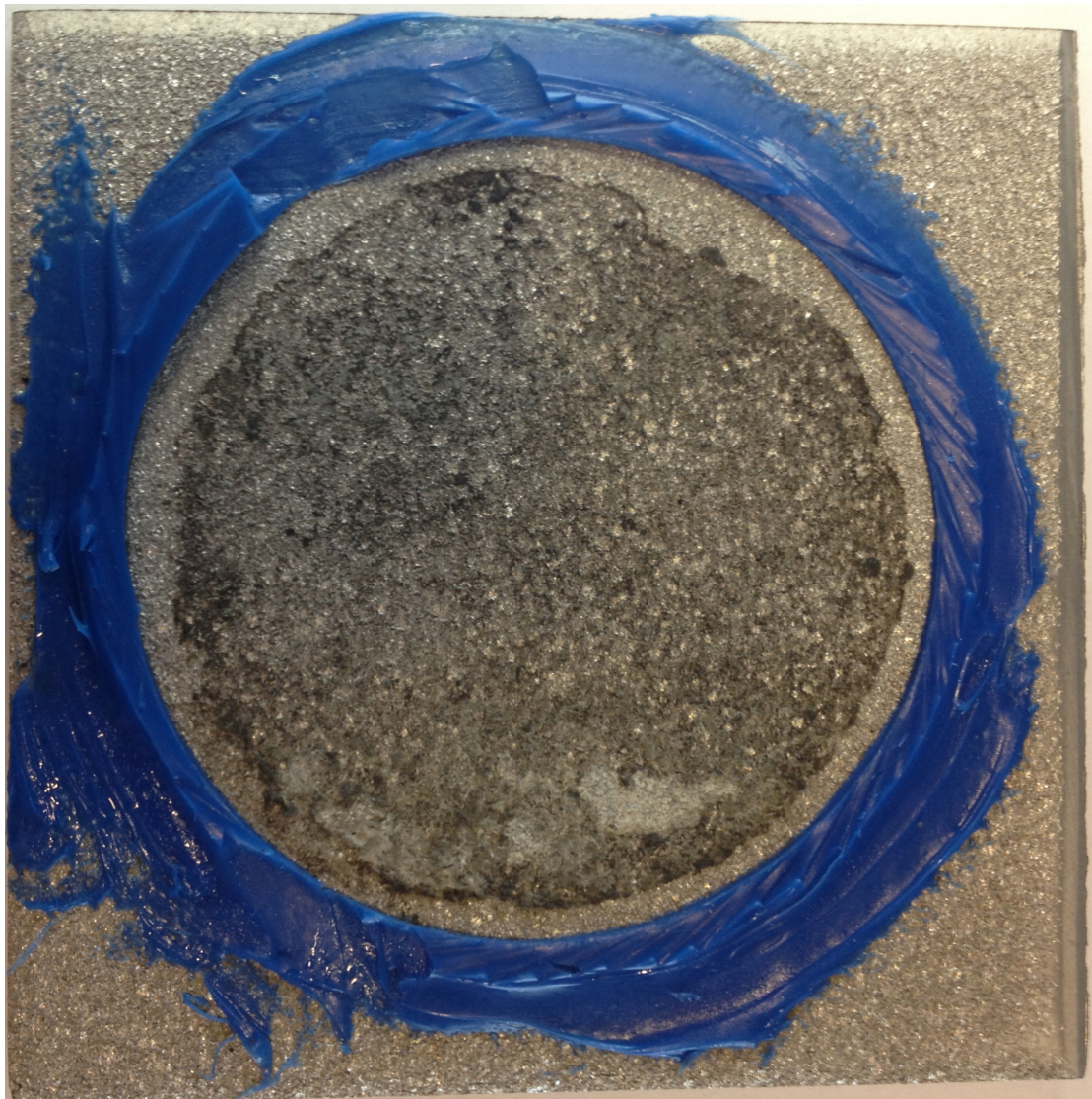
Appendix C

Individual Current Density Curves for all Samples

Sample 1:

Sample 2:

Sample 3:

Anodic density vs time for sample 3

Sample 4:

4: -1050 mV
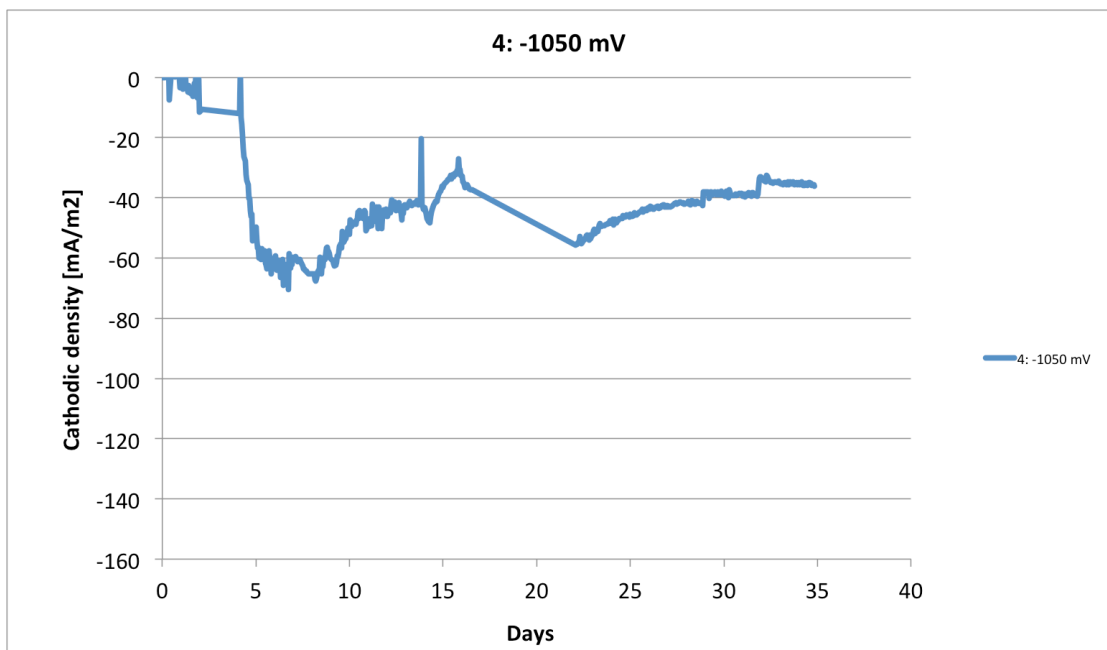
Sample 5:
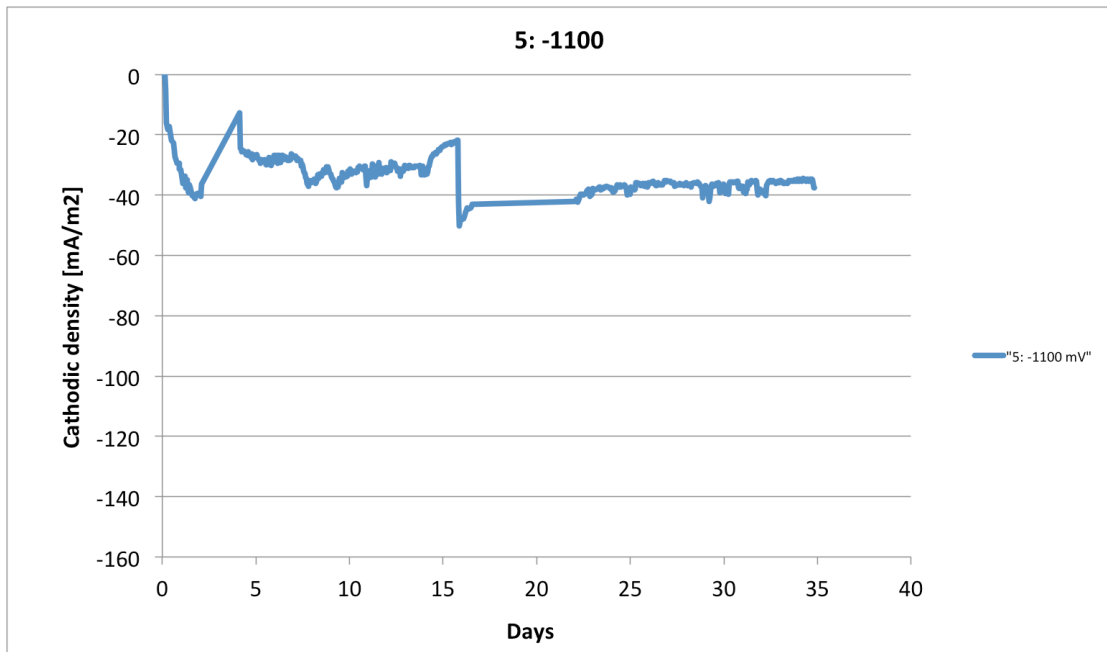
APPENDIX D

pH Measurements

pH Sample 3

pH Sample 4

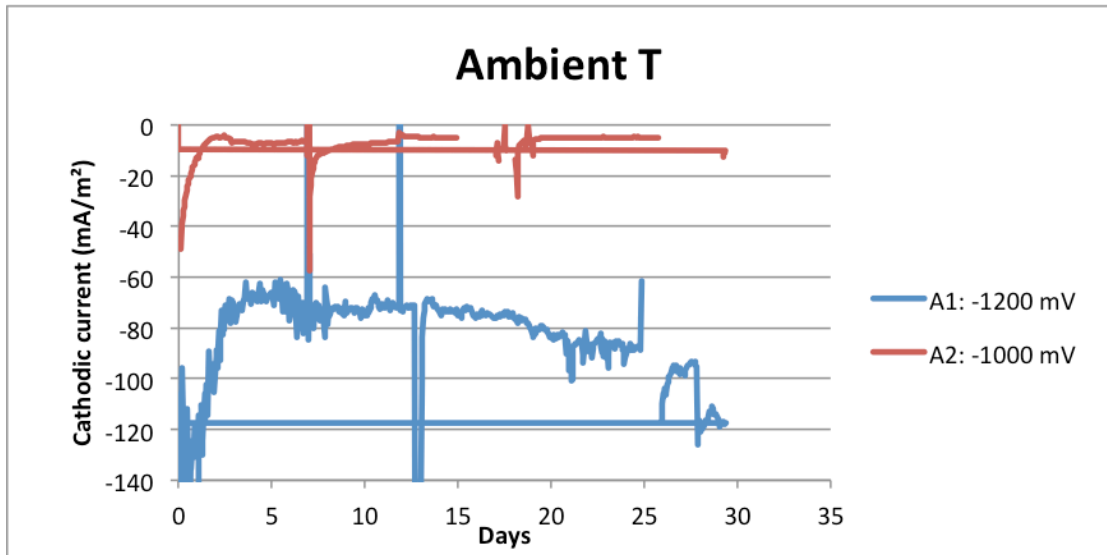pH Sample 5
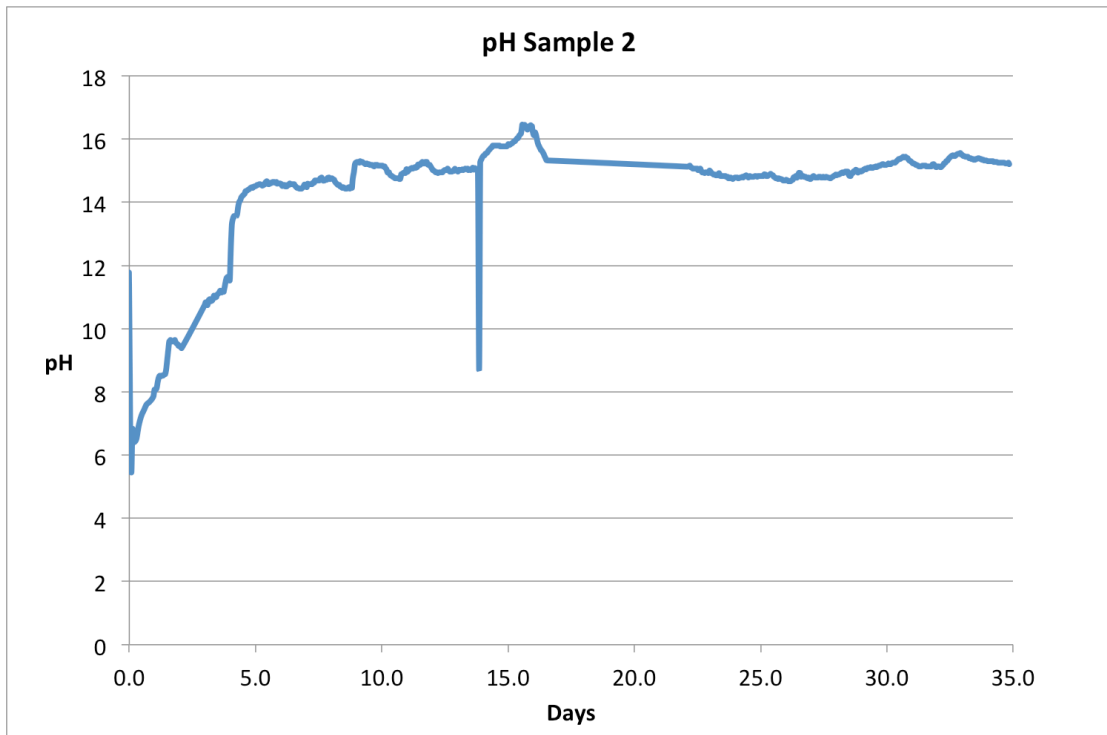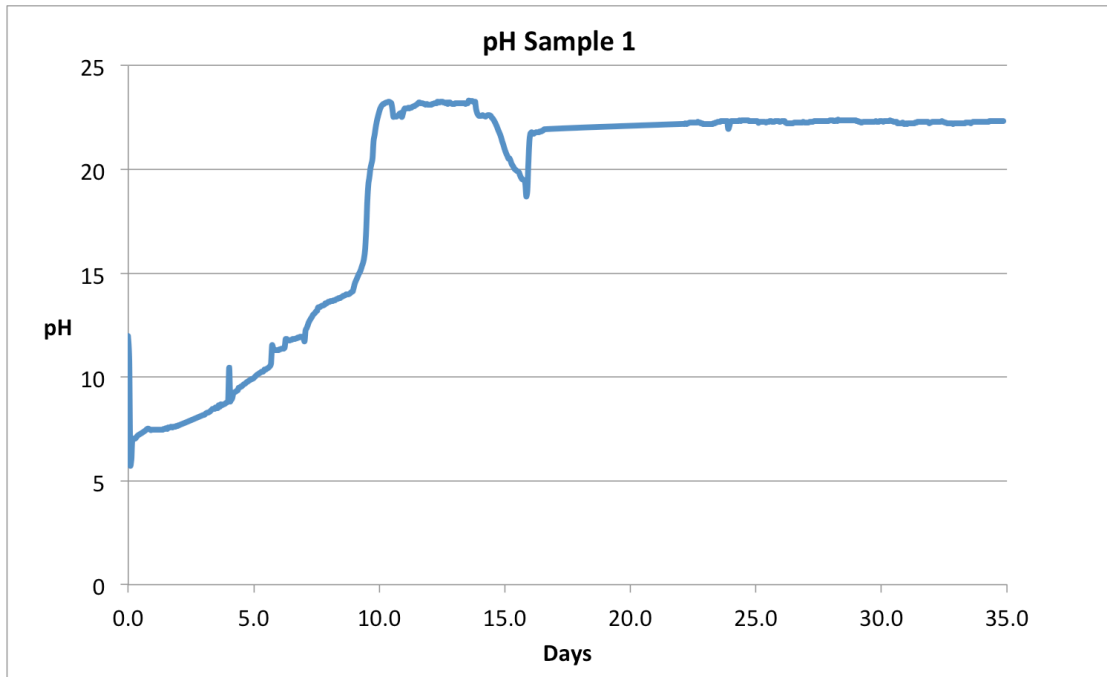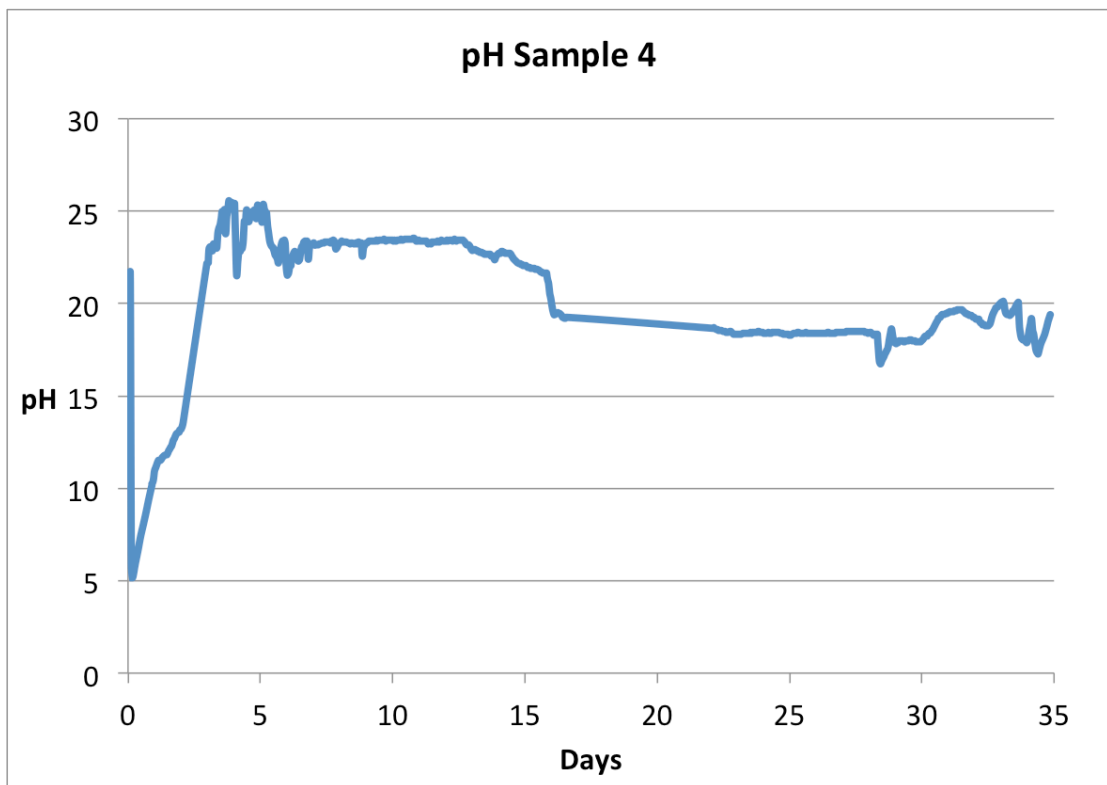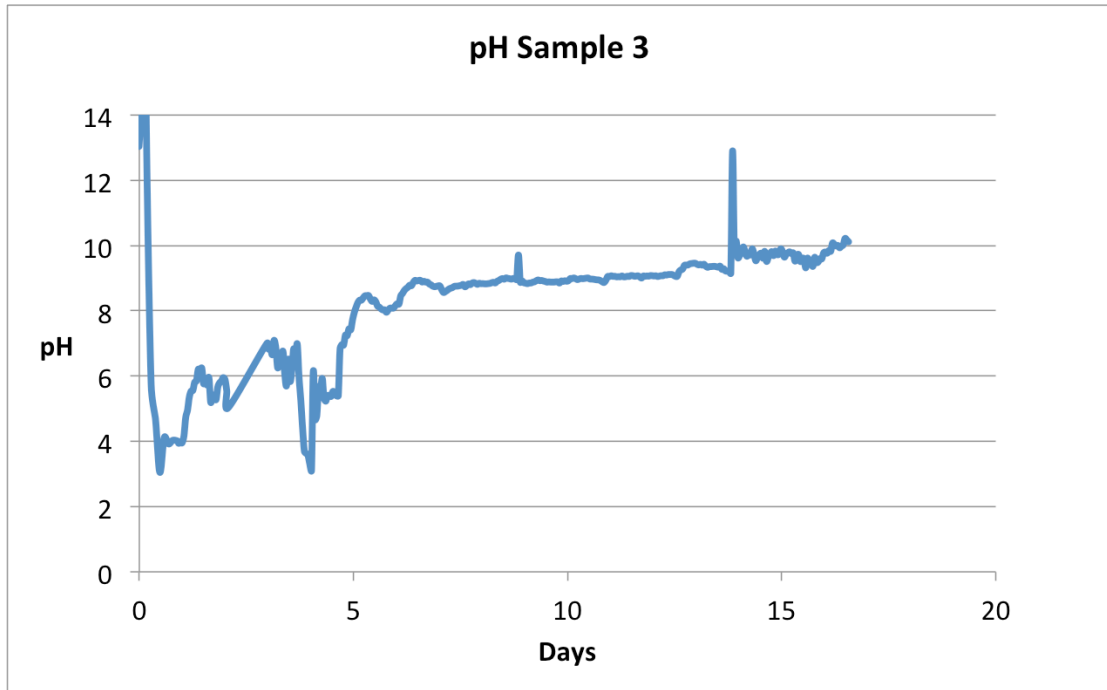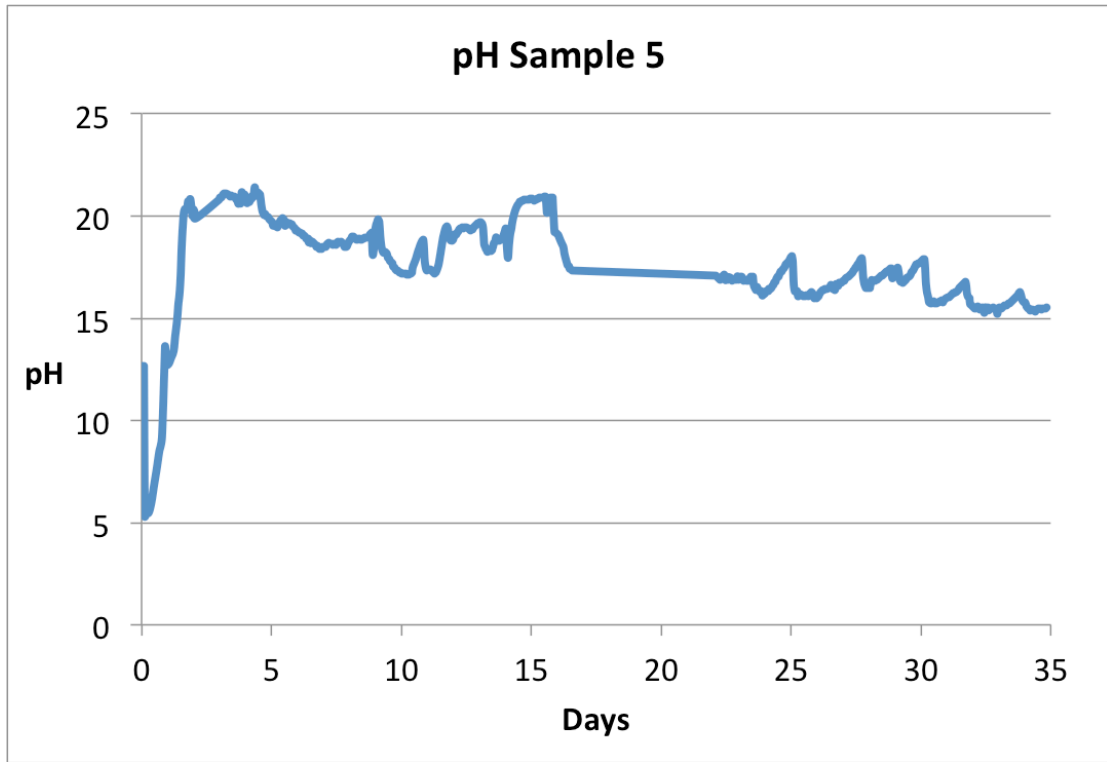
APPENDIX E

POTENTIAL LOG
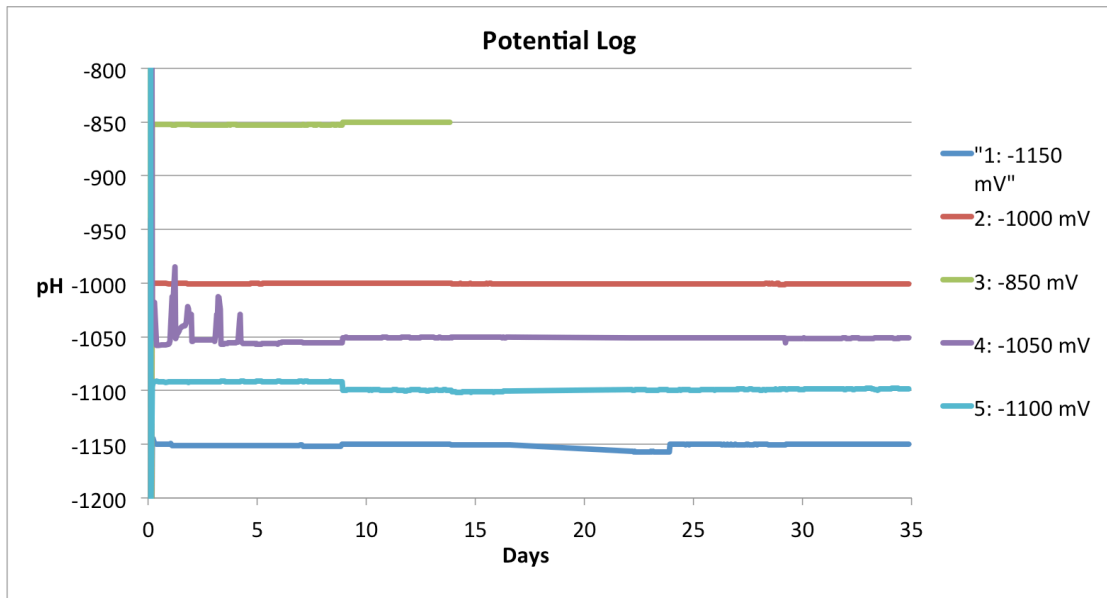
APPENDIX F

TEMPERATURE LOG
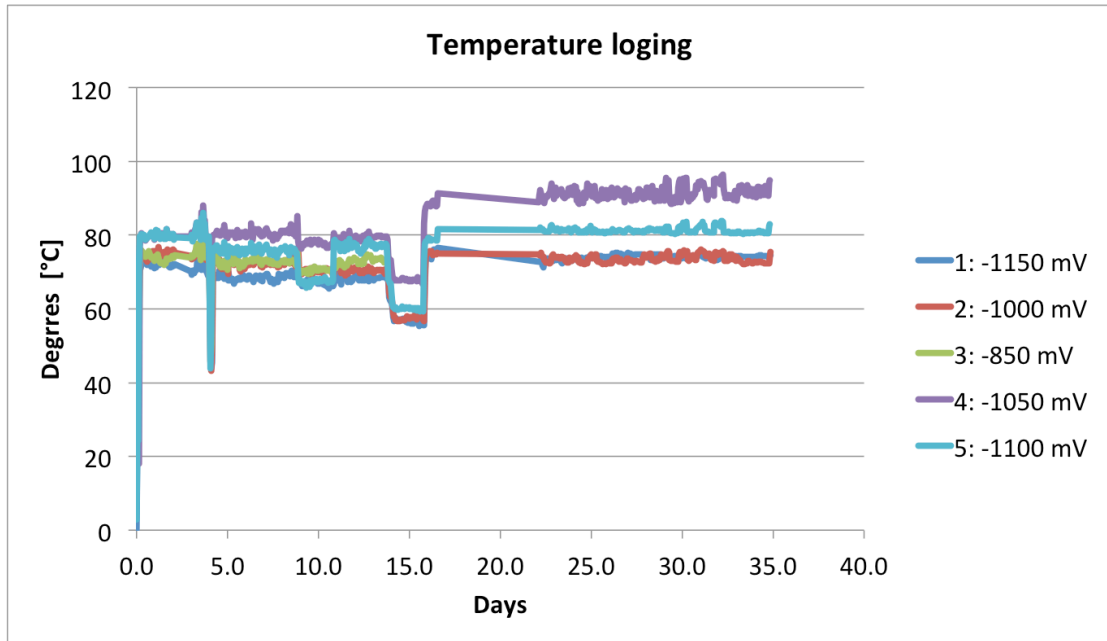
APPENDIX G

CURRENT DEMAND WITHOUT SEALERS

Note: these measurements were not done in this project but are obtained from an earlier project done at SINTEF Material and Chemistry on the same topic.
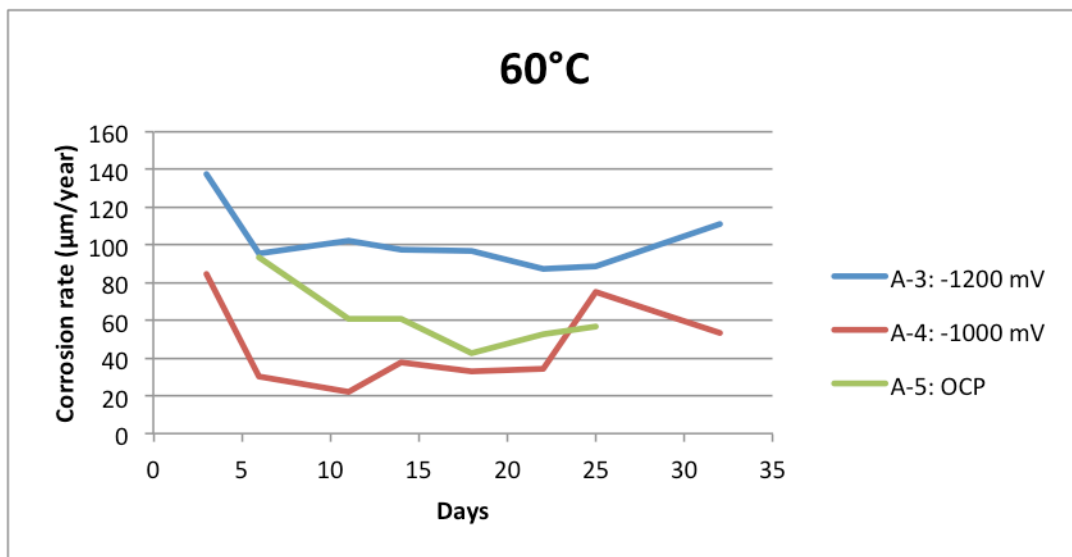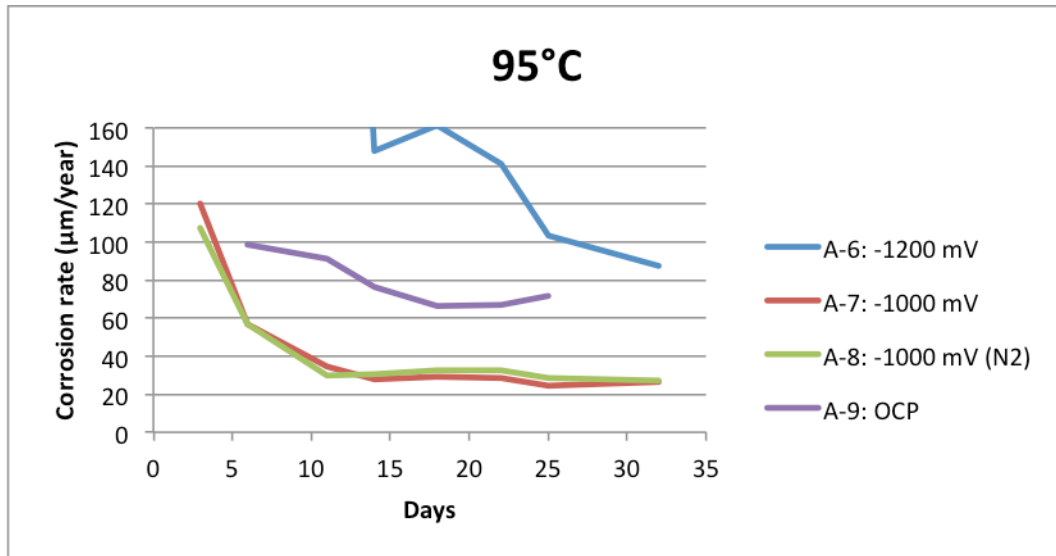
Ambient T

A1: -1200 mV
A2: -1000 mV

S
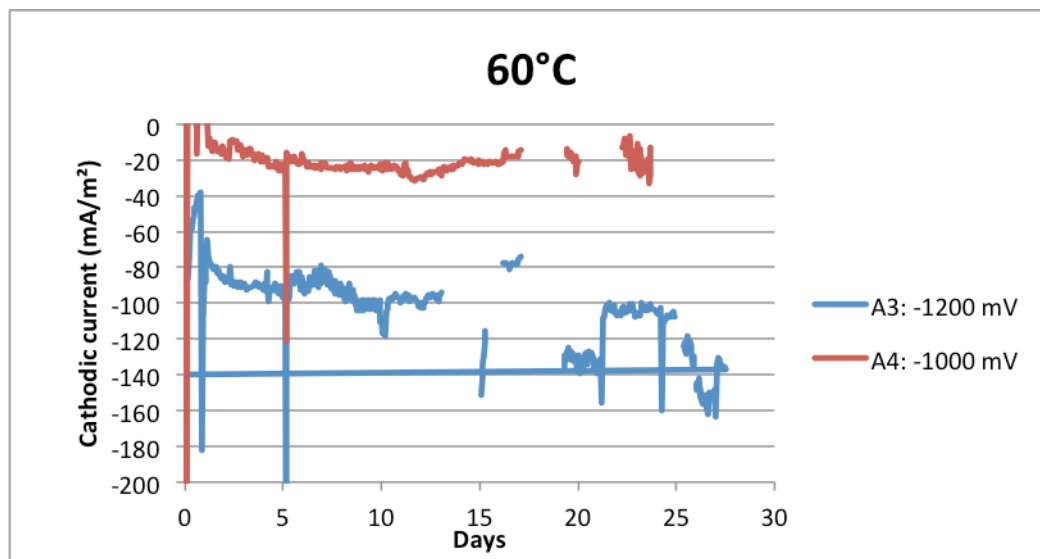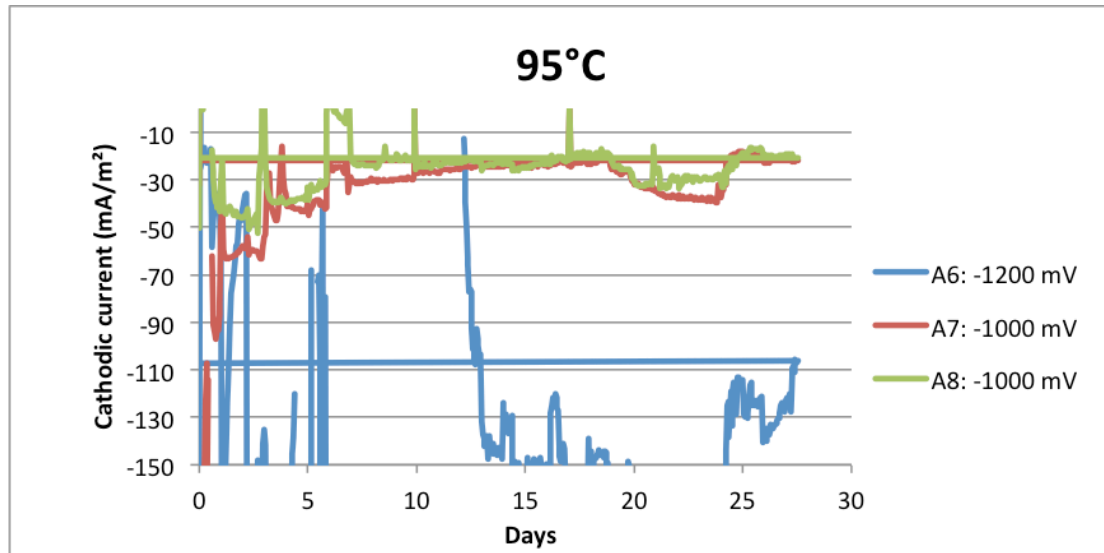
Appendix H

Corrosion Rate without Sealer

Note: these measurements were not done in this project but are obtained from an earlier project done at SINTEF Material and Chemistry on the same topic.
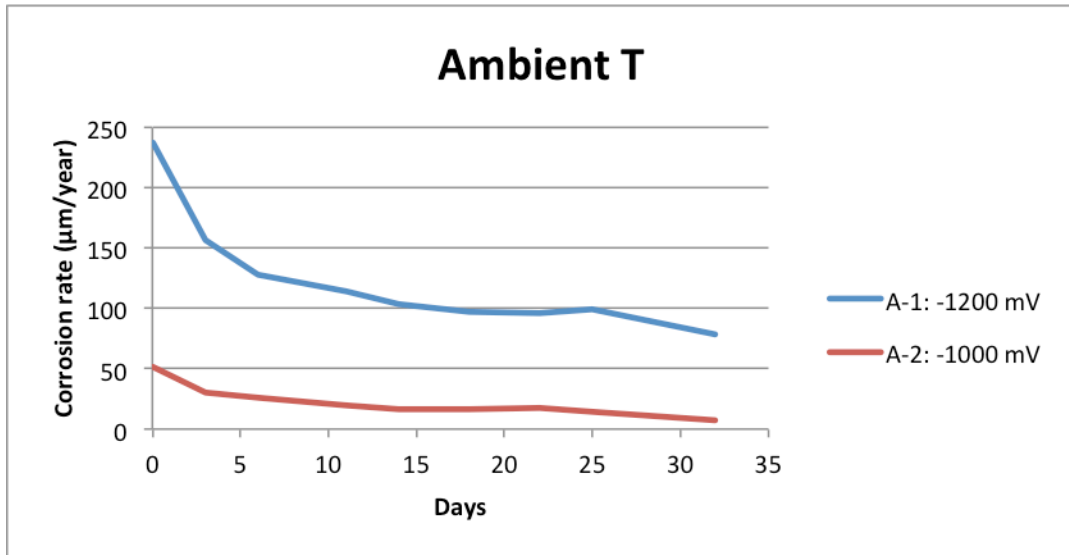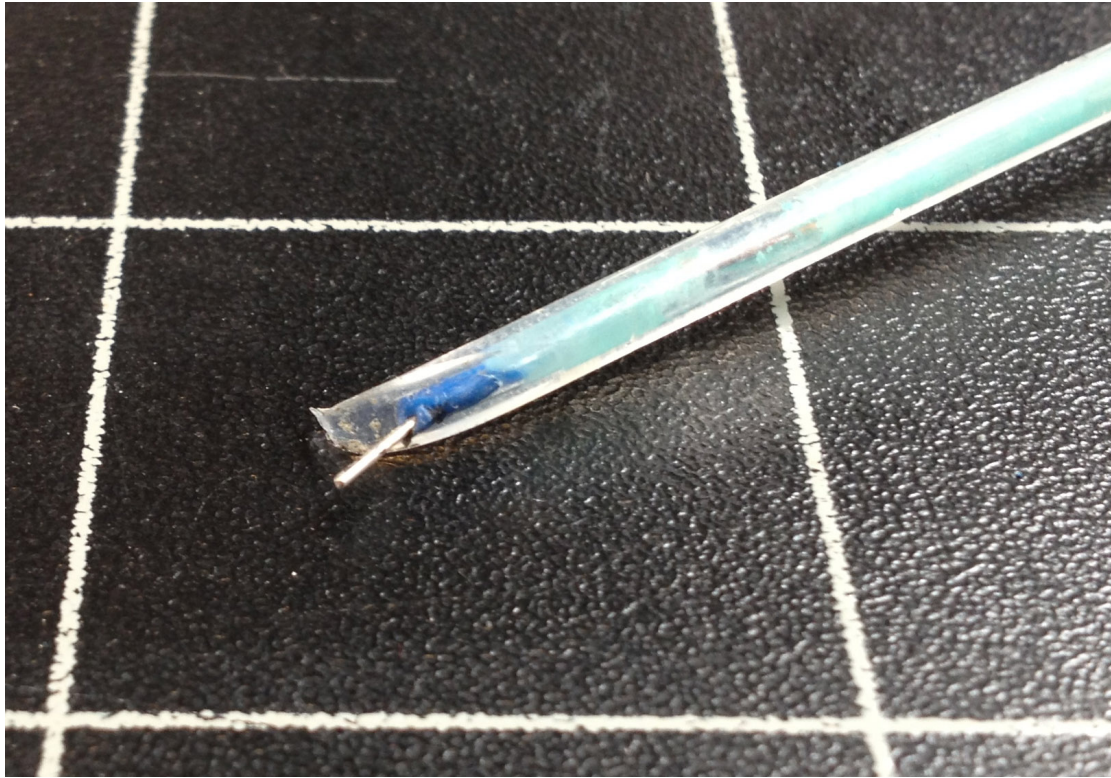
Ambient T

Corrosion rate (µm/year) vs Days

A-1: -1200 mV
A-2: -1000 mV

U

Appendix I

Detachment of Iridium Oxide

In the picture below is an iridium oxide electrode that has suffered from detachment of the oxide layers shown

APPENDIX J

STANDARD DEVIATION VALUES FOR THE E°´VALUES AND THE SENSOR SENSITIVITY

Standard Deviation Values for the E°´values and the Sensor Sensitivity compered to the values Wang et al reported in [30]

Project	E°´	Sensor sensitivity
Current	72	6.6
Wang et.al from [30]	0.4	0.1

APPENDIX K

ANODIC AND CATHODIC TAFEL CURVE FOR SAMPLE 2